

Diss. ETH No. 14100

# On the Dynamics of Tidewater Glaciers

A dissertation submitted to the  
SWISS FEDERAL INSTITUTE OF TECHNOLOGY ZURICH  
for the degree of  
**Doctor of Natural Sciences**

presented by  
Andreas Vieli  
Dipl. Phys. ETH  
born 21. June 1970  
citizen of Vals (GR)

accepted on the recommendation of  
Prof. Dr. H. Blatter, examiner  
Dr. M. Funk, co-examiner  
Prof. Dr. K. A. Echelmeyer, co-examiner  
Prof. Dr. A. Ohmura, co-examiner

2001

# Contents

Contents	1
Abstract	V
Zusammenfassung	VII
Introduction	1
O r g a n i z a t i o n o f t h e t h e s i s .	3
<b>Paper 1: Tidewater glaciers: frontal flow acceleration and basal sliding</b>	5
1 . 1 I n t r o d u c t i o n . .	6
1 . 2 D a t a b a s e a n d f i e l d o b s e r v a t i o n s .	6
1 . 3 M o d e l d e s c r i p t i o n .	8
1 . 3 . 1 B a s a l s l i d i n g .	9
1 . 3 . 2 B a s a l w a t e r p r e s s u r e a n d s l i d i n g .	11
1 . 4 M o d e l r e s u l t s a n d c o m p a r i s o n w i t h o b s e r v a t i o n s .	12
1 . 4 . 1 C o n s t a n t s l i d i n g c o e f f i c i e n t .	12
1 . 4 . 2 S p a t i a l l y d e p e n d e n t s l i d i n g c o e f f i c i e n t .	12
1 . 4 . 3 H i g h l y c r e v a s s e d z o n e .	14
1 . 5 C o n c l u s i o n .	15
1 . 6 A c k n o w l e d g e m e n t .	16
<b>Paper 2: Short-term velocity variations on Hansbreen, a tidewater glacier in Spitsbergen</b>	17
2 . 1 I n t r o d u c t i o n .	18
2 . 1 . 1 H a n s b r e e n .	19

2.2	Observational program . . . . .	21
2.3	Observation results . . . . .	23
2.3.1	Climatic conditions . . . . .	23
2.3.2	Variations in water pressure . . . . .	23
2.3.3	Velocities and vertical displacement . . . . .	24
2.4	Interpretation and discussion of observations . . . . .	29
2.4.1	General flow characteristics . . . . .	29
2.4.2	Short-term variations . . . . .	31
2.5	Conclusions . . . . .	35

<b>Paper 3:</b>	<b>Flow dynamics of tidewater glaciers: a numerical modelling approach</b>	<b>37</b>
3.1	Introduction	38
3.1.1	Motivation	38
3.1.2	Current knowledge on tidewater glaciers	39
3.1.3	Previous modelling work	40
3.2	Governing processes	41
3.2.1	Calving	41
3.2.2	Basal sliding	44
3.3	Model description	45
3.3.1	Field equations and flow law	45
3.3.2	Basal boundary condition	46
3.3.3	Surface boundary condition	46
3.3.4	Calving front and upper boundary	47
3.3.5	Numerical Solution technique	47
3.4	Model experiments	48
3.4.1	Model input	48
3.4.2	Model results	49
<b>3.5</b>	<b>Discussion</b>	<b>57</b>
<b>3.6</b>	<b>Conclusions</b>	<b>59</b>

<b>Paper 4: The retreat of a tidewater glacier: observations and model calculations on Hansbreen</b>	<b>61</b>
4.1 Introduction . . . . .	62
4.2 Hansbreen: Geographical setting and observations . . . . .	65
4.2.1 Frontal positions 1982-1998 . . . . .	65
4.2.2 Observations related to calving . . . . .	68
4.2.3 Flow velocities . . . . .	68
4.3 Interpretation and discussion of observations . . . . .	69
4.3.1 Long term changes 1982-1998 . . . . .	69
4.3.2 Seasonal variations . . . . .	70
4.3.3 Calving rate water depth relation . . . . .	72
4.4 Modelling the retreat of 1982-1998 . . . . .	72
4.4.1 Model description . . . . .	72
4.4.2 Model input . . . . .	74
4.5 Model results and discussion . . . . .	77
4.6 Conclusions and prospects . . . . .	82
<b>A Interferometric radar observations of Hansbreen</b>	<b>85</b>
A.1 Introduction and method . . . . .	85
A.2 SAR-data for Hansbreen region . . . . .	86
A.3 SAR interferogram April 9/10 1996 . . . . .	86
A.4 Concluding remarks . . . . .	90
<b>Bibliography</b>	<b>93</b>
<b>Acknowledgements</b>	<b>101</b>
<b>Curriculum vitae</b>	<b>103</b>

# Abstract

This thesis investigates the dynamics of tidewater glaciers and the involved processes such as calving and basal sliding. This is done by two different approaches.

The first observational part of this study is focussed on Hansbreen, a 16km long tidewater glacier situated in South Spitsbergen. A detailed analysis of a 16year time series of front position and geometry was used to identify and investigate the important processes and factors that control calving and changes in front position between 1982 and 1998 and on a seasonal scale. The observed abrupt retreat in 1990 is found to be related to a basal depression in the terminus region. The additionally observed seasonal variations of the front positions are mainly due to variations of the calving rate and not due to seasonal variations in ice velocity. Observations of Hansbreen further indicate that melting at the water line may play an important role by triggering the process of calving during periods of slow front position changes.

The flow behaviour of Hansbreen is studied in detail during two field investigations performed in summer 1998 and 1999 in cooperation with J. Jania from University of Silesia, Poland. Temporal variations of the flow of Hansbreen were measured on time scales from hours to seasons. During the melting season, short events of strongly increased surface velocities were observed, rather than generally enhanced 'spring' velocities. These *speed-up events* are related to periods of strongly increased water input to the glacier, due to rainfall or enhanced surface melt during a föhn weather situation. The close correlation between water pressure recorded in a moulin and the observed surface velocities suggests that the speed-ups are caused by a strong increase of basal water pressure which leads to enhanced basal sliding. The speed-up was associated to a short peak of the longitudinal strain, which may lead to additional fracture in the terminus region and therefore affect the process of calving. The observed short-term velocity variations and associated processes on Hansbreen are very similar to those observed on landbased valley glaciers. This suggests that the relevant mechanisms and physical processes that control the flow and its temporal variations are the same.

Spatially, a strong increase of the flow towards the calving front was observed on Hansbreen. It could be shown that increased basal sliding due to decreased effective pressure towards the front is responsible for the increase in flow. Using a glacier flow model including a water pressure dependent sliding law the observed velocity pattern, especially the frontal acceleration, could be well reproduced.

In a second part of the thesis the dynamics of tidewater glaciers is approached by numerical modelling. A time dependent numerical flow model for tidewater

glaciers has been developed which solves the full equations for the stress and velocity fields and includes a water pressure dependent sliding law. A calving criterion is implemented which removes at each time step the part of the glacier that is thinning below a critical height above buoyancy. In contrast to previous modeling approaches, the calving rate is an output quantity of the model and not prescribed.

Model experiments are performed for a synthetic but typical tidewater glacier with a basal depression in the terminus region. With these model experiments the qualitatively described mechanisms and concepts suggested to explain changes in front positions are examined and the importance of different factors and processes, such as basal topography, calving and basal sliding on the dynamics of tidewater glaciers is investigated.

The linear relation between calving rate and water depth proposed on empirical grounds is qualitatively reproduced by the model for the situation of a slowly retreating or advancing terminus, but not for situations of rapid changes. Length changes of tidewater glaciers, especially rapid changes, are dominantly controlled by the basal topography and are to a minor degree a direct reaction to a mass balance change. Rapid changes in terminus positions preferably occur in places where the bed slopes upwards in ice flow direction. In the present model calculations thinning due to a change in mass balance is only the triggering process of a rapid retreat through a basal depression. The results also confirm the suggested cycles of slow advance and rapid retreat through a basal depression by different authors (Meier and Post, 1987). We conclude that accurate information on the near terminus bed topography is required for reliable predictions of terminus changes due to climate changes.

The glacier dynamics model is additionally applied to Hansbreen to analyse the observed retreat from 1982 to 1998. A seasonal calving rate, estimated from the observed front positions, is additionally prescribed in the model. The model calculations show that the process of buoyancy-induced calving is controlling the abrupt retreat of Hansbreen through the basal depression. The modelled location of the jump in retreat is found to be independent of the assumed mass balance and the prescribed seasonal calving rate and is fixed to the position where the basal depression is located. Thus, the abrupt retreat of Hansbreen is mainly an effect of basal topography in the terminus region and not a direct response to a change in mass balance or climate.

# Zusammenfassung

In der vorliegenden Arbeit wird die Dynamik von kalbenden Gletschern und der daran beteiligten Prozesse wie die Kalbung von Eisbergen, das Gletscherfließen und basale Gleiten untersucht. Die Studie beschränkt sich auf kalbende Gletscher, welche auf dem Gletscherbett aufliegen, sogenannte *tidewater glacier*. Mit numerischen Modellierungen des Gletscherfließens und direkten Feldmessungen werden die relevanten Prozesse untersucht.

Die Feldbeobachtungen stammen im wesentlichen vom Hansbreen, einem 16 km langen kalbenden Gletscher, welcher im Süden von Spitzbergen liegt. Die Feldarbeiten wurden in Zusammenarbeit mit Professor J. Jania von der Universität Schlesien in Polen durchgeführt. Die Auswertung von gemessenen Positionen der Gletscherfront und -geometrie zwischen 1982 und 1998 bildete die Basis für die Untersuchung und Identifikation der relevanten Prozesse und Faktoren, welche die Kalbung und Gletscherveränderungen in saisonalen und längeren Zeitskalen kontrollieren. Der beobachtete abrupte Rückzug des Gletschers im Jahre 1990 steht im Zusammenhang mit einer basalen Übertiefung des Gletscherbettes im Gebiet der Kalbungsfrent. Die Beobachtungen am Hansbreen zeigen weiter, dass während Phasen langsamer Änderungen der Frontposition die Schmelze an der Wasserlinie den Kalbungsprozess dominiert.

Während zwei Feldkampagnen in den Sommern 1998 und 1999 wurden Veränderungen der Oberflächengeschwindigkeiten des Hansbreen in verschiedenen Zeitskalen (von Stunden bis Monaten) genauer untersucht. Während der Schmelzperiode wurden Beschleunigungsereignisse beobachtet, an welchen die Oberflächengeschwindigkeiten auf das fünffache des ursprünglichen Wertes anstiegen und 1 bis 2 Tage dauerten. Aufgetreten sind diese Speed-up Ereignisse in Perioden mit stark erhöhter Wasserzufuhr in den Gletscher, welche durch Niederschlagsereignisse oder stark erhöhte Oberflächenschmelze während Föhn Wetterlagen verursacht wurden. Der beobachtete Zusammenhang zwischen dem Anstieg der Oberflächengeschwindigkeiten und dem zunehmenden basalen Wasserdruck, welcher in einer Gletschermühle gemessen wurde, weisen darauf hin, dass diese Speed-up Ereignisse durch erhöhtes basale Gleiten verursacht werden. Die Beschleunigungsereignisse wurden durch eine Störung in der Längsdehnung (in Fließrichtung) begleitet, wodurch zusätzliche Brüche und Spaltenbildungen vorkommen können und damit der Prozess der Eisbergkalbung beeinflusst wird. Die beobachteten kurzzeitigen Variationen der Geschwindigkeiten und die dabei auftretenden Prozesse sind vergleichbar mit denjenigen von nicht kalbenden Talgletschern. Dies zeigt, dass für Talgletscher und kalbende Gletscher die für das Fließen und deren zeitlichen

Änderungen wesentlichen Prozesse dieselben sind

Am Hansbreen konnte eine starke Zunahme der Oberflächenfliessgeschwindigkeiten zur Kalbungsfront hin beobachtet werden. Diese Geschwindigkeitszunahme kann durch erhöhtes basales Gleiten als Folge vom abnehmenden effektiven basalen Wasserdruck gegen das Gletscherende hin erklärt werden. Mit einem numerischen Gletscherfliessmodell, welches die Abhängigkeit des basalen Gleitens vom Wasserdruck berücksichtigt, konnte die beobachtete Geschwindigkeitszunahme gut reproduziert werden.

Im zweiten Teil dieser Arbeit wird die Dynamik von kalbenden Gletschern mittels numerischer Modellierung untersucht, Dazu wurde ein numerisches Modell für die Evolution von kalbenden Gletschern entwickelt, welches die vollen Gleichungen zur Berechnung der Spannungs- und Geschwindigkeitsfelder löst, sowie ein vom Wasserdruck abhängiges Gleitgesetz beinhaltet. Die Gletscherkalbung wird durch ein Kriterium berücksichtigt, nach welchem die Position des Gletscherendes nach jedem Zeitschritt so versetzt wird, dass ein kritischer Wert über dem Schwimmgleichgewicht nie über- oder unterschritten wird (*Auftrieb* induzierte *Kalbung*). Im Gegensatz zu früheren Modellansätzen ist die Kalbungsrate ein Resultat der Modellrechnungen und wird nicht durch eine Parameterisierung vorgeschrieben. Für eine synthetische aber für tidewater *glaciers* typische Geometrie mit einer basalen Übertiefung im Frontbereich, sind Modellexperimente mit je einem positiven und negativen Massenbilanz Szenario durchgeführt worden. Mit diesen Modellrechnungen werden die von verschiedenen Autoren vorgeschlagenen qualitativ beschriebenen Mechanismen und Konzepte zur Erklärung von Veränderungen bei kalbenden Gletschern überprüft und die Bedeutung verschiedener Faktoren und Prozesse, wie basale Topographie, Kalbung oder basales Gleiten, für die Dynamik dieser Gletscher untersucht.

Die Modellresultate bestätigen qualitativ die empirisch bestimmte, lineare Beziehung zwischen Kalbungsrate und Wassertiefe (Brown and others, 1982). Allerdings ist sie nur bei langsamen Gletscherveränderungen gültig. Schnelle Längenänderungen werden meistens durch die basale Topographie im Bereich der Kalbungsfront verursacht und sind keine direkte Reaktion auf Massenbilanzänderungen. Schnelle Vorstösse oder Rückzüge treten bevorzugt an Stellen auf, wo das Gletscherbett am Gletscherende in Fliessrichtung ansteigt. Liegt das Gletscherende unmittelbar vor einer basalen Übertiefung, ist eine Absenkung der Gletscheroberfläche als Folge einer negativen Massenbilanz der Auslöser für einen schnellen Gletscherrückzug. Wie sich tidewater *glaciers* bei einer Klimaveränderung verhalten werden, hängt deshalb stark von der basalen Topographie ab und eine Prognose setzt deren genaue Kenntnis voraus. Die Modellrechnungen bestätigen auch die von verschiedenen Autoren vorgeschlagenen Zyklen von langsamen Vorstössen und schnellen Rückzügen von kalbenden Gletschern durch eine basale Übertiefung (Meier and Post, 1987).

Das entwickelte numerische Modell wurde auf Hansbreen angewendet zur genauen Untersuchung des durch Messungen gut dokumentierten Rückzugs zwischen 1982 und 1998. Dazu wurde, neben dem zuvor beschriebenen Kalbungskriterium, eine aus Beobachtungen abgeschätzte saisonale Kalbungsrate vorgeschrieben. Die Modellrechnungen haben gezeigt, dass der beobachtete schnelle Rückzug von 1990



durch *Auftrieb induzierte Kalbung* verursacht wurde. Der Ort des modellierten sprunghaften Rückzugs hängt dabei nicht von der angenommenen Massenbilanz oder vorgeschriebenen saisonalen Kalbungsrate ab, sondern ist auf das Gebiet der basalen Übertiefung fixiert. Der abrupte Rückzug im Jahre 1990 ist deshalb eine Folge der Bettgeometrie und keine direkte Reaktion auf Änderungen der Massenbilanz oder des Klimas.

# Introduction

The general purpose of this thesis is to improve the understanding of the dynamics of tidewater glaciers and to identify and investigate the most relevant processes and their interactions.

The dynamics of glaciers that end in the sea or in a lake, is beside changes in mass balance or climate, additionally affected by the process of calving at the terminus. Calving is the dominating ablation mechanism for the existing ice masses on the world and accounts for  $\sim 70\%$  of the annual mass transfer from glaciers and ice sheets to the oceans (Van der Veen, 1997). It has been proposed as a major factor in the retreat of the Northern Hemisphere ice sheets during the last deglaciation.

This study is focussed on tidewater glaciers, which are defined as glaciers that end in the sea with a grounded ice cliff from which icebergs are discharged. Tidewater glaciers are mostly temperate or polythermal and occur in temperate oceanic regions (Alaska and Patagonia) or subpolar or polar regions (Svalbard, Canadian and Russian Arctic, Coastal Greenland or Antarctic Peninsula). The dynamical behaviour of tidewater glaciers is important with respect to changes in climate, but the interaction between climate and the dynamics of tidewater glaciers is not well understood (Van der Veen, 1997). Rapid retreats related to increased calving rates have been observed for several tidewater glaciers (Meier and Post, 1987), although the climatic conditions were more or less constant. These observations indicate that such rapid front position changes are not an immediate response to changes in climate. Other processes such as calving and basal sliding or factors like water depth and basal topography play an important role for the control of the terminus position.

Iceberg calving is a very efficient mechanism for ice loss and permits a much larger mass loss than surface melting, but the details of the process are not well understood. Based on observations, an empirical relation has been suggested, in which the calving rate is expected to increase linearly with water depth (Brown and others, 1982). This empirical relation results in an accelerated retreat of a tidewater glacier through a basal depression, but it does not describe the physical mechanism of calving. Observations indicated that in the case of a rapidly retreating tidewater glaciers the empirical relation should be questioned (Meier, 1994, Van der Veen, 1996). In addition, observed seasonal variations of the calving rate are not correlated to the water depth at the terminus (Sikonia, 1982).

Basal sliding is known to be an important factor for the control of the dynamics of tidewater glaciers. The generally fast flow of these glaciers is mainly due to high basal sliding because of the high basal water pressure in the terminus region.

Increased calving rates were found to be associated with increased basal sliding in the terminus region, which in turn reduces the retreat. An increase in basal sliding leads to longitudinal stretching, which may lead to enhanced calving and thinning. Observation at rapidly retreating Columbia Glacier showed that the part of the terminus which thins below a critical height above flotation breaks off, probably due to buoyancy forces and the formation of bottom crevasses (Van der Veen, 1996). In this interpretation the increase of the calving or retreat rate is initiated and maintained by thinning and hence, affected by the dynamics of the entire glacier.

The various processes involved in the control of the terminus Position, such as calving, basal sliding, longitudinal stretching and thickness changes are not isolated to the calving front. These processes also lead to strong interactions and feedback mechanisms, which are crucial for the control of the changes of terminus Position.

The first observational part of this study is focussed on Hansbreen, a 16km long slowly flowing tidewater glacier situated in South Spitsbergen. A detailed analysis of a comprehensive data set of front positions of Hansbreen is done and additional velocity measurements have been performed on the glacier. The aims of this case study are:

- to determine the characteristics of the flow of Hansbreen and its spatial and temporal variations and to derive a pattern for basal sliding
- to identify and investigate the most relevant processes and factors that control the flow, front position changes and calving for the case of Hansbreen

The second part of this study intends to approach the dynamics of tidewater glaciers in general by the use of a numerical glacier flow model. The objectives of this modeling part are:

- to develop a time dependent numerical flow model for tidewater glaciers that includes and couples the most important processes controlling the dynamics: glacier flow, calving and basal sliding

With model experiments performed for a tidewater glacier with a basal depression in the terminus region the author intends:

- to demonstrate the Performance of the model
- to examine the qualitative concepts and mechanisms suggested for calving and the control of the front position of tidewater glaciers
- to investigate the reaction of tidewater glaciers and their sensitivity to changes in mass balance or climate
- to apply the model on the case of Hansbreen and compare the results with the observed retreat

# Organkation of the thesis

This thesis consists of four papers. In each paper a detailed introduction to the considered topic is given. Interferometric analysis on the flow field of Hansbreen is additionally presented in Appendix. The references to all papers are summarily presented at the end of the thesis.

## **PAPER 1:**

### **Tidewater glaciers: frontal flow acceleration and basal sliding**

Andreas Vieli, Martin Funk, Heinz Blatter  
*Annals of Glaciology*, **31**, 2000

This paper aims to explain the observed spatial flow pattern of Hansbreen. Basal sliding is recognized to play an important role to control the flow behind the calving front of Hansbreen. A glacier flow model is used, which solves the full equations of stress and in which a water pressure dependent sliding law is implemented.

## **PAPER 2:**

### **Short-term velocity variations on Hansbreen, a tidewater glacier in Spitsbergen**

Temporal variations of the flow of Hansbreen are investigated on time scales of hours to seasons to identify and explain the controlling processes. Continuous velocity measurements recorded in summer 1999 with a temporal resolution of 3 to 4 hours are presented. Possible mechanisms and processes related to the observed temporal variations of the flow are discussed with emphasis on observed short-term Speed-up events.

## **PAPER 3:**

### **Flow dynamics of tidewater glaciers: a numerical modelling approach**

In this paper the dynamics of tidewater glaciers is investigated with a time dependent version of the numerical flow model presented in Paper 1. Calving is implemented by a flotation criterion and is an output quantity of the model. The model is applied for a synthetic but typical tidewater glacier geometry with a basal depression in the terminus region. Model calculations were performed for different mass balance scenarios to investigate the sensitivity of tidewater glaciers on climate changes and to demonstrate how the glacier change is affected by the considered physical processes and feedback mechanisms. We also intend to examine the so far qualitatively described concepts and processes suggested for tidewater glaciers on the base of observations.

## **PAPER 4:**

### **The retreat of a tidewater glacier: observations and model calculations on Hansbreen**

Based on observations and model calculations the retreat over the last two decades of Hansbreen is investigated. Front position variations between 1982 and 1998 are presented and the possible controlling factors and mechanisms for the front position and the calving process are discussed. To give more insight on the cause of an observed abrupt retreat of Hansbreen in 1990, its evolution is simulated with the numerical model for the dynamics of tidewater glaciers presented in Paper 3.

# Paper 1

## Tidewater glaciers: frontal flow acceleration and basal sliding

Andreas Vieli<sup>1+2</sup>, Martin Funk<sup>1</sup>, Heinz Blatter<sup>1</sup>

*<sup>1</sup>Geographisches Institut ETH\*, Winterthurerstr. 190, CH-8057 Zürich, Switzerland*

*<sup>2</sup>VAW, ETH Zentrum, Gloriastr.37/39, CH-8092 Zürich, Switzerland*

### Abstract<sup>†</sup>

A numerical glacier flow model (finite-element method) is used to suggest the processes that control the flow behind the calving front of a tidewater glacier. The model is developed for grounded calving glaciers and includes an effective pressure dependent sliding law. The sliding law is implemented by adding a soft basal layer with a variable viscosity. The model is applied on Hansbreen, a tidewater calving glacier in Svalbard. Comparison between modelled surface velocities and observed velocity data shows a good agreement. We conclude that the flow of a grounded calving glacier can be modelled with an effective pressure dependent sliding law.

---

\*now Institute of Climate Research ETH

†Annals of Glaciology, 31, 2000

## 1.1 Introduction

The flow dynamics of tidewater calving glaciers is of great interest, but poorly understood (Van der Veen, 1996; Meier, 1994). Increasing surface flow velocities towards the calving front were observed on several grounded calving glaciers, such as Hansbreen, Spitsbergen; Columbia Glacier, Alaska (Krimmel and Vaughan, 1987); Moreno Glacier, Patagonia (Rott and others, 1998) and Nordbo Glacier, Greenland (Funk, 1990). Understanding the processes controlling the flow field behind a calving front is essential for developing a physically based model for calving. It is known that basal sliding strongly affects the flow of grounded calving glaciers (Meier and others, 1994; Kamb and others, 1994; Van der Veen, 1996). Effective pressure (ice overburden minus water pressure) is suggested as one important controlling factor of basal sliding (Iken, 1977; Budd and others, 1979; Bindshadler, 1983).

This study concentrates on Hansbreen, a grounded calving glacier in Svalbard, for which an extensive data set exists. A numerical glacier flow model, including basal sliding, is used to suggest the important processes that control the flow behind the calving front.

## 1.2 Data base and field observations

Hansbreen is a tidewater calving glacier situated at Hornsund in southern Spitsbergen. The glacier covers an area of 57 km<sup>2</sup> and is about 16 km long (Fig. 1.1). It ends in the sea with a 1.3 km wide calving front. The front height above water level varies between 30m and 40m. The glacier bed along the frontal 10 km is below sea level. Since the establishment of the Polish Polar Station in the vicinity of Hansbreen in 1957, several glaciological investigations were carried out, and an extensive data set of Hansbreen is available (Jania and Kaczmarek, 1997). It includes glacier surface topography from photogrammetry, bed topography from radio-echosoundings (Glazovsky and others, 1991) and depth soundings of the fjord in front of the glacier (Gizejewski, 1997). Furthermore, annually measured frontal positions and surface velocity data determined by terrestrial photogrammetry are available since 1982 (Jania and Kolondra, 1982; Jania, 1988).

In summer 1998 additional surface velocity measurements were made on Hansbreen by terrestrial survey of 7 stakes along a flowline with a temporal resolution of 1 to 2 days. The velocity data show a high variability in time and space (Fig. 1.2). Spatially, surface velocity increases significantly towards the calving front, starting 4km behind the ice cliff (Fig. 1.5 shown later). Temporally, periods of substantially higher surface velocity were observed to last for 2 to 3 days (Fig. 1.2). These “fast-flow” events occurred during periods with significantly higher surface melt rates. Daily mean temperature recorded at Hornsund meteorological station of the Institute of Geophysics of Polish Academy of Science and water runoff data from the neighbouring land-based Werenskjeldbreen (personal communication from M. Pulina, Oct.1998) correlate well with the observed velocity variations (Fig. 1.2). At the lateral part of the frontal ice cliff, an outflow channel at sea level was observed. During periods with high surface melt rates, the outflowing water was under

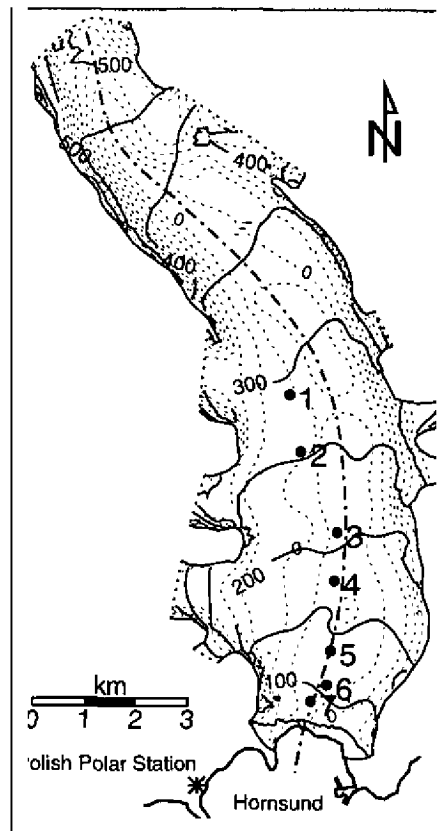


Figure 1.1: Map of Hansbreen showing surface (solid contour lines) and bed (dashed contour lines) topography. The contour intervals are 50m. The location of the stakes, used for velocity measurements by terrestrial Survey, are shown with the corresponding stake numbers (1 to 7) used in the text. The dashed-dotted line indicates the flowline used for the model calculations.

high pressure (fountains of water were observed, accompanied by loud noise). The measured fast-flow velocities are mean values taken over a three-day period. True maximum values are probably higher. The last ten days of the Observation period show relatively constant low velocities. This “slow-flow” period may correspond to a winter flow regime.

Based on extensive studies on valley glaciers, several authors have pointed out that short term velocity variations are related to changes of basal water pressure (Iken, 1977; Iken and Truffer, 1997; Meier and others, 1994). The observations on Hansbreen suggest that basal sliding predominantly determines the flow field and is affected by variations of surface melt water production.



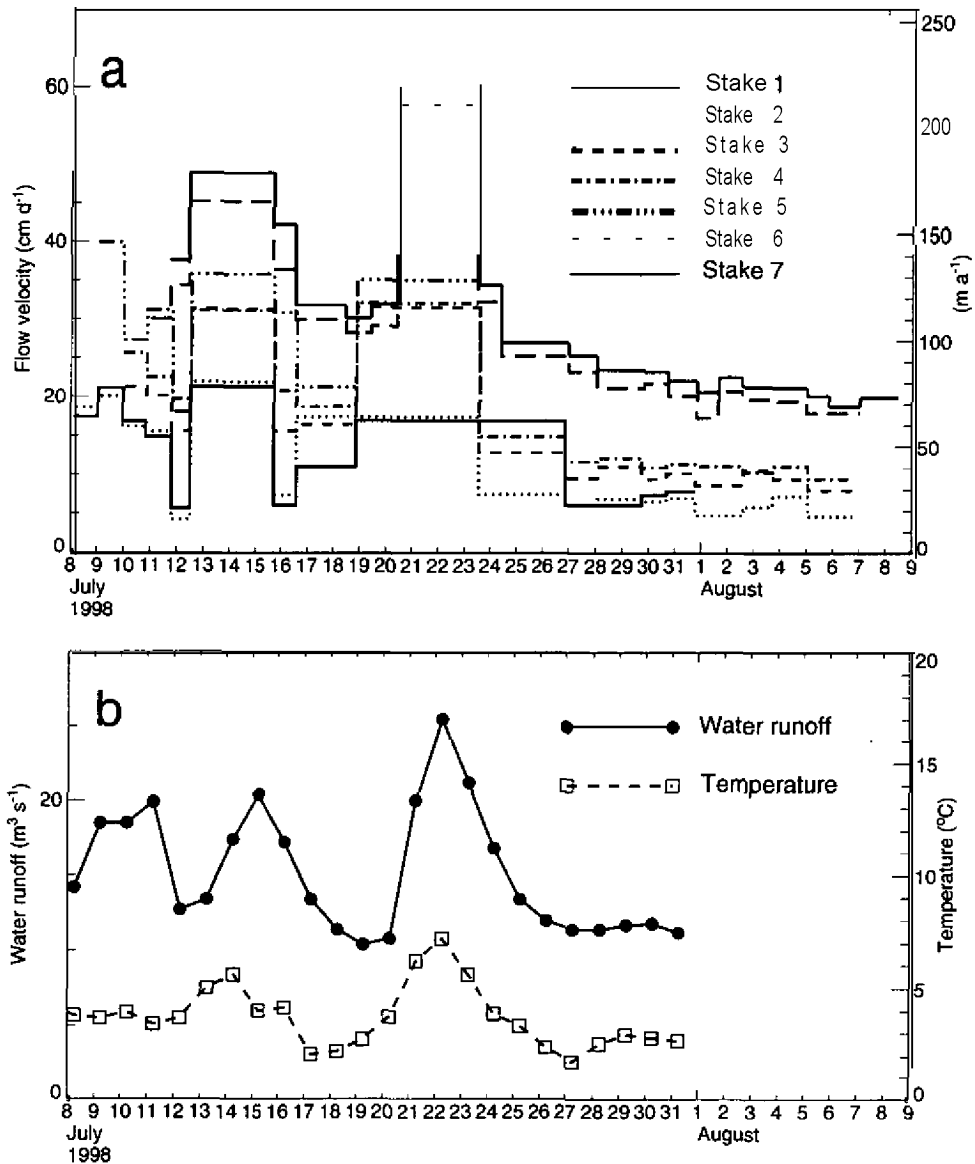


Figure 1.2: (a) Variation of flow velocities with time at the stakes 1 to 7 measured by terrestrial Survey. (b) Variation with time of mean daily temperature at Hornsund meteorological Station and daily water runoff at neighbouring Werenskjøldbreen.

### 1.3 Model description

A flow model based on the finite-element method (MARC, 1997) is used. The code solves the full equations for the stress and velocity fields. A two-dimensional version

of the model is used to calculate stress and velocity fields along the flowline shown in Fig. 1.1.

Glen's flow law,

$$\dot{\epsilon}_{ij} = A\tau^{n-1}\tau_{ij}^n \quad (1.1)$$

with common values for the flow law exponent  $n = 3$ , and the rate factor  $A = 0.1 \text{ bar}^{-3}\text{a}^{-1}$  has been used in the model (Paterson, 1994).  $\dot{\epsilon}_{ij}$  are the components of the strain rate tensor,  $\tau_{ij}$  are the components of the deviatoric stress tensor and  $\tau$  is the effective stress ( $2^{\text{nd}}$  invariant of deviatoric stress tensor).

### 1.3.1 Basal sliding

The glacier flow model requires an appropriate boundary condition at the glacier bed to account for basal sliding. We assume a relation between sliding velocity  $v_b$  and basal shear traction  $\tau_b$  of the form:

$$v_b = c(x) \cdot \tau_b^{n'}, \quad (1.2)$$

where  $c(x)$  is the sliding coefficient and  $n'$  a Parameter to be specified (Lliboutry, 1968 and 1979).

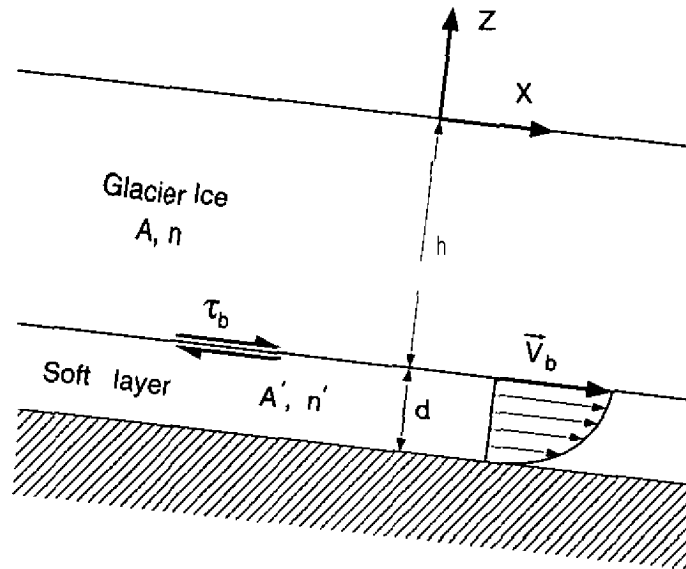


Figure 1.3: Schematic view of the glacier with a soft basal layer for implementing a sliding law that relates the basal velocity  $\vec{v}_b$  to basal shear traction  $\tau_b$ .

This relation for basal sliding is implemented in the model by adding a thin soft layer at the glacier base (Leysinger, 1998; personal communication from H. Gudmundsson, 1998) with a flow law corresponding to equation (1.1) and with flow Parameters  $n'$  and  $A'$  (Fig. 1.3). The approach of a different rheology for a subglacial layer has been used previously by MacAyeal (1989) and Alley and others (1987b) to model ice streams in Antarctica. In both cases the subglacial layer was assumed to be a till layer and a linear viscous rheology was used. Here the soft layer with a variable viscosity is used as a method to implement the suggested sliding law (1.2) for a given sliding coefficient  $c(x)$ . The glacier bed corresponds to the interface between glacier ice and the introduced soft layer (Fig. 1.3). Although the physics of the sliding in consideration may not coincide with the soft slab approach, the described method is mathematically correct. For a prescribed basal boundary condition such as the given sliding law (1.2), the Solution for the stress and velocity field is unique (Colinge, 1998).

For an ice slab of thickness  $h$ , with an underlying thin soft layer of thickness  $d$  and slope angle  $\alpha$ , the analytical Solution of the basal velocity  $v_b$  (Fig. 1.3) in the shallow ice approximation (Hutter, 1983) is:

$$\begin{aligned} v_b &= \int_{-(h+d)}^{-h} 2A' \cdot (\rho g \sin(\alpha) z)^{n'} dz \\ &= 2A'(\rho g \sin(\alpha))^{n'} \left[ h^{n'} d + \frac{n'}{2} h^{n'-1} d^2 + O(d^3) \right] \end{aligned} \quad (1.3)$$

With  $d \ll h$  terms of order  $O(d^2)$  can be neglected and we get

$$v_b \approx 2dA'\tau_b^{n'} \equiv c(x) \tau_b^{n'}, \quad (1.4)$$

which corresponds to the assumed sliding law (1.2). For the flow model we assume a linear sliding law by setting  $n' = 1$ . Layer thickness  $d$  is constant and  $A'(z)$  is given with the sliding coefficient  $c(x)$  and is a function of the distance  $x$  along the flowline.

The formulation (1.4) is correct for the shallow ice approximation which neglects longitudinal stress gradients and approximates the basal shear traction with the local driving stress. This may be a poor assumption, especially near the calving front of a tidewater glacier. By using equation (1.4) in our model we can estimate the errors due to the said simplification. For a given sliding coefficient  $c^{in}(x) = 2dA'(x)$  we obtain from model calculations the basal shear traction  $\tau_b^{model}$  and basal velocity  $v_b^{model}$  at the upper boundary of the basal layer. Introducing these values into equation (1.2) we obtain the sliding coefficient  $c^{model}(x) = v_b^{model} / \tau_b^{model}$  which should be identical with  $c^{in}(x)$ . While for the shallow ice approximation  $c^{in}(x)$  is equal to  $c^{model}(x)$ , for a real glacier Situation these coefficients are different. For a model run of Hansbreen a comparison between  $c^{in}$  and  $c^{model}$  is shown in Fig. 1.4. The differences are very small in the upper part of the glacier (less than 2%) and exceed 10% only in the frontmost 300 m.

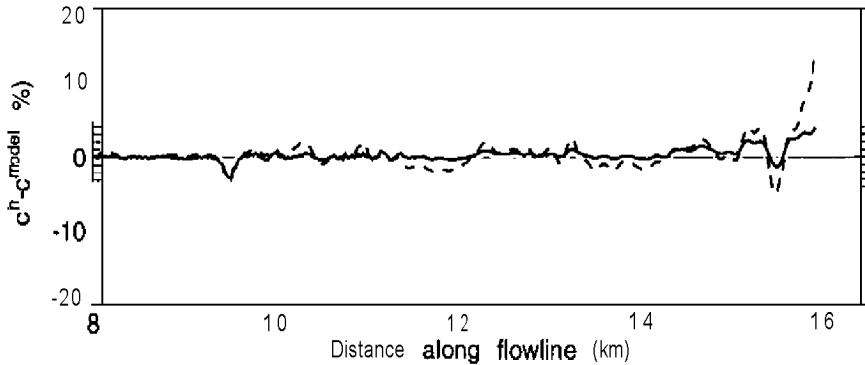


Figure 1.4: **Difference between input** sliding coefficient  $c(x)^{in}$  and calculated sliding coefficient from model results  $c(x)^{model}$  expressed as a **percentage** of  $c(x)^{in}$  for slow-flow (solid line) and fast-flow (dashed line) scenarios.

### 1.3.2 Basal water pressure and sliding

Basal sliding is strongly affected by changes in water pressure  $p_w$  (Iken, 1981; Kamb and others, 1994; Meier and others, 1994; Jansson, 1995). For experiments of sliding over hard bed, Budd and others (1979) proposed a sliding law of the form

$$v_b \propto \tau_b^m p_e^d, \quad (1.5)$$

where  $p_e$  is the effective pressure (ice overburden minus water pressure). Bind-schadler (1983) successfully applied a similar form to measured data on glaciers, and Fowler (1987) has derived a similar relationship on theoretical grounds. The exponent  $m$  is often replaced by Glen's flow law exponent  $n$  and  $d$  is an empirical positive number.

For sliding over a soft glacier bed, Boulton and Hindmarsh (1987) proposed a viscous behaviour for sediment deformation of the form

$$\dot{\epsilon} \propto \tau^a p_e^{-b}, \quad (1.6)$$

where  $\dot{\epsilon}$  is the strain rate. On the basis of observations, they determined the exponents to be  $a = 1.33$  and  $b = 1.8$ . Equation (1.6) results in a sliding law analogous to equation (1.5). Recent studies suggest that subglacial till behaves like a Coulomb-plastic material (Iverson and others, 1998). Deformation takes place in discrete shear zones whose positions fluctuate with changing basal water pressure. The mean deformation over time results in a very similar equation, as proposed in (1.6).

For the present flow model, we assume a simple sliding law taking into account the effective pressure  $p_e$  and which is based on current sliding theories. For our model, the sliding coefficient  $c(x)$  of equation (1.2) is assumed to be:

$$c(x) = q \frac{1}{p_e(x)^m}, \quad (1.7)$$

with the effective pressure  $p_e(x) = p_i(x) - p_w(x)$ , where  $p_i(x)$  is the ice overburden pressure and  $p_w(x)$  the water pressure at the glacier bed. The Parameter  $m$  is set to unity and  $q$  is tuned to fit modelled to observed velocities.

## 1.4 Model results and comparison with observations

For the surface geometry of the year 1998 the model was run with various sliding scenarios. The results are shown in Figure 1.5 and discussed in this section.

### 1.4.1 Constant sliding coefficient

First, we set  $c(x) = 0$ , which corresponds to ice flow without sliding. The calculated surface velocities from internal deformation of the ice are much smaller than the observed values (Fig. 1.5). According to the observations, the surface velocities start to increase 4km behind the calving front. From the difference between modelled velocities with  $c(x) = 0$  and measurements, we estimate the amount of basal sliding to be about 3 times the deformation velocity in the upper part and to increase up to 20 times immediate behind the front. With a constant sliding coefficient,  $c(x) > 0$  the surface velocity can be increased by nearly a constant value (Fig. 1.5), but the modelled velocity increase is limited to the frontmost 300m. It follows that the observed surface velocity distribution cannot be explained with a constant sliding coefficient.

### 1.4.2 Spatially dependent sliding coefficient

To provide a spatially dependent  $c(x)$  we introduce the effective pressure as suggested in equation (1.7) in the sliding law (1.2). Since the basal water pressure during the velocity measurements is not known, test-scenarios need to be assumed. The basal water pressure behind a calving front must be at least equal to the pressure of the vertical water column at the calving face. During the melt season, the basal water pressure increases above this minimal pressure to force water to flow toward the front. Because our observations identified periods of fast-flow and slow-flow (Fig. 1.2), we select two different flow periods for the model calculations.

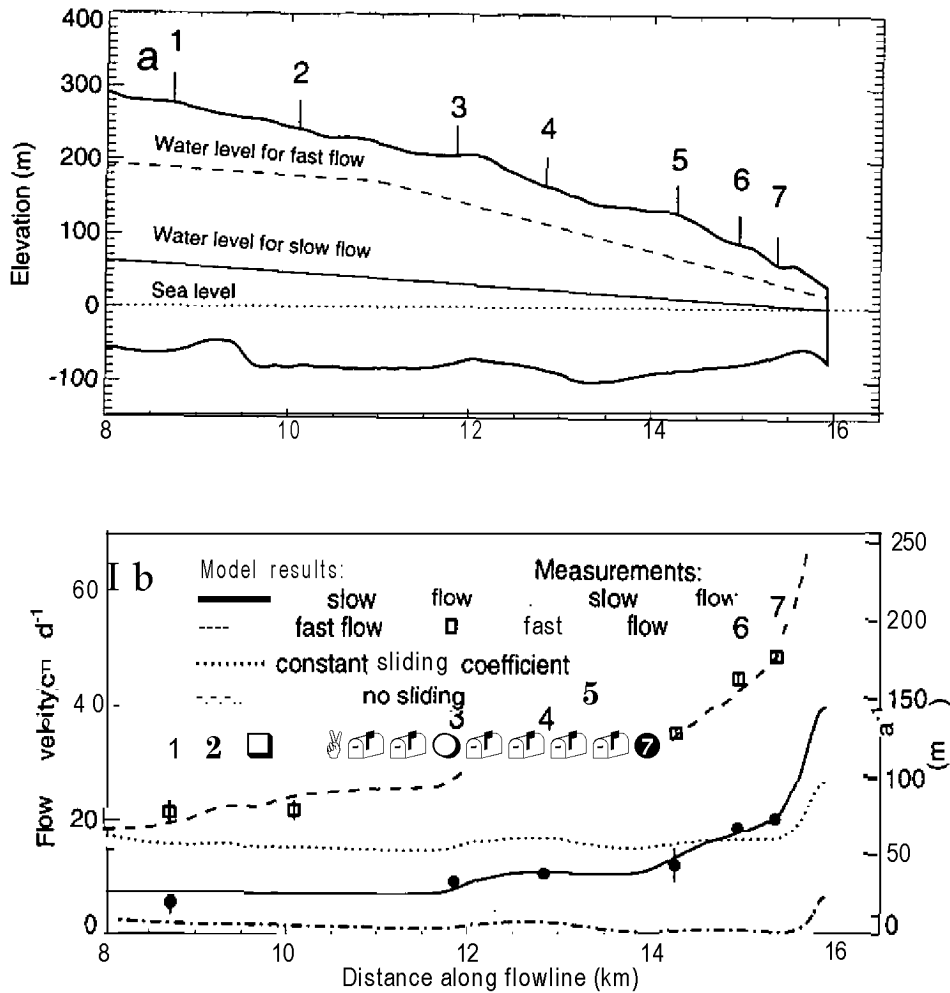


Figure 1.5: (a) Profile along the flowline of Hansbreen with glacier bed and surface topography. The lines within the glacier show the assumed water level scenarios. (b) Measured (Symbols) and modelled (lines) surface flow velocities for the slow and fast flow periods of summer 1998.

### Slow-flow period

The observed velocities for this period correspond to the mean measured velocities of the period from July 31, to August 8, 1998. The sliding Parameter  $q$  and the water level gradient are adjusted to fit the velocity measurements with the method of least-squares matching (Fig. 1.6). The resulting water level gradient is 0.45'' and is shown in Figure 1.5. This seems to be a reasonable value, however Figure 1.6 shows that the model is not sensitive to small changes in the water level gradient. The model results are shown in Figure 1.5 and are in good agreement with the observed velocities. Note that the velocity increase, starting 4 km behind the front, is well reproduced by the model.

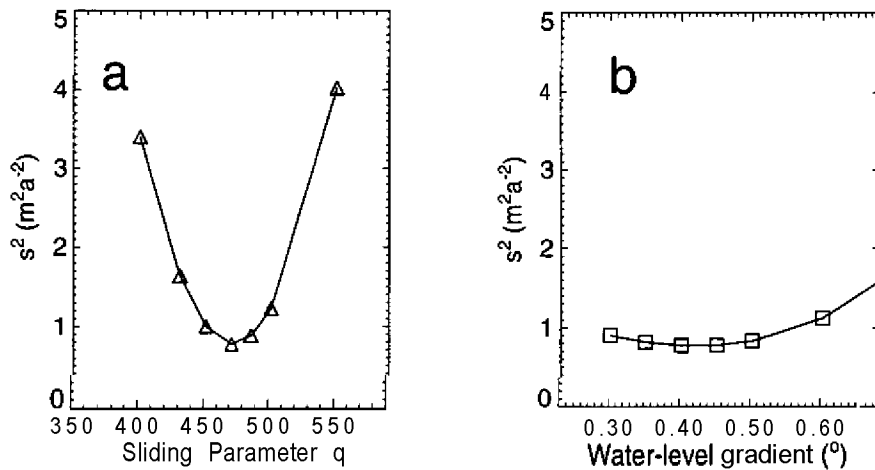


Figure 1.6: Sensitivity of the model on Parameter adjustment done by least-squares matching of modelled and measured velocities for the slow-flow scenario. The vertical axis shows the mean square error  $s^2$  of the modelled and measured velocities. In (a) the mean square error is shown as a function of the sliding Parameter  $q$  and a constant water level gradient (0.45°). In (b) the mean square error is shown as a function of the water level gradient and a constant sliding Parameter ( $q = 470$ ).

### Fast-flow period

The fast-flow velocities correspond to the mean measured velocities of the period from July 12, to July 15, 1998. The sliding Parameter  $q$  is the same as for the slow-flow scenario. By increasing the water level at the front by 17 m and the water level gradient to 1.79° we get the best fit to observations (least-squares matching).

This higher water level takes into account the observed increased meltwater production and observed water outflow under high pressure at the lateral part of the calving front. In the upper 11 km we assume a reduced water level gradient of 0.5°, to take into account the smaller surface slope in the upper part of the glacier. The modelled velocities are in good agreement with the measurements, especially the frontal increase in flow velocity is well reproduced (Fig. 1.5). The rather good agreement for stakes 1 and 2 suggest that the assumed reduced water level gradient for the upper 11 km is reasonable, at least for the region where stakes 1 and 2 are located. Using the same sliding Parameter as adjusted for the slow-flow scenario, the model is able to simulate the fast-flow Situation if we increase the water level accordingly.

### 1.4.3 Highly crevassed zone

The frontmost 500m of Hansbreen are highly crevassed. The formation of these crevasses is related to the stress field, which is also calculated in the used flow

model. The modelled effective stress  $\tau_{\text{eff}}$  at the surface is particularly large over a distance of 500m immediately behind the calving front (Fig. 1.7). It exceeds 1 bar in all modelled scenarios. If we consider a “Von Mises Criterium” for the formation of crevasses corresponding to an effective stress above 1 bar (Vaughan, 1993 ), the observed extent and location of the crevasse zone are in good agreement with the calculated high values of the effective stress.

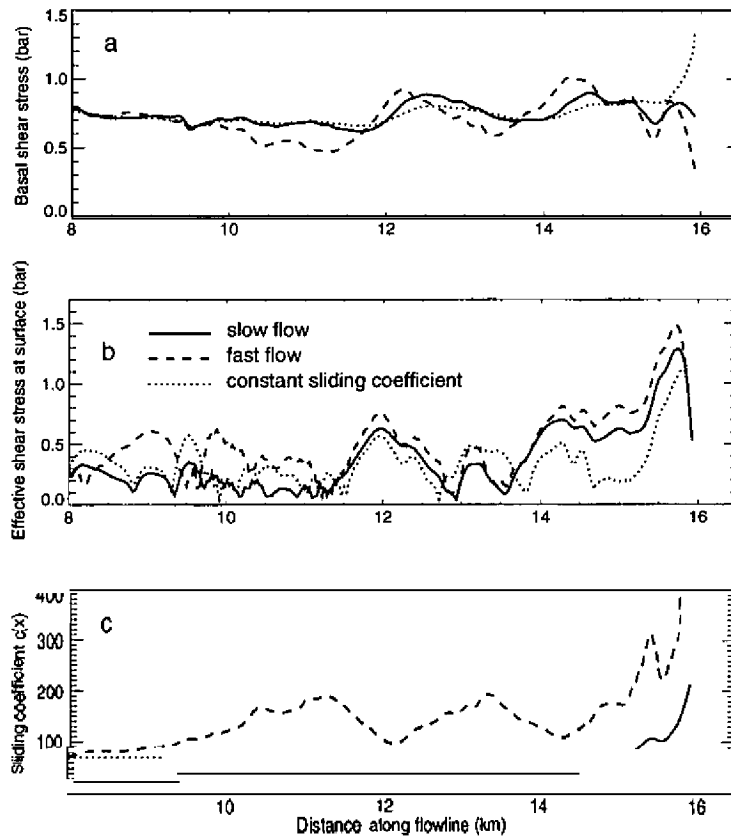


Figure 1.7: (a) Basal shear traction along the flowline from model calculations. (b) Effective shear stress at the surface along the flowline from the model calculations. (c) Sliding coefficient of the model along the flowline.

## 1.5 Conclusion

Surface velocity measurements suggest that basal sliding processes play an important role in the dynamics and calving of tidewater glaciers, and need to be considered in the ice flow modelling. It is shown that a sliding law dependent on basal shear stress can be successfully implemented in the finite-element glacier flow model by adding a thin soft layer with variable viscosity at the base of the model. Results from model calculations with constant or zero sliding coefficient only show a frontal velocity



increase over a distance of 300m (2 to 5 times the frontal ice thickness) instead of the observed 4 km. By using a sliding law which relates the sliding coefficient, and thus the basal velocity, to effective basal pressure, the model results reasonably reproduce the observed velocity increase behind the calving front. We conclude that basal sliding processes which strongly depend on the effective pressure, dominantly control the flow of a grounded calving glacier such as Hansbreen.

## **1.6 Acknowledgement**

The authors thank J. Jania of the Geomorphological Institut of University of Silesia, Poland. He made this field investigation on Hansbreen possible and helped a lot in the field. The Geophysical Institut of Polish Academy of Science provided the infrastrucur on the Polish Polar Station in Hornsund, Svalbard during the field investigation. The work was supported by the Eidgenössische Technische Hochschule, Zürich, Switzerland, grant no. 0-20-400-97. B. Bindshadler and E. G. Josberger reviewed an earlier version and helped to improve the manuscript substantially.

# Paper 2

## Short-term velocity variations on Hansbreen, a tidewater glacier in Spitsbergen

### Abstract

In this study spatial and temporal variations of the flow of Hansbreen, a tidewater glacier in South Spitsbergen, are investigated. During summer 1999, variations of the surface flow velocities were measured in the ablation zone of Hansbreen with a temporal resolution of 3 to 4 hours. During the melting season, short events with strongly increased surface velocities and a typical duration of 1 to 2 days were observed. These speed-up events are related to periods of strongly increased water input to the glacier, due to rainfall or enhanced surface melt during föhn weather conditions. A close correlation between the surface velocities and water pressure recorded in a moulin is found and suggests that the observed speed-up is caused by changes in basal water pressure. The strong increase of basal sliding is suggested to be due to the opening of basal cavities or decoupling at the glacier bed resulting from the high basal water pressure. This explanation is supported by the locally observed uplift and slight change in the flow direction during a speed-up event. The location of the velocity peak is found to propagate downglacier and leads to short peaks of the longitudinal strain, which may cause additional fracture in the terminus region and therefore affect the process of calving. The observed short-term velocity variations and associated processes on Hansbreen are very similar to those observed on landbased valley glaciers. This suggests that the relevant mechanisms and physical processes that control the flow and its temporal variations are the same. In addition, relatively high sliding velocities and a velocity increase towards the calving front, independent on temporal changes, were observed on Hansbreen, which seems to be typical for tidewater glaciers.

## 2.1 Introduction

The purpose of this study is to present observations of temporal variations of surface flow of Hansbreen, a small tidewater glacier in Spitsbergen and to identify the controlling processes and mechanisms on time scales of hours to seasons. Emphasis is directed towards observed short-term speed-up events and the processes related to them.

The flow of glaciers undergoes temporal variations on time scales of daily cycles to seasons, which are mainly due to changes in the basal boundary condition (Willis, 1995). Geometry and the driving stress do not significantly change over such time scales. On a seasonal time scale, a velocity increase is often observed at the beginning of the melting season, when high basal water pressure occurs, which leads to enhanced basal sliding. An increased basal water pressure is a consequence of enhanced water input and an insufficiently developed basal drainage system. During winter the water input is generally small or zero and the subglacial drainage system is poorly developed. When surface melting starts in spring, the drainage system is not adjusted to the enhanced water input and the water pressure increases and leads to enhanced basal sliding. With progressive adaption of the drainage system to enhanced water input, the water pressure will drop, leading to a decrease in basal sliding.

Velocity measurements with high temporal resolutions (hours to days) showed distinct short-term velocity increases throughout melting seasons on several glaciers, such as Findelengletscher (Iken and Bindschadler, 1986), Unteraargletscher (Iken and others, 1983), Variegated Glacier (Kamb and Engelhardt, 1987), Storglaciären (Jansson and Hooke, 1989; Hanson and Hooke, 1994) and Black Rapids Glacier (Truffer, 1999). Repeated short events with a two to fivefold increase of the surface velocities and a typical duration of 1 to 2 days were observed. Such velocity anomalies are often termed ‘mini-surge’ or ‘spring Speed-up events’ because they often occur at the beginning of the melting season. Such ‘Speed-up events’ are often associated with a vertical uplift in the order of a few decimeters (Iken and others, 1983; Kamb and Engelhardt, 1987; Truffer, 1999).

On Variegated Glacier high basal water pressure was found to be the cause of the observed surface Speed-ups (Kamb and Engelhardt, 1987). In this case the velocity peak propagated down glacier at a speed of about  $300 \text{ m h}^{-1}$  and was related to a down propagating pressure wave. Very similar on Findelengletscher, a high pressure wave propagating down glacier at a speed of about  $100 \text{ m h}^{-1}$  was related to an event of accelerated surface motion (Iken and Bindschadler, 1986). Due to the temporal shift of the velocity peak, such an event is accompanied by a Variation of longitudinal surface strain as observed for Variegated Glacier (Raymond and Malone, 1986) and Storglaciären (Jansson and Hooke, 1989). The short-term velocity variations observed on Storglaciären were found to correlate with subglacial water pressure variations, which were related to enhanced water input to the glacier (Hanson and others, 1998; Hanson and Hooke, 1994).

The current knowledge of the temporal variations of the flow on time scales of seasons to hours and the related mechanisms are derived from studies and observations

on alpine valley glaciers with generally small sliding velocities. The flow of tidewater glaciers, which are defined as grounded calving glaciers ending in the sea, is dominantly controlled by basal sliding (Van der Veen, 1996). The generally high basal sliding velocities (Meier and Post, 1987) and the typically increased flow velocities towards the calving front are mainly due to the persistent high water pressure in the terminus region (Vieh and others, 2000). This difference in the general water pressure and flow pattern between tidewater and valley glaciers indicates that the temporal variations of glacier flow and the relevance of the controlling mechanisms are not necessarily the same.

In the 1960s, Voigt (1979) observed enhanced surface velocities at the beginning of the melting period on tidewater glacier Kongsvegen and Kongsbreen (Spitsbergen) and detected short events of velocity increase similar to speed-up events. For the large and rapidly flowing tidewater Columbia Glacier both clear diurnal cycles of the flow and speed-up events similar to those observed on valley glaciers were observed (Meier and others, 1994). These events were related to enhanced water input due to rainfall or intensive melting. Although the observations show that rapid sliding is caused by high basal water pressure, they do not support a direct relation between basal sliding and water pressure. Instead, a relation between basal sliding and water storage at the bed was recognized (Kamb and others, 1994). In addition for Columbia Glacier a clear seasonal variation of the flow was observed with a maximum in late fall at the terminus, which occurred delayed further upglacier (Meier and others, 1985). The period of maximum speed also corresponds to the period of highest englacial water storage estimated from meteorological observations (Tangborn, 1997). The velocity during speed-up events is only 30% higher than the average flow, whereas for the landbased glaciers mentioned above a two to fivefold velocity increase was observed. The sliding velocities of Columbia Glacier are very high throughout the entire year (3 to 9 m d<sup>-1</sup>) and therefore strongly affect the basal drainage system. Up to now no comprehensive study on the flow of slower, smaller tidewater glaciers, such as Hansbreen, has been performed.

### 2.1.1 Hansbreen

Hansbreen is a tidewater glacier situated in southern Spitsbergen, which calves into Hornsund (Fig. 2.1). The glacier is about 16 km long, flows from a glacierized saddle at an altitude of 500 m a. s. l. down to the sea and the average surface slope is 1.8 degrees. The lowest 12 km of the glacier bed are below sea level, with a maximum basal depression depth of -100 m and a maximum ice thickness of about 350 m.

The flow regime of the frontal region of Hansbreen was first investigated by Jania and Kolondra (1982) using terrestrial photogrammetry. Increased velocities towards the glacier terminus were detected. Velocity variations on seasonal and shorter time scales were observed (Jania, 1988), however the measurement intervals were generally longer than 5 days. In addition to the velocity measurements, glacier quakes were recorded (Jania and others 1985; Gorski, 1997).

In summer 1998, surface velocity measurements were performed by terrestrial survey of 7 stakes with a temporal resolution of one day (Vielí and others, 2000; Fig. 2.1).

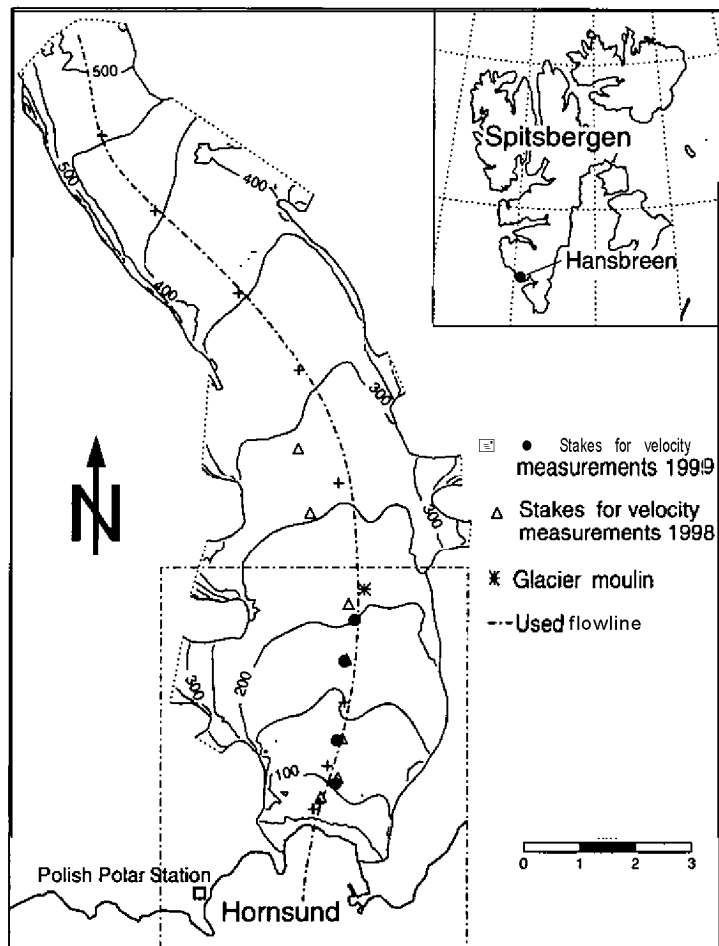


Figure 2.1: Map of Hansbreen showing surface topography. The **contour intervals** are **50** m. The location of **stakes** used for velocity measurements are indicated.

Strong variations of the surface flow velocity were observed in time and space. Short periods of substantially higher surface flow velocities were detected and occurred during periods of significantly increased melt rates related to föhn. The duration of these speed-up events was 1 to 3 days. In the frontal 4 km, a significant increase of flow velocities along the flowline towards the calving front was observed. Vieli and others (2000) showed that the decreasing effective pressure towards the front is responsible for the increase in basal sliding. Using a numerical glacier flow model including an effective pressure dependent sliding law, a good agreement between measured and modelled velocity was obtained, in particular for the frontal acceleration pattern.

In summer 1999 a field investigation was performed looking at the temporal and spatial variations of the flow velocities of Hansbreen with high temporal resolution. The measurement period lasted from June 21 to July 26, 1999 and the results obtained are presented in this paper.

## 2.2 Observational program

Four GPS stations were set up along a flowline on Hansbreen, labelled as *A*, *B*, *C*, *D*. The lowest Station was located 800m behind the calving front and the highest one 3.6 km away from it (Fig. 2.2). The GPS stations were mounted on aluminium poles drilled 5 m into the ice (Fig. 2.3) and the electric power supply was provided from a solar panel. A fifth GPS receiver was installed outside the glacier close to the Polish Polar Station and was used as reference Station. Three (*A*, *B*, *D*) of the four permanent stations were in Operation continuously from June 21 to July 26. For a short period, GPS Station *C* was moved to a fixpoint outside the glacier (Fig. 2.2). Position measurements were repeated at intervals of three to four hours, depending on satellite availability. The mission duration was about 20min. Both the L1 and L2 phase Signals were recorded. Data processing was performed with the Leica SKI Software (Version 2.2).

The a priori error of a GPS measurement is specified as  $\pm 3\text{ mm} \pm 2\text{ ppm}$  for the horizontal position and about twice as much in the vertical direction. From a detailed analysis using data from the additional fixpoint outside the glacier, the a posteriori error is determined as shown in Table 2.1 (Vieser, 2000). For the horizontal position the a posteriori error  $\sigma_{hor}$  is specified with  $\pm 3\text{ mm}$  fl ppm and is slightly better than the a priori value. The vertical a posteriori error  $\sigma_{ver}$  is specified with 3.2 times the horizontal value, which is significantly worse than the a priori value. This is due to the fact that no satellites are passing near zenith at such high latitudes ( $77^\circ\text{ N}$ ).

Table 2.1: Horizontal and vertical a posteriori error of the GPS-Position measurement at the different stations.

Station name	Baseline length	Difference in Elevation to Reference Station	$\sigma_{hor}$	$\sigma_{ver}$
Fixpoint	1.8 km	26m	4 mm	13mm
A	3.0 km	69m	5 mm	17mm
B	3.5 km	113m	5 mm	17mm
C	4.8 km	148 m	7 mm	23 mm
D	5.5 km	183 m	9 mm	29 mm

In addition nine poles were set up along the flowline at regular distances between the calving front and the glacier top (Fig. 2.1) and six additional poles in a transverse profile located 800 m upglacier from the calving front (Fig. 2.2). For both profiles the GPS position measurements were repeated up to four times during the investigation period at intervals of a few days to weeks.

Water pressure was measured with a vibrating wire pressure sensor in an active moulin, situated 500m upglacier from to the highest GPS receiver *D* (Fig. 2.2). Pressure measurements were carried out every 30sec and the averaged values over

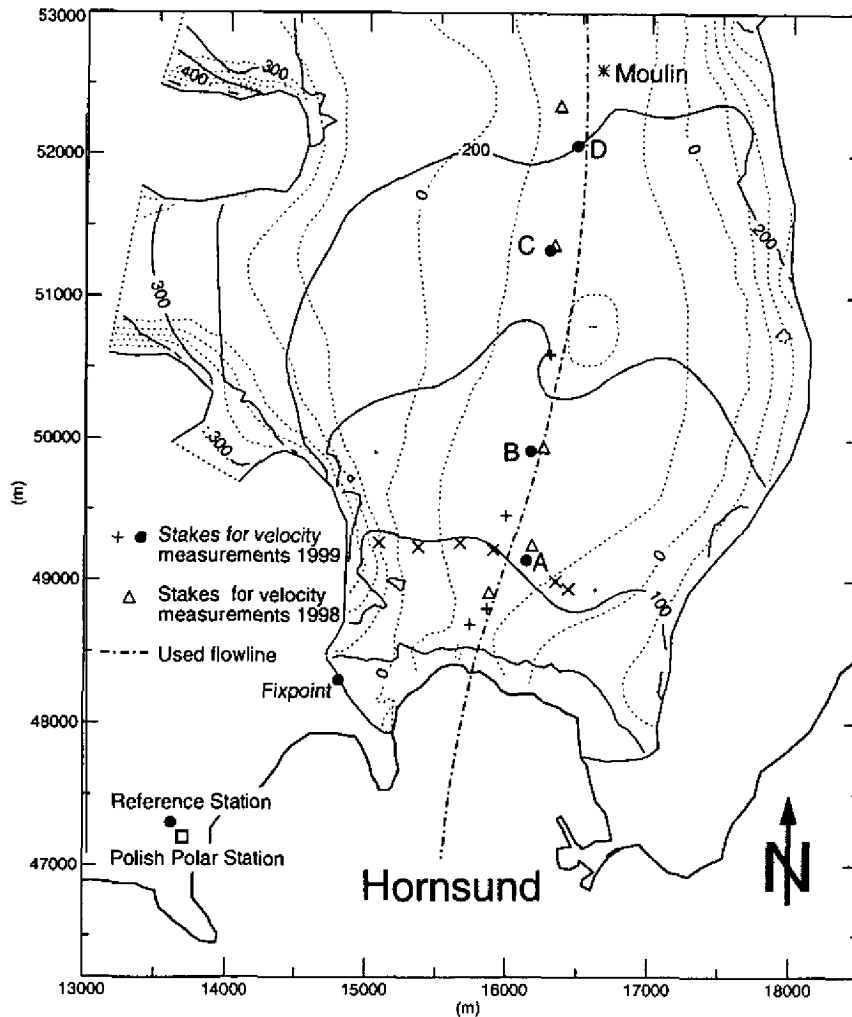


Figure 2.2: Map of the frontal region of Hansbreen showing the location of the stakes used for the velocity measurements. The permanent GPS stations are indicated with the solid black dots. The solid and the dashed contours indicate the glacier surface and bed topography, respectively. The contour intervals are 50 m. The cross symbols mark the positions of the additional poles for the transverse (x) and longitudinal (+) velocity profile.

15 min were stored. The pressure data was converted in meters of water level above sea level. The absolute depth of the sensor was estimated at  $173 \text{ m} \pm 7 \text{ m}$  below the glacier surface corresponding to  $25 \text{ m} \pm 7 \text{ m}$  above sea level. The glacier bed at this location is  $81 \text{ m}$  below sea level. The sensor was installed on July 12, one day after the moulin became free from the winter snow pack.

Meteorological data were recorded at the meteorological station of the Institute of Geophysics of the Polish Academy of Science, situated at the Polish Polar Station,  $15 \text{ m}$  above sea level about  $2 \text{ km}$  away from the glacier terminus. Ablation was measured several times during the investigation period on the same poles used for the GPS measurements. Runoff from the neighbouring landbased Werenskioldbreen was estimated by measuring the water level of its outflow river at half day intervals (personal communication from J. Jania, University of Silesia, August 1999).

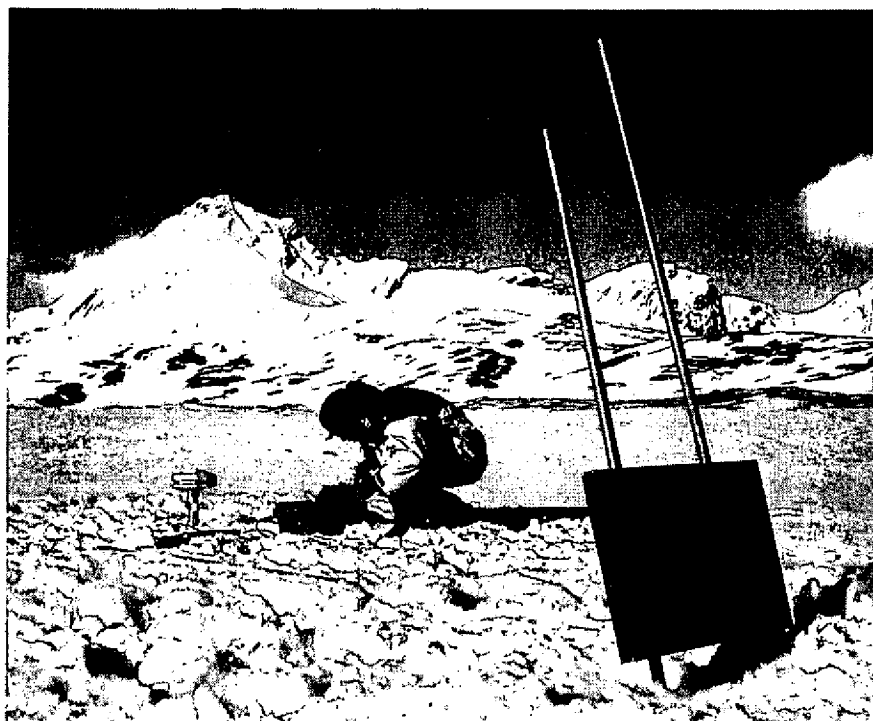


Figure 2.3: Uppermost, permanent GPS-Station *D* installed on Hansbreen with the controller box and the solar panel to provide electric power.

## 2.3 Observation results

### 2.3.1 Climatic conditions

Surface melting started before the beginning of the measurement period. At that time the glacier was still covered with snow, which was wet in the lower part. After July 12, the lower part of the glacier surface, where ablation was measured, became snow free. The temperature measured at the meteorological station was above the freezing point during the entire investigation period (Fig. 2.4d). From June 22 to June 29 several rainfall events occurred. In the accumulation area, precipitation fell as snow several times, indicating temperatures below zero degrees there. A 4 day föhn period started on July 15 and was characterized by strong easterly winds, clear sky and increased mean daily air temperatures at the meteorological station by about 5° (Fig. 2.4d). This föhn period was briefly interrupted in the night from July 17 to 18. During the föhn period surface ablation was enhanced by a factor of 2 to 3 at the stake locations in the lower part of the glacier (Table. 2.2). Melt water streams formed at the surface and the color of the glacier surface in the terminus region changed from white to blue within a few hours.

### 2.3.2 Variations in water pressure

The water level measured in the glacier moulin located 500m upglacier of station *D* is shown in Fig. 2.4c. In the period of Observation from July 12-26 the water



Table 2.2: Amount of ice melted ( $\text{cm d}^{-1}$ ) for three different time periods. Period 1 (21.6.-15.7.) is before the föhn period, Period 2 (15.7.-18.7.) during the föhn period and Period 3 (21.7.-23.7.) after it. The error of the ablation measurements is  $\pm 1 \text{ cm d}^{-1}$ .

Station name	Ablation of ice ( $\text{cm d}^{-1}$ )		
	Period 1	Period 2	Period 3
A	2.7	9.8	4.3
B	3.5	6.7	3.0
C	2.3	7.2	-
D	-	9.3	3.5

pressure underwent strong temporal variations. First the water level was 80 m below the surface. At the beginning of the föhn period on July 15, it started to increase strongly and reached the maximum value of 29 m below the surface, corresponding to the flotation level at this location. This water level peak was followed by a drop of about 120 m to a level of 155 m below the surface. Daily fluctuations with an amplitude of roughly 5 m were superimposed on the described longterm water level changes.

### 2.3.3 Velocities and vertical displacement

Temporal variations

The measured vertical displacement and the horizontal velocities of the four permanent GPS stations are shown in Fig. 2.4a and 2.4b. The horizontal velocities shown in Fig. 2.4b and 2.5b are derived from a smooth cubic spline interpolation of the horizontal displacement by the IMSL based routine CSSMOTH available in PV-WAVE (1995). Due to gaps in the data for Station C only the velocities and vertical displacement for the three others stations are shown.

The velocity records of all stations show two distinct speed-up events, both lasting about 2 days. During speed-up event 1 (SE 1) the velocities increased by a factor of two and reached the maximum on June 26. During speed-up event 2 (SE2) the velocities increased by a factor of about six and reached the maximum value in the evening of July 16. Between the two speed-up events the velocities were on a low and rather constant level, with a slight slow down after SE 1. The second speed-up event (SE2) is much more pronounced than the first. After SE2, the velocities dropped to a significantly lower level than before the event. The diurnal velocity fluctuations noticeable in Figure 2.4b are within the error bar of the GPS measurements. From the available data we cannot decide whether those fluctuations are diurnal variations of the ice flow or a systematic error in the position determination by the differential GPS method (Vieser, 2000; Meinck, 1998).

The first event (SE 1) took place at all 4 stations, but only the observations of station A and B covered the full event (Fig. 2.4b). The two measured motion events are simultaneous and no significant change of the vertical displacement was observed.

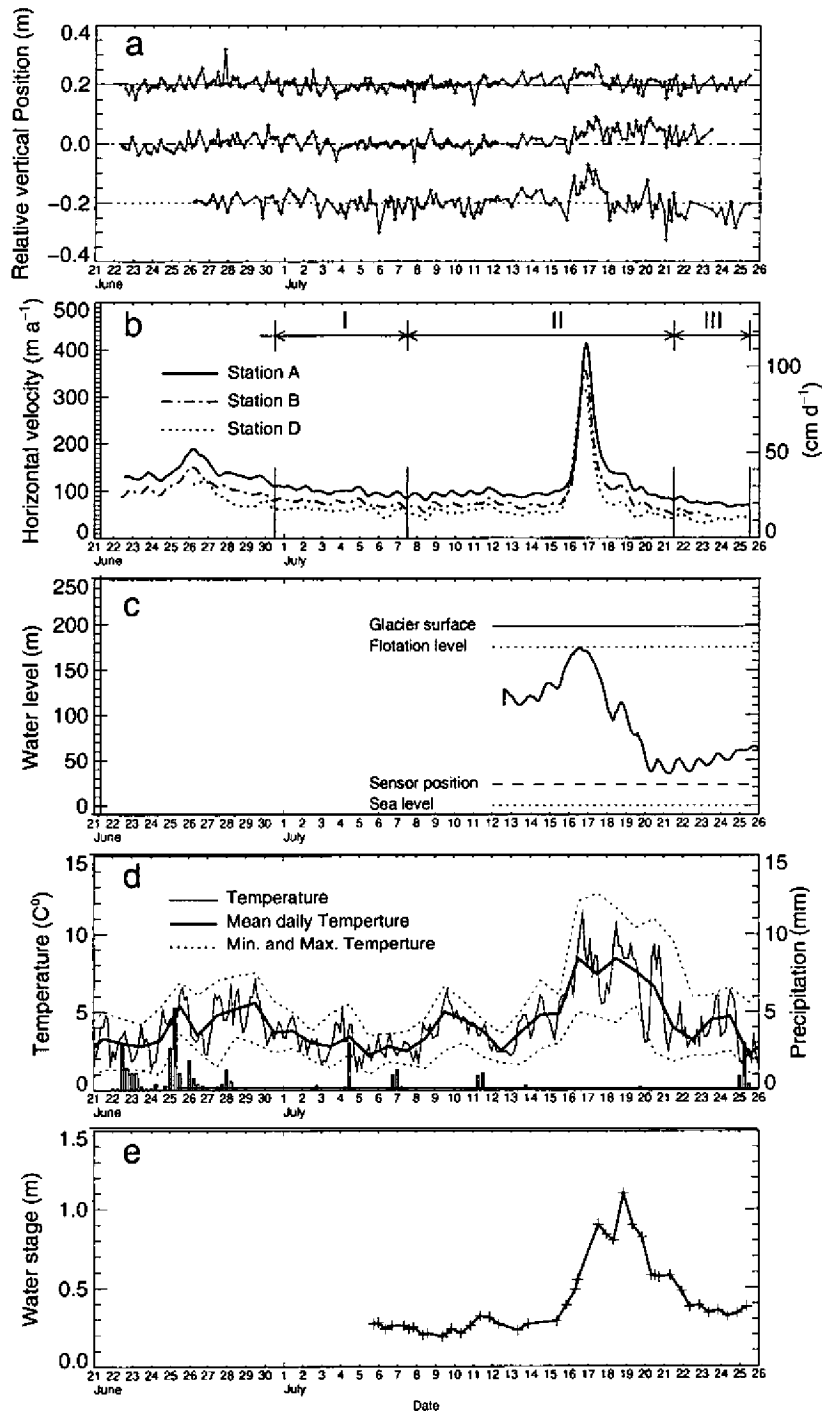


Figure 2.4: Measured data shown with time during the investigation period in summer 1999. (a) Measured relative vertical position (subtracted from general trend) of Station *A* (top), *B* (middle) and *D*. (b) Horizontal velocities calculated from the position measurements for the three permanent stations. *I*, *II* and *III* refer to the time periods used for the velocity measurements in the longitudinal profile (see Table 2.4). (c) Pressure record measured in a moulin shown as water level above sea level. (d) Temperature and precipitation measured at the meteorological station at Hornsund in the vicinity of Hansbreen. (e) Water level of the outflow river of neighbouring Werenskioldbreen

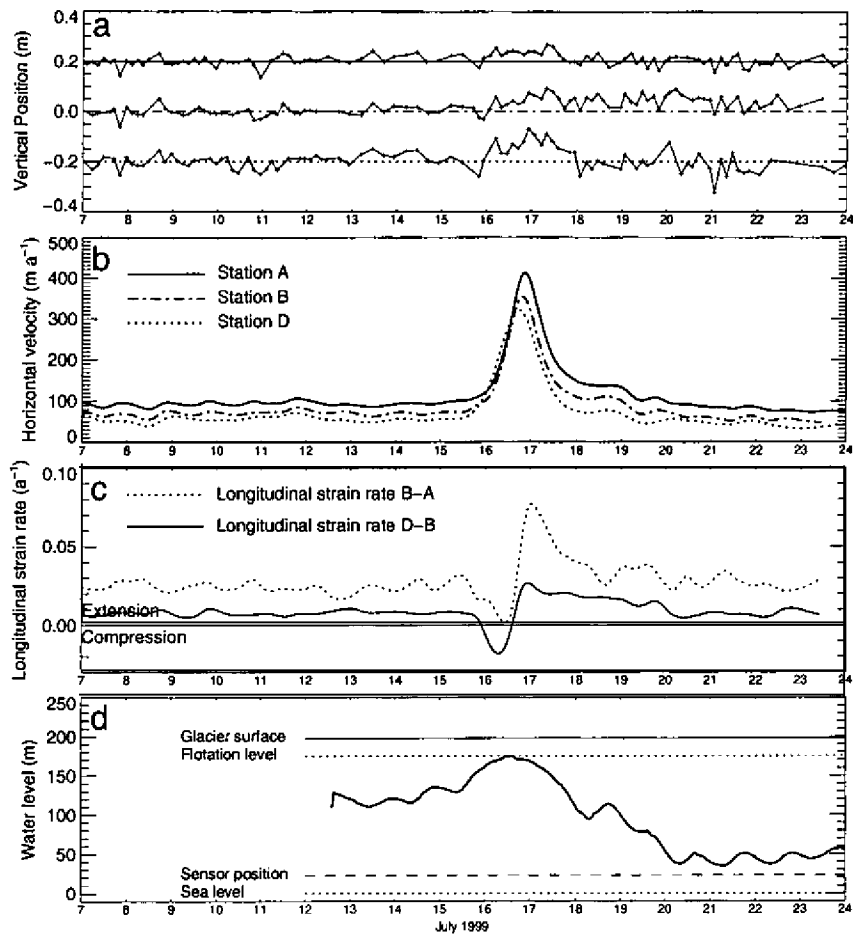


Figure 2.5: Zoomed section of the time record around SE2 showing (a) the relative vertical position, (b) horizontal surface velocities, (c) longitudinal strain rates between stations *B* and *A*, and *D* and *B* and (d) the water pressure measured in a moulin.

The second speed-up event occurred 20 days later, after a period of more or less constant surface velocities and climatic conditions (Fig. 2.4). Again this event was recorded at all four stations. The duration of SE 2 was about 2 days and occurred at the beginning of a 4 day föhn period with the velocity maximum in the evening of 16 July (Fig. 2.4 and 2.5). The maximum velocities of SE 2 at the different stations are shifted in time (Fig. 2.5 and 2.6). The maximum velocity is first reached at the highest station *D* and occurred with some delay at station *B* and station *A*. The temporal shift of the velocity peak between station *D* and *A* is about 3 hours, which is close to the temporal resolution of the Observation. For a distance of 2940m between these two stations a propagation velocity for the velocity peak of about  $1000 \text{ m h}^{-1}$  results.

#### *Vertical displacement*

The relative vertical position change with time of station *A*, *B* and *D* is shown in Fig. 2.4a. The symbols represent single measurements for the vertical position minus a mean vertical displacement trend over the Observation period. The measured strong fluctuations of the vertical position have an amplitude of about 3cm and are

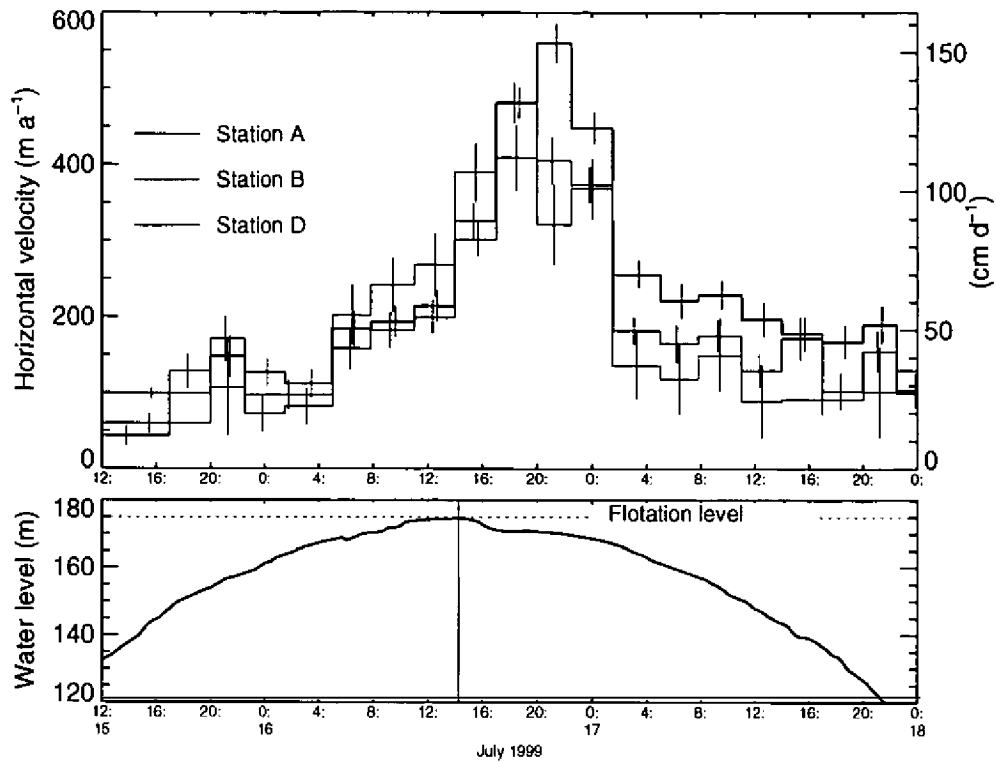


Figure 2.6: Close up view of speed-up event 2 showing the measured (top) horizontal surface velocities of the permanent stations. Below the water level recorded in the glacier moulin is shown with the time of maximum water level (vertical line).

within the a posteriori error (Table. 2.1). For station *D* a significant uplift ( $\sim 10$  cm) is observed between July 16 and 18, simultaneous to SE 2 (Vieser, 2000). For stations *A* and *B* similar uplifts are indicated, but the signals are weak. In addition to the uplift a slight change of the flow direction is observed for station *D* and *B* during SE 2 (Fig. 2.7). Both stations moved about 6cm to the right of the general flow direction during the speed-up event and switched back after it. Such a flow direction change is not significant for the two other stations *A* and *C*.

Table 2.3: Time periods for velocity measurements along the flowline and the transverse profile.

Period I	30.6.-7.7.1999	Slow flow before speed-up event 2
Period II	7.7.-21.7.1999	Including speed-up event 2
Period III	21.7.-25.7.1999	Slow flow after speed-up event 2
1998	August 98	Slow flow after a speed-up event in 1998

### Spatial Variation

For different periods in 1999 and 1998 surface flow velocities were measured along the flowline (Fig. 2.1). These periods are specified in Table 2.3 and indicated in Figure 2.4b. The corresponding surface flow velocities along the flowline are shown in Figure 2.8. For all periods a strong increase of the surface movement towards the

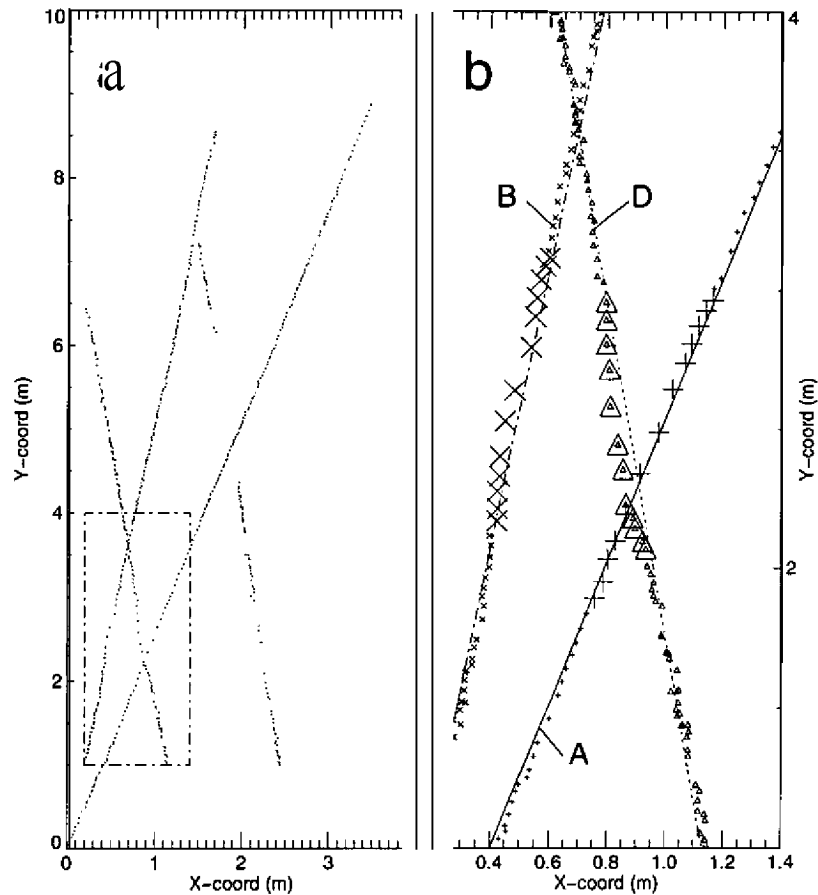


Figure 2.7: (a) Map view of all relative positions of the four permanent GPS-stations (shown in arbitrary coordinates). (b) Close up of the indicated section in (a). Large Symbols indicate position measurements between July 16:00 h and July 17 16:00 h, which corresponds to the Speed-up event 2.

terminus was observed. Lowest velocities occurred for the two periods after strong speed-up events in 1999 and 1998. In the upper 5 km of the glacier the velocities did not significantly change for the different periods. In Figure 2.8 an additional velocity value from April 9/10, 1996 is shown, which was derived from interferometric analysis (personal communication from H. Rott, University of Innsbruck, August 1998).

Surface velocities in a transverse Profile, located 800m behind the terminus (Fig. 2.2), are shown in Figure 2.9. The measurements do not cover the orographic left side of the glacier because of crevasses. Maximum velocities are located in a 500m wide zone in the middle of the glacier and decrease to zero towards the orographic right margin.

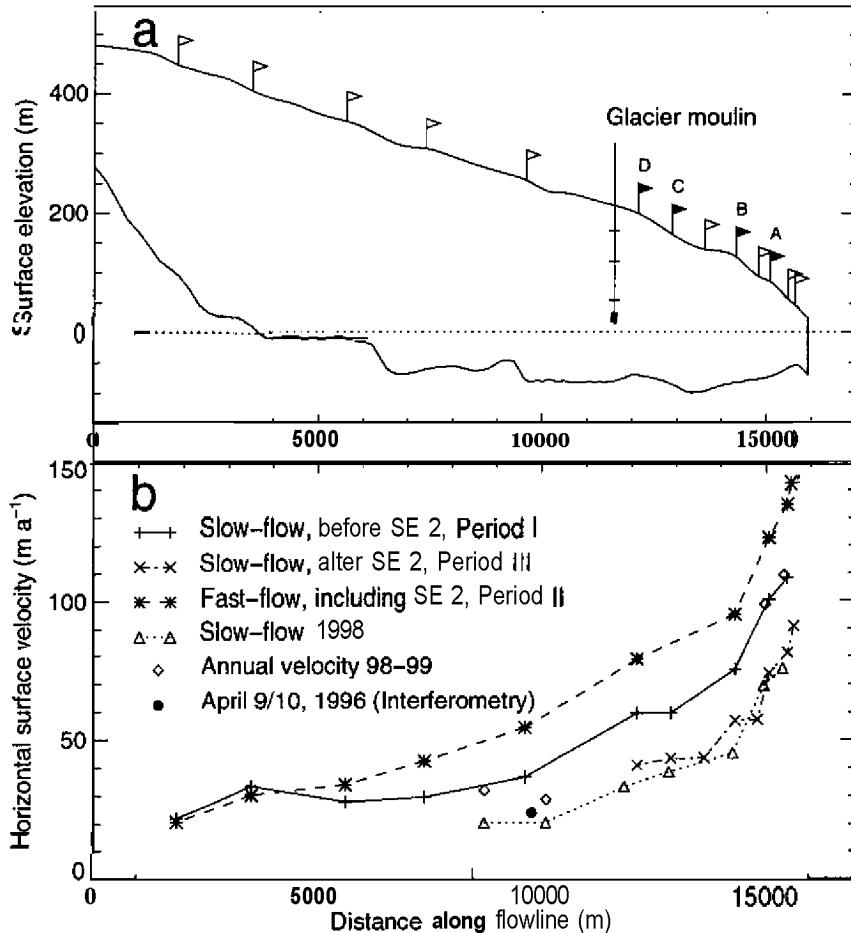


Figure 2.8: (a) Glacier geometry shown along a flowline of the glacier. The location of the four permanent GPS stations are indicated by the solid flags, the white flags indicate the poles of the longitudinal velocity profile. In addition, the approximate location of the pressure sensor in the glacier moulin is shown together with the mean water level before SE2 (middle), the maximum water level (top) and the minimum level after SE2 (lowest). (b) Measured horizontal velocities along the flowline for different time periods which are specified in Figure 2.4b and Table 2.4.

## 2.4 Interpretation and discussion of observations

### 2.4.1 General flow characteristics

The observations on Hansbreen show a few but distinct short-term speed-up events during the melt season (Fig. 2.4b). This is in contrast to the anticipated general increase of ice velocities during the entire melt season. The data of Hansbreen shows that the occurrence of such speed-up events is not limited to the beginning of the melting season. Periods of enhanced melt due to strong föhn weather situations can occur during the whole ablation period and cause such speed-up events. After

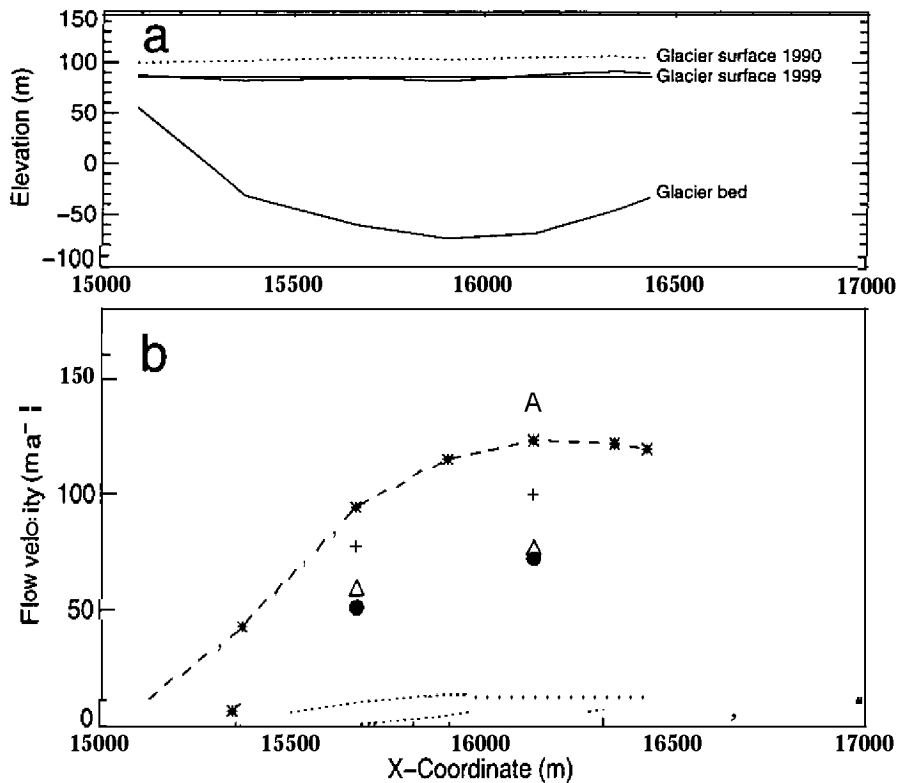


Figure 2.9: Profile across Hansbreen at station A showing (a) geometry and (b) horizontal velocities for different time periods. The stars with the dashed line indicate the velocities for the measurement Period II (including speed-up), the crosses for July 7 to 8, the triangles for July 21 to 23 and the dots for July 23 to 25. The dotted line represents the velocities due to ice deformation estimated by the shallow ice approximation using the local ice thickness and surface slope.

the Speed-up events, the velocities return to a slightly lower value than before. The observations from Hansbreen in 1998 indicated a very similar general flow behaviour during the melt season, but the temporal resolution of the velocity measurements was only 1 to 2 days (Viel and others, 2000).

The annual velocities between summer 1998 and 1999 are in the range of the velocities observed in a period between the two Speed-up events (Period 1) but they are above the slow flow values observed in 1998 and 1999 after a strong Speed-up event (Period 111, Fig. 2.8). The interferometrically derived velocity from April 9/10 1996 is a representative value for the arctic winter and is close to the annual and summer slow flow values. These observations, together with earlier studies on the flow of Hansbreen (Jania, 1988) indicate that during winter no significant increase of the flow occurs and the surface motion is in the range of the slow flow observed during summer. The observations show that apart from these short-term Speed-up events the glacier movement is almost steady with the seasons. The seasonal flow behaviour of Hansbreen seems to be similar to the flow of tidewater glacier Kongsvegen (Voigt, 1979).

### *Spatial variation of the flow*

The accelerated flow along the flowline towards the glacier terminus observed on Hansbreen is typical for tidewater glaciers (Fig. 2.8). Vieli and others (2000) showed that this increase in the flow is mainly due to enhanced basal sliding towards the terminus. Although the flow pattern in the frontal part of Hansbreen is very different from valley glaciers, it can be explained with the same water pressure dependent sliding law (Vieli and others, 2000). The strong velocity increase towards the terminus implies increased longitudinal extension (Fig. 2.5c), which causes the observed enhanced surface crevassing towards the terminus. Except during the speed-up event, the differences of horizontal velocities between the different stations are more or less constant with time (Fig. 2.4b and 2.8), which is illustrated by the rather constant longitudinal strain rates in the periods between the speed-up events (Fig. 2.5c). The flow in the upper accumulation area is found to be more or less constant during the Observation period.

The measured velocities in the transverse profile show that the shape of the velocity distribution between fast and slow flow does not change significantly (Fig. 2.9). This illustrates how difficult it is to detect spatial variations of the basal flow field with surface observations. A rough estimation of the ice deformation by the shallow ice approximation using the local ice thickness, surface slope and a rate factor of  $0.214 \text{ a}^{-1} \text{ bar}^{-3}$  and the exponent  $n = 3$  (Paterson, 1994) shows that even during slow flow periods the longitudinal flow is dominated by basal sliding (Fig. 2.9).

## **2.4.2 Short-term variations**

### *Glacial hydrological system*

SE 1 is related to a period of enhanced water input to the glacier due to a pronounced rainfall event, with little changes in air temperatures. The snow cover in the lower part was thin and already wet before SE 1. Therefore, water storage capacity of the snow pack was small and an enhanced water input to the drainage system due to precipitation is likely.

In the second part of the Observation period, when SE2 took place, precipitation was close to zero and the surface at the four stations was snow free. SE2 is related to a föhn event with enhanced surface melting. Temperature is a good index value for surface melting on the glacier (Ohmura, 2001) and therefore the significantly higher air temperatures during the föhn period led to enhanced surface melt and to a strong increase of water input to the glacier. The temperature was measured at the meteorological Station, located at the shore of Hornsund. On the glacier, the temperature increase due to föhn is probably even higher than at the meteo station, because the glacier is located on the leeward side of a 1000 m mountain ridge, whereas the meteo station is more exposed to the fiord climate. During the föhn period the sky was clear and therefore enhanced direct solar radiation additionally increased surface melting on the glacier.

Using temperature as an index for the surface melt a 4 day period of much higher water input to the glacier results for SE2, with a short interruption during the night



from July 17 to 18. A small time lag between the temperature signal and the water input to the glacier is expected to be in the order of hours. The observed doubling of the ablation rate confirms the increased water input during the föhn period (Table 2.2) and the water pressure measured in the moulin reflects this enhanced water input. Flotation level was reached in the afternoon of July 16. Although the water input was still high, the water level started to decrease because of changes in the intra or subglacial drainage system.

The relatively constant meteorological condition before the föhn period indicates a constant water input to the glacier and therefore the basal drainage system was well adjusted to this water input. At the beginning of the föhn period the drainage system was not efficient enough to drain the sudden enhancement of the water input and leads to the observed increase of water pressure in the moulin. When the water pressure reaches the flotation level, local decoupling at the bed may increase the basal discharge by additional flow through basal cavities. Due to this reorganization to a more efficient drainage system, the water level within the moulin starts to decrease even if the water input remains high. The outflow record of landbased neighbouring Werenskioldbreen situated in the east of Hansbreen also indicates a continuing high water input to the glacier (Fig. 2.4e). At the end of the föhn period the water input decreases, but the drainage system is still adjusted to the high water input. Therefore the water pressure drops to a lower value than before the föhn event. The following slow increase of the water pressure indicates a renewed adjustment of the drainage system to this reduced water input, most likely by channel closure due to viscous deformation, when ice pressure exceeds water pressure (Röthlisberger, 1972). The duration of the enhanced water supply for SE2 was longer than the responding pressure and surface speed-up event associated with it. We propose that the observed duration of the pressure event of 1 to 2 days represents the time scale required by the subglacial drainage system to adjust itself to a water input perturbation. In the period before and after the peak, the diurnal cycles in water level reflect the diurnal variation of melt water input. The time scale of these fluctuations seems to be below the suggested time needed for the subglacial drainage system to adjust to changes in water input, which explains the discernable daily variations in water level. The moulin in which water pressure was measured was already active before SE 2, which indicates that a channelized drainage system already existed to some extent before SE 2.

The observed water pressure was measured in a moulin and not at the glacier bed itself. Thus, the observed pressure is expected to represent the water pressure variations of the drainage system in the vicinity of the moulin and not the local pressure at the bed. It is not known where or how the moulin or channel is hydraulically connected to the terminus or glacier bed, which is below sea level. In the orographic left part of the calving front, where the sea is very shallow, an outflow channel at the glacier bed was observed during periods of high discharge. The outflowing water was enriched with sediment which also indicates contact of the drainage system with the glacier bed.

Speed up events detected in summer 1998 (Vielí and others, 2000) were also related to föhn periods with enhanced surface melting and confirm the typical time scale of 2 days.

### Speed-up, water pressure and *water storage*

The velocities of SE2 are closely related to the observed peak in water pressure in a moulin. With increasing or decreasing water pressure the surface velocities were observed to increase or decrease, respectively. The maximum velocity was reached when water pressure was almost at flotation level.

The very short time scales involved in the observed speed-up events suggest that the drastic changes of surface flow are caused by changes in basal sliding and not by internal ice deformation. For Hansbreen, ice flow in the terminus region is known to be mainly due to basal sliding (Vielí and others, 2000). From other studies and theory we expect that such short-term changes in basal sliding are mainly due to a sudden increase of basal water pressure (Iken and Bindshadler, 1986; Kamb and Engelhardt, 1987; Fischer and Clarke, 1997). According to the present knowledge basal sliding is expected to increase progressively with increasing water pressure under a fixed basal shear stress, due to enhanced formation of basal cavities (Bindshadler, 1983; Budd and others 1979; Iken, 1981) or decreased strength of a basal Sediment layer (Boulton and Hindmarsh, 1987). The observational data set of SE 2 from Hansbreen shows that the horizontal speed-up and the recorded water pressure peak occurred almost simultaneously (Fig. 2.4 and 2.5). When formation and growth of basal cavities take place due to high basal water pressure, the sliding velocity is rather related to water storage at the bed than directly to water pressure. Maximum velocities would then occur when water storage is highest. Water storage was also found to control basal sliding for short-term velocity variations on tidewater glacier Columbia (Kamb and others, 1994) and Le Conte (personal communication from K. Echelmeyer, University of Alaska, March 2001). When the water pressure reached the flotation level, bed Separation and basal decoupling may have occurred in larger areas and led to additionally enhanced sliding. In these decoupled areas, which are expected to occur mainly in the central part of the bed, the basal shear drag would be transferred to regions which are still sticky (Blatter and others, 1998).

The velocities after SE2 were slightly lower than before it. This slow down can be explained with the observed record of the water level, which was at a lower level after the event than before. For SE1 no water pressure data are available, but increased water pressure is expected due to the additional water input from a pronounced rainfall event in the morning of June 25 (Fig. 2.4).

### Temporal *shift*

The observed temporal shift of the location of the velocity peak during SE 2 suggests that a pressure wave was propagating down glacier with an approximate velocity of  $1000 \text{ m h}^{-1}$ . Enhanced water input occurred simultaneously over the whole ablation zone and therefore an increase of the water pressure is also expected to occur everywhere at the same time. The drainage system was probably less efficient upglacier than in the terminus region. As a consequence the water pressure rose faster in the upper ablation area and first reached the flotation level there and then propagated downwards. Because speed-up events were not recorded in the upper accumulation zone (Fig. 2.8) a basal water pressure rise probably took place only in the lower 10 km. In the upper 5 km less ablation occurred and the glacier was covered by firn.

The melt water penetrates regularly over the whole glacier surface and is first stored in the firn. Thus, the disturbance in water input to the basal drainage system is strongly delayed and damped.

Such velocity or pressure peaks moving downwards were observed on several other glaciers. For Findelengletscher (Iken and Bindshadler, 1986) and Variegated Glacier (Kamb and Engelhardt, 1987) propagation velocities of the pressure peak were  $100 \text{ m h}^{-1}$  and  $300 \text{ m h}^{-1}$ , respectively. Low propagation velocities were suggested to be related to enhanced water storage outside the basal conduits (Iken and Bindshadler, 1986). Thus, the significantly higher value found for Hansbreen compared to other glaciers indicates rather low water storage. Another reason for the high propagation velocity may be that the water pressure reached flotation and caused ice-bed decoupling of larger areas at the bed

The temporal shift of the velocity peak implies changes of the longitudinal strain rate between the different stations shown in Fig. 2.5c. Longitudinal compression results on the front side of the velocity peak and longitudinal extension on the leeward side. The generally higher extension rate found between two lower stations is related to the strong acceleration towards the calving front. The high peak in the longitudinal extension rate that occurs during the speed-up event may lead to additional fracture and to crevasse opening at the surface. Because of the associated high water pressure the formation of bottom crevasses is expected (Van der Veen, 1998). Thus, changes in the flow on such short time scales may affect the process of calving at the terminus, but not vice versa.

For SE1 no significant temporal shift of the velocity peaks between the different stakes can be ascertained (Fig. 2.4). Because the velocity peaks are much less pronounced for SE 1 than for SE 2 and only the two stations *B* and *A* cover the whole speed-up event, such a temporal shift could not be detected. For SE1, a rainfall event is the cause for the velocity peak, whereas enhanced surface melting was responsible for SE 2.

#### *Uplift and change of flow direction*

A small vertical uplift during SE2 could be inferred from the measurements (Fig. 2.4 and 2.5). For Station *D* the vertical uplift was 10 cm, which is significantly above measurement errors, whereas for Station *A* and *B* it is within the errors. The vertical uplift occurs during the period of enhanced velocities and water pressure. A consequence of the high basal water pressure, attaining the flotation level, can be the formation of basal cavities and water storage at the bed, which may explain the measured vertical uplift. The high water pressure may also lead to an extension of the basal Sediment and result in a vertical uplift, as suggested for the case of Black Rapids Glacier (Truffer, 1999). This explanation requires the existence of a basal Sediment layer of sufficient thickness.

At the beginning of the speed-up event, when longitudinal compression occurs, vertical extension is expected because of mass conservation and incompressibility. Assuming constant horizontal strain rates from surface to the base, the uplift due to vertical extension is estimated to be one to two orders of magnitude smaller than the 10 cm observed at Station *D*. From the observations we suggest that water storage

at the bed by the formation of basal cavities or bed Separation is the most probable reason for the observed uplift.

SE 2 was also associated with a slight change of the flow direction at Station *D* and *B* but not for the two other stations *A* and *C*, which indicates the local Character of this phenomenon. The high water pressure may cause local decoupling and Separation of the glacier from the bed and lead to high basal velocities in this area. Thus the sliding pattern at the glacier bed is expected to be inhomogeneous in space. In the decoupled areas the basal shear drag has to be transferred to the sides which are still sticking. The resulting surface flow distribution to this spatial Variation of the basal velocity is damped and smoothed. The observed small changes in flow direction may reflect important spatial variations of the basal flow field, due to local ice-bed decoupling during periods of high basal water pressure.

The local Character of the observed uplift and change in flow direction supports the idea that these effects are related to basal cavitation and local decoupling of the glacier from the glacier bed.

## 2.5 Conclusions

The study performed on Hansbreen during the melt season shows that sporadic well pronounced short-term Speed-up events with a typical duration of 1-2 days occur, rather than generally enhanced flow velocities during the melt season. Such events are related to periods of enhanced water input to the glacier, either due to rainfall or intensive melt events (föhn Situation). The rapid velocity changes suggest that such events are due to enhanced basal sliding. The close correlation between surface flow and recorded water pressure in a moulin suggests that the speed-up is caused by enhanced basal water pressure. The rapid increase of sliding is expected to be due to a rapid opening of basal cavities resulting from the high basal water pressure. When the water pressure reaches flotation, additional decoupling over larger areas may occur at the glacier bed, leading to further increase in local sliding rates. Thus, for the observed Speed-up events, water storage at the bed is an important factor for basal sliding.

The speed-up was observed at all stations in the ablation zone, but the velocity peak is found to be shifted slightly with time. The location of the maximum velocity propagates down glacier with roughly  $1000 \text{ m h}^{-1}$ , suggesting a pressure wave with the same propagation velocity. This temporal shift in the speed-up results in local longitudinal compression during the ascending phase of the velocity peak and longitudinal extension during the descending phase. These short strain peaks do not substantially contribute to the observed uplift, but may lead to additional fracture and crevasse formation in the terminus region and may therefore affect the process of calving. The observed small change in flow direction and uplift additionally support the idea that basal cavitation (water storage at the bed) or bed Separation due to high water pressure cause the rapid basal sliding. In addition, this indicates that the basal flow field is inhomogeneous and local decoupling at the bed causes the generally increased surface velocities.

The general flow pattern of tidewater glacier Hansbreen differs from landbased valley glaciers of similar size. A general velocity increase towards the terminus and high basal sliding rates occur, which are both related to the generally high water pressure in the terminus region (Vielí and others, 2000). Basal sliding is high all year round, even in periods without surface melt. But the observed variations of the flow on short time scales and the associated processes are very similar and suggest that the relevant mechanisms and physical processes that control the flow and its temporal variations are the same. In addition, the observations of Hansbreen indicate no fundamental difference in the subglacial drainage system and glacial hydrology known from studies of landbased glaciers, although most part of the glacier bed is below sealevel. The observed typical duration of 1 to 2 days for the speed-up events on Hansbreen was also found for landbased valley glaciers. This study of Hansbreen suggests that the duration of a short-term speed-up event associated with a pressure increase is controlled by the time it takes for the basal drainage system to adjust to a change in water input, which is proposed to be 1 to 2 days.

# Paper 3

## Flow dynamics of tidewater glaciers: a numerical modelling approach

Andreas Vieli,<sup>1+2</sup> Martin Funk,<sup>2</sup> Heinz Blatter<sup>1</sup>

*Institute for Climate Research ETH, Winterthurerstr. 190, CH-8057 Zürich, Switzerland*

*<sup>2</sup>Section of Glaciology, VAW, ETH Zentrum, Gloriastr.37/39, CH-8092 Zürich, Switzerland*

### Abstract

The dynamics of grounded tidewater glaciers is investigated with a time dependent numerical flow model, which solves the full equations for the stress and velocity fields and includes a water pressure dependent sliding law. The calving criterion implemented in the model shifts the calving front at each time step to the position where the frontal ice thickness exceeds flotation height by a prescribed value. With this model, the linear relation between calving rate and water depth proposed on empirical grounds is qualitatively reproduced for the situation of a slowly retreating or advancing terminus, but not for situations of rapid changes. Length changes of tidewater glaciers, especially rapid changes, are dominantly controlled by the bed topography and are to a minor degree a direct reaction to a mass balance change. Thus, accurate information on the near terminus bed topography is required for a reliable prediction of the terminus changes due to climate changes. The results also confirm the suggested cycles of slow advance and rapid retreat through a basal depression. Rapid changes in terminus positions preferably occur in places where the bed slopes upwards in ice flow direction.

## 3.1 Introduction

This study investigates tidewater glaciers which are defined as glaciers that end in the sea with a *grounded* ice cliff from which icebergs are discharged. The present paper approaches the dynamics of tidewater glaciers with a time dependent numerical flow model. The model solves the full equations for the stress and velocity fields, including a water pressure dependent sliding law. A calving criterion is implemented which removes at each time step the part of the glacier terminus that is thinning below a critical height above buoyancy. Thus, the calving rate, which is defined as the ice velocity at the terminus minus the rate of change in the terminus position, is an output quantity of the model. This is an important progress in the investigation of the evolution of tidewater glaciers with a numerical glacier flow model.

The model is applied on a synthetic but typical tidewater glacier geometry with a basal depression in the terminus region. Model calculations were performed for two mass balance scenarios leading to an advancing and a retreating situation mainly over the basal depression. With these model experiments we intend to demonstrate how the changes of the calving front are affected by the considered physical processes and their feedback mechanisms. We also want to examine the qualitatively described concepts and processes suggested for tidewater glacier on the basis of observations (Meier and Post, 1987; Van der Veen, 1996).

### 3.1.1 Motivation

The dynamical behaviour of tidewater glaciers is important because of their reaction to climate change, but is still poorly understood (Meier, 1994; Van der Veen, 1997). Observations of several glaciers, such as Columbia Glacier (Meier and Post, 1987), Uppsala Glacier (Warren and others, 1995a), Glacier San Rafael (Warren and others, 1995b) and records of past glacial expansion (Powell, 1991) show that tidewater glaciers have a great potential for dramatic retreats of the terminus position. For example, Columbia Glacier retreated at a rate of about  $0.7 \text{ km a}^{-1}$  from 1985 to 1991 (Krimmel, 1992). Iceberg calving is a very efficient ablation mechanism and permits a much larger rate of mass loss than surface melting (Van der Veen, 1996). A generally high calving activity can strongly increase the freshwater input into the ocean in form of icebergs and may have a strong impact on the environment. During the rapid retreat of Columbia Glacier, drifting icebergs posed a serious threat to oil tankers (Dickson, 1978). The additional fresh water may also affect the marine ecosystem in the surrounding sea. During the last glaciation, huge quantities of icebergs were discharged six times by the Laurentide ice sheet. They were recorded in a set of ice-rafted debris deposited in sediment layers in the North Atlantic (Heinrich, 1988). These so called Heinrich-events are connected with rapid climate variations in the North Atlantic region. It was speculated (Broecker, 1994) that the additional freshwater from the discharged icebergs disrupted the deep-water formation, thereby switching the thermohaline ocean circulation between glacial and interglacial modes (Dansgaard-Oeschger events). Thus studying the present tidewater glaciers may provide a better understanding of the past changes.

The rapid changes in terminus position of Columbia Glacier in the last decades (Meier and Post, 1987) and several Patagonian grounded calving glaciers (Warren, 1993; Naruse and others, 1997) are not directly related to climate. Meier and Post (1987) mentioned that longer periods of warm climate may have triggered rapid retreats by thinning of the glacier in the terminus region. Clarke (1987) suggested that tidewater glaciers inherently have an unstable response to a long-term mass balance deficit. In view of the potential for rapid changes of tidewater glaciers as a response to climate changes, an improved knowledge of the dynamics is essential.

### **3.1.2 Current knowledge on tidewater glaciers**

Several processes that influence the dynamics of tidewater glaciers have been identified, and these may be important for controlling the position of the terminus. Empirical studies showed that the calving rate increases linearly with water depth at the terminus (Brown and others, 1982). It was also recognized that bed topography plays an important role in the control of changes in terminus position (Meier and Post, 1987). Tidewater glaciers typically end at a submarine frontal moraine. When the terminus starts to retreat into deeper water the calving activity increases and results in a dramatic retreat, which has been observed for many tidewater glaciers (Venteris, 1999; Van der Veen, 1997). Meier and Post (1987) suggested that tidewater glaciers undergo a cycle of slow advance (on the order of a few hundred to a thousand years) and a rapid retreat (decades to a century) through a depression in the basal topography.

Basal sliding is known to be an important factor for controlling the dynamics of tidewater glaciers (Van der Veen, 1996; Meier and Post, 1987) and is related to basal water pressure (Bindschadler, 1983; Iken, 1981). Observations from Columbia Glacier showed that the sliding velocity at the terminus increases with increasing calving rate, thus reducing the rate of position change (Van der Veen, 1996). Data from many tidewater glaciers show that there is a good correlation between calving rate and ice speed at the terminus (Van der Veen, 1996; Jania and Kaczmariska, 1997). For glaciers in steady state this correlation is a direct consequence of the definition of the calving rate, but for rapidly changing glaciers it is not obvious (Van der Veen, 1996). Furthermore, it is still not clear whether increased calving leads to increased sliding or vice versa.

Backpressure from the terminal moraine may also affect the ice flow (Van der Veen, 1997; Fischer and Powell, 1998). When the terminus retreats and loses contact to the frontal moraine, the backstress is expected to decrease and the velocity at the terminus will increase due to enhanced horizontal stretching (Meier and Post, 1987) and the rate of retreat will be reduced.

On long time scales (hundreds of years) Sedimentation processes and the formation of a terminal moraine become important (Fischer and Powell, 1998; Hunter and others, 1996; Powell, 1991). The infilling of the basal depression in front of the glacier and the growing terminal push-moraine reduce the water depth and therefore the calving activity. Hence an advance of the glacier through a basal depression is facilitated,



which was already observed at Taku Glacier (Motyka, 1997) and Hubbard Glacier (Mayo, 1989).

Which processes initiate a retreat or advance of a calving glacier is still an open question. Even the comprehensive data set of rapidly retreating Columbia Glacier does not allow the identification of the mechanisms that cause and control a terminus retreat. Two different conceptions have been proposed.

Meier (1994, 1997) suggested that calving is the driving mechanism for a retreat. His conception is based on the proportionality of the calving rate with water depth (Brown and others, 1982). Meier claims that increased calving causes additional horizontal stretching at the terminus because the increased cliff height will cause higher unbalanced lithostatic Stresses. Increased horizontal stretching will lead to thinning of the glacier terminus, the effective pressure will decrease, followed by an increase in basal sliding and additional horizontal stretching. If calving rate is related to extension rate, calving activity will increase and enhance the retreat. On the other hand, the increase of sliding due to glacier thinning will reduce the retreat (Meier and Post, 1987).

A different concept is proposed by Van der Veen (1996, 1997a). He argues that if thinning takes place at the terminus due to increased flow velocity and horizontal stretching, the calving activity and therefore the rate of retreat will increase. Observations at Columbia Glacier (Van der Veen, 1996; Meier and Post, 1987) and rapidly retreating grounded calving glaciers in Patagonia (Venteris, 1999) showed that the part of the terminus which is thinning below a critical height above flotation, breaks off because of buoyancy. In this interpretation, the retreat is initiated and maintained by thinning and stretching of the glacier. Meier's and Van der Veen's opposing concepts show that the involved physical processes lead to complex feedback mechanisms. We therefore propose to approach the problem with a numerical glacier model, which allows to couple the relevant processes concerning the dynamics of tidewater glaciers.

### 3.1.3 Previous modelling work

At the beginning of the rapid retreat of Columbia Glacier in the early 1980's several numerical models were developed to predict the future retreat of this tidewater glacier. Rasmussen and Meier (1982) used a one dimensional model based on mass conservation. In this model the calving rate was specified by a linear function of the water depth at the terminus. A drastic retreat that strongly depends on the Parameters of the calving function was predicted.

Sikonia (1982) modeled the flow in a vertical section along the flowline. Basal sliding was simulated by using a thin soft layer at the glacier bed. The calving rate was related to ice thickness above buoyancy and to seasonal variations of freshwater runoff. The modeled length change was extremely sensitive to the Parameters used in the calving function. For small variations of these Parameters the reaction of the glacier ranged between no retreat at all and a rapid retreat.

Bindschadler and Rasmussen (1983) developed a finite-difference model that calculates the ice flux for a finite number of cross sections and updates the glacier

geometry using the continuity equation. The ratio of the sliding velocity to the total surface velocity was determined from observed velocities and was assumed to be a constant for each point in space. Different parameterisations for the calving rate were used which relate the calving rate linearly to water depth or front height. If flotation was reached at the terminus, the floating ice was removed. According to the model results a rapid retreat was expected. Calculations could only be performed for a few hundred meters of retreat due to limitations in computing time. According to the results of all three models a rapid retreat of Columbia Glacier was expected. Surprisingly the observed glacier retreat was much slower than predicted, mainly because the flow velocities increased more than expected (Meier, 1994).

In a similar setting, the retreat of Unteraargletscher ending in a planned new reservoir was estimated. Funk and Röthlisberger (1989) proposed and used an approach in which they estimated the mass flux and the empirical calving rate as a function of water depth. For a similar problem on Austdalsbreen Hooke and others (1989) followed this approach, but in addition, the effect of a changing water level on basal sliding was discussed.

## 3.2 Governing processes

A model of the dynamics of a tidewater glacier must incorporate realistic descriptions of calving and basal sliding, and must consider interactions between the calving process and the dynamics of the entire glacier (Van der Veen, 1997).

### 3.2.1 Calving

The calving rate  $u_c$  is defined as the volume of ice that breaks off per unit time and per unit vertical area from the glacier terminus (Paterson, 1994, page 376). It is equal to the ice velocity at the terminus,  $u_i$ , minus the rate of change in the terminus position  $L$ :

$$u_c = u_i - \frac{dL}{dt} \quad (3.1)$$

With this formulation the ice lost by melting at the calving front is included in the calving rate. Most theoretical studies of calving were applied on floating glaciers and ice shelves (Reeh, 1968; Holdsworth, 1978). Hughes (1992) developed a theoretical model for calving of grounded glaciers based on the idea that bending shear is the controlling mechanism for calving. This theory is not able to explain unambiguously the observations on tidewater glaciers and cannot be applied to tidewater glaciers that are close to flotation at the terminus (Van der Veen, 1996).

Several quantities show a close relationship to the calving rate, such as water depth, front height or ice velocity. Based on data of 12 Alaskan tidewater glaciers, Brown and others (1982) proposed a proportionality between calving rate and water depth  $d$  at the terminus:

$$u_c = \beta \cdot d \quad (3.2)$$

with a coefficient of  $27.0 \text{ a}^{-1}$ . Pelto and Warren (1991) proposed a similar, linear relationship with additional data from glaciers in Greenland and Svalbard. For glaciers calving into fresh water a 15 times smaller slope coefficient  $\beta$  of the linear relationship between calving rate and water depth has been found (Funk and Röthlisberger, 1989). Recent studies of the large Patagonian glaciers calving into lakes, such as Glaciar San Rafael (Warren and others, 1995b) and Glaciar Moreno (Rott and others, 1998) do not confirm a smaller slope coefficient  $\beta$  for fresh water calving glaciers. The proposed relations are empirical and do not describe the mechanisms of calving. Van der Veen (1996) pointed out that the empirical linear relation (3.2) is based on data from glaciers which are in or close to steady state. The observed calving rates during the rapid retreat of Columbia Glacier and several other grounded calving glaciers (such as Hansbreen, Jania and Kaczmarska, 1997; Glaciar San Rafael, Warren and others, 1995b; Maud Glacier, Kirkebride and Warren, 1997) are not in agreement with the linear calving relation. A linear calving relation may not be valid during rapid changes of glacier termini (Meier and Post, 1987), as observed for Columbia Glacier. However, these empirical relations can be adopted as a working hypothesis and a calving model should meet these relations.

#### Flotation model

Based on the observations of Columbia Glacier, an alternative treatment of calving is suggested in the *flotation* model (Van der Veen, 1996). During rapid retreat of Columbia Glacier, the terminus appeared to retreat to a position where it approached flotation thickness (Meier and Post, 1987). In the *flotation model*, the terminus of the glacier retreats to the position where the ice thickness  $h$  exceeds the flotation height by an amount  $h_o$  (Van der Veen, 1996). The height at the terminus  $h_c$  is then given by

$$h_c = \frac{\rho_w}{\rho_i} d + h_o, \quad (3.3)$$

where  $\rho_w$  is the density for sea or freshwater ( $1030$  or  $1000 \text{ kg m}^{-3}$ ) and  $\rho_i$  is the density of glacier ice. This implies that the part of the terminus where the ice thickness is below the critical thickness  $h_c$ , calves off because the ice can no longer resist the buoyancy force. The final detachment is probably due to additional weakening of the ice by the formation of bottom crevasses when flotation is approached (Van der Veen, 1998). Applying this model to the rapid retreat of Columbia Glacier, Van der Veen (1996) found  $h_o = 50\text{m}$ . The flotation model is consistent with the observed rapid retreating calving glaciers in Patagonia, where a similar critical height above buoyancy was derived (Venteris, 1999). In the flotation model the calving mechanism does not need to be entirely understood, which favours its use in a numerical model to calculate the evolution of tidewater glaciers.

To date the flotation model was only tested with data sets of large fast flowing tidewater glaciers (water depths of  $150\text{-}300 \text{ m}$ , flow velocities of  $1000\text{-}6000 \text{ m a}^{-1}$ ). For smaller glaciers (water depths less than  $150 \text{ m}$ , flow velocities less than  $200 \text{ m a}^{-1}$ ) the observed frontal cliff heights generally do not exceed  $50 \text{ m}$  and the height above flotation is expected to be well below the  $50\text{m}$  suggested for Columbia Glacier.

Therefore we propose a *modified flotation criterion* where the fixed minimum height above flotation  $h_o$  in Equation (3.3) is replaced by a small fraction  $q$  of the flotation thickness at the terminus. The height at the terminus is then

$$h'_c = \frac{\rho_w}{\rho_i} (1 + q) d = \frac{\rho_w}{\rho_i} d + h'_o. \quad (3.4)$$

For this modified flotation criterion, the terminus moves to the position where the ice thickness corresponds to  $h'_c$ . Choosing  $q = 0.15$ , the resulting  $h'_o$  is equal to the observed value of  $h'_o = 50$  m for Columbia Glacier.

#### *Melt induced calving* model

For small and slowly flowing tidewater glaciers, parts or all of the terminus are generally far above the critical height  $h'_c$  and the calving rates are small (below  $150 \text{ m a}^{-1}$ ). In this case, the observed calving rates cannot be described with the flotation model, and other processes are controlling the calving rate. For these slowly flowing tidewater glaciers melting at the front may become important. The average amount of ice lost by melting is small compared to the mass loss by calving (Powell, 1988). According to observations melting is concentrated at the waterline (Fig. 3.1), due to wave erosion. Observations from Glaciar San Rafael (Warren and others, 1995b) and Le Conte Glacier (Personal communication K. A. Echelmeyer, March 2001) indicate that there may also be a lot of melting below the waterline. For the deterioration of icebergs, melting at the waterline was found to be one order of magnitude higher than subaqueous melting forced by buoyancy convection (El-Tahan and others, 1987). Thus, the vertical ice front is undercut by melting at the waterline and the ice above the notch breaks off in thin lamellas. The resulting calving rate is equivalent to the melt rate at the waterline. This process was observed on several glaciers and described in detail for fresh water calving Maud Glacier (Kirkebride and Warren, 1997). Assuming that melting at the waterline is the driving process for calving, the melt rate must be on the order of magnitude of the flow velocity at the terminus. From laboratory and field experiments and from theoretical studies on the deterioration of icebergs an equation for the melt rate  $M_w$  at the waterline per degree above the melting point was derived (El-Tahan and others, 1987):

$$M_w = 0.000146 \left( \frac{R}{H} \right)^{0.2} \frac{H}{P}, \quad (3.5)$$

where  $M_w$  is the melt rate at the waterline in  $\text{m s}^{-1} \text{ K}^{-1}$ ,  $H$  is the wave height in meters,  $P$  the mean wave period in seconds and  $R$  the roughness height of the ice water boundary in meters. The melt rate is controlled by wave activity and water temperature. According to literature a reasonable value for surface roughness of ice in sea water is 1 cm. Assuming a sea temperature of  $1^\circ \text{ C}$ , a wave height of 0.1 to 0.2 m and a wave period of 3 to 5 s, melting rates between 0.2 to  $0.5 \text{ m d}^{-1}$  are calculated (Equation 3.5), corresponding to annual melt rates up to  $180 \text{ m a}^{-1}$ . If the sea is covered with ice during the winter season, no melting will take place at the waterline and therefore the annual value will be reduced. Thus, for slowly flowing

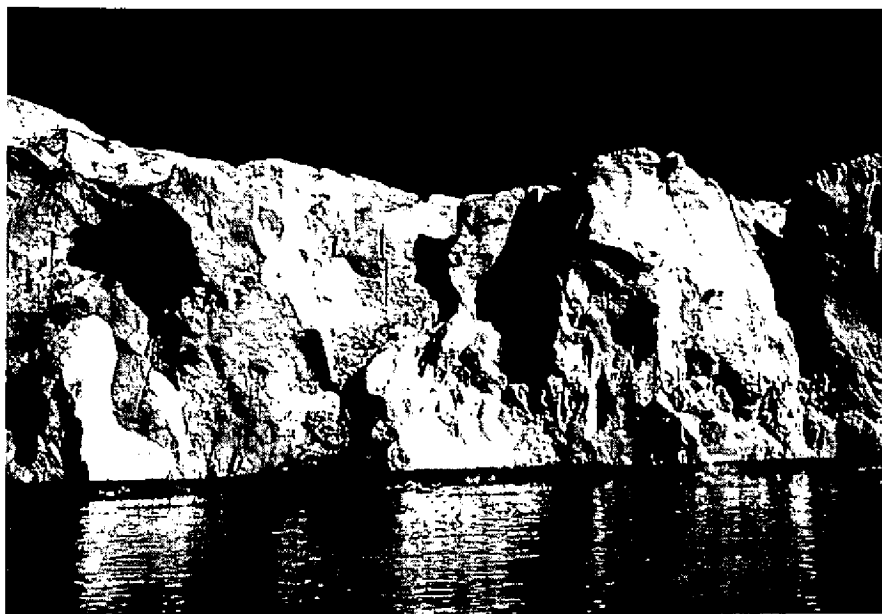


Figure 3.1: Calving front of Hansbreen, a tidewater glacier located in Spitsbergen. The notch melted out at the waterline shown on the Photograph extends all along the calving face and persisted throughout the entire melting season. The height of the calving face on the shown section is between 18 m and 25 m. The Photograph was taken at low tide in July 1998.

tidewater glaciers, melting at the waterline seems to be a controlling process of the calving rate. This is confirmed by observations on Hansbreen, a tidewater glacier in Spitsbergen (Fig. 3.1; Jania, 1988). Salinity additionally affects melting and may explain the reduced calving rates for small fresh water calving glaciers (Funk and Röthlisberger, 1989).

### 3.2.2 Basal sliding

The fast Aow observed on many tidewater glaciers (Meier and Post, 1987) is primarily due to high sliding velocities (Clarke, 1987; Meier and others, 1994; Kamb and others, 1994). Also for small slowly flowing tidewater glaciers, such as Hansbreen, basal sliding dominates the flow in the terminus region (Vieh and others, 2000). Basal water pressure was recognized to be an important controlling factor for basal sliding (Budd and others, 1979; Iken, 1981; Bindschadler, 1983; Jansson, 1995). A commonly used description for basal sliding is (Budd and others, 1979; Bindschadler, 1983):

$$v_b = k \cdot \tau_b^m p_e^{-r}, \quad (3.6)$$

where the basal velocity  $v_b$  is related to the basal shear stress  $\tau_b$  and  $k$  and  $r$  are adjustable empirical positive Parameters. The effect of the effective pressure  $p_e$ ,

which is defined as the ice-overburden minus the basal water pressure, is included in the sliding relation.

The inverse proportionality of the sliding velocity  $v_b$  to  $p_e^r$  has a strong effect on the flow of tidewater glaciers. The basal water pressure of a tidewater glacier undergoes seasonal and long-term variations, depending on the water input and the state of the subglacial water drainage system. The water level within a tidewater glacier decreases towards the calving front to a value corresponding to sea level. In the situation of a tidewater glacier the effective pressure is also expected to decrease towards the terminus.

According to the sliding law (3.6), the reduced effective pressure induces increased sliding velocities. This is supported by the observed high sliding rates (Meier and Post, 1987) and increased flow velocities towards the calving front on tidewater glaciers, such as Hansbreen (Vielí and others, 2000), Columbia Glacier (Krimmel and Vaughan, 1987), Moreno Glacier (Rott and others, 1998) and Nordbo Glacier (Funk, 1990). Vielí and others (2000) used a water pressure dependent sliding law in a glacier flow model to explain the observed velocity increase on Hansbreen. In the evolution with time of tidewater glaciers a strong interaction between basal sliding and glacier geometry takes place. An increase of basal water pressure or a thinning of the glacier in the terminus region leads to enhanced basal sliding due to the reduction of effective pressure. The velocity increase induced by sliding leads to additional thinning and a further increase of sliding. It is therefore essential to include the effect of water pressure on basal sliding when modelling the dynamics of tidewater glaciers (Van der Veen, 1997).

### 3.3 Model description

The tidewater glacier model presented in this paper calculates the surface evolution and the two-dimensional flow regime (velocity, strain rate and stress-field) for a longitudinal section of a glacier.

#### 3.3.1 Field equations and flow law

Ice is treated as an incompressible viscous fluid. The equation for mass continuity and for linear momentum can be written as

$$\frac{\partial v_i}{\partial x_i} = 0 \quad (3.7)$$

and

$$\frac{\partial \tau_{ij}}{\partial x_i} + \rho g_j = 0 \quad (3.8)$$

where  $v_i$  are the velocity components,  $\rho$  is the ice density,  $g_j$  are the components of the acceleration due to gravity and  $\tau_{ij}$  the components of the stress tensor. The horizontal coordinate is  $x_1 = x$  and the vertical coordinate  $x_2 = z$ , which is positive

in upward direction. Glen's flow law relates the deviatoric stresses to the strain rates and can be written as

$$\dot{\epsilon}_{ij} = A\tau^{n-1}\sigma_{ij} \quad (3.9)$$

where  $\dot{\epsilon}_{ij}$  are the components of the strain rate tensor,  $\sigma_{ij}$  are the components of the deviatoric stress tensor and are given by  $\sigma_{ij} = \tau_{ij} - \frac{1}{3}\delta_{ij}\tau_{kk}$ . The effective shear stress  $\tau$  is defined by  $\tau^2 = \frac{1}{2}\sigma_{ij}\sigma_{ij}$ . Typical values for the flow law exponent  $n = 3$  and the rate factor  $A = 0.1 \text{ bar}^{-3}\text{a}^{-1}$  have been used in the model (Gudmundsson, 1999; Hubbard and others, 1998; Albrecht and others, 2000).

### 3.3.2 Basal boundary condition

The glacier flow model requires an appropriate boundary condition at the glacier bed to account for basal sliding. For the present flow model the proposed sliding law (Equation(3.6)) is used, which takes into account the effective pressure  $p_e$  and is based on current sliding theories. We set  $r = 1$  and  $m = 1$  such that we get a linear sliding law. Relation (3.6) is implemented in the model by adding a thin soft layer at the glacier base (Vieh and others, 2000). The viscosity of this basal layer has been chosen in order to fulfill the sliding relation (3.6) for a specific location. A detailed implementation is described in Vieli and others, 2000. The factor  $k \cdot p_e^{-1}$  in relation (3.6) is given as input for the model and the basal velocity and basal shear traction result by solving the system of field equations and boundary conditions.

The effective pressure changes in each time step and has to be calculated from the actual ice thickness and basal water pressure. The basal water pressure along the flowline of a glacier is poorly known and therefore assumptions must be made. For the model calculations presented in this paper water level is assumed to be on sea level which is the lower limit for a tidewater glacier. The water level is usually higher, especially during melting seasons, but in such a way the effect of a decreasing effective pressure towards the glacier front is taken into account. Changes in basal topography due to Sedimentation in the sea in front of the glacier or the formation of a terminal moraine are not considered in the model.

### 3.3.3 Surface boundary condition

The time evolution of the glacier surface is calculated. The surface boundary condition for the glacier surface is

$$\frac{\partial S}{\partial t} = b - v_x^s \frac{\partial S}{\partial x} + v_z^s, \quad (3.10)$$

where  $S(x, t)$  is the surface elevation,  $t$  the time,  $v_x^s(x, t)$  is the horizontal and  $v_z^s(x, t)$  the vertical component of the flow velocity at the surface and  $b(x, t)$  the surface mass balance. A linear relation between mass balance  $b$  and surface altitude  $S$  is assumed.

### 3.3.4 Calving front and upper boundary

At the upper boundary the horizontal velocity  $v_x(x = 0, z, t)$  is set to zero from the surface to the bed, but in vertical direction the ice can move, that means no ice flux into the model occurs through this boundary. With this boundary condition we simulate an ice saddle Situation.

For the frontal vertical ice cliff standing in the sea the hydrostatic pressure of the ocean water  $p_w$  is taken into account:

$$p_w = \begin{cases} 0 & z \geq \text{sea level} \\ -\rho_w g z & z < \text{sea level} \end{cases} \quad (3.11)$$

The *modified flotation* criterion (Equation (3.4)) is used to calculate the position of the calving front. For each time step the new terminus is moved to the position where the ice thickness  $h$  exceeds the flotation height by the fraction  $q=0.15$ . The ice mass that is removed corresponds to the mass loss due to calving. Following this method the calving rate is a result of the numerical model and is controlled by the ice velocity and the surface changes. This is in contrast to earlier models that included ad hoc assumptions for the calving rate. A floating terminus cannot be treated in our model.

In the case of slowly flowing tidewater glaciers melting at the water line is important. Therefore a prescribed calving rate can be included in the model, which is derived from the melt rates at the waterline according to Equation (3.5).

### 3.3.5 Numerical Solution technique

The stress and velocity fields are calculated with the commercial finite-element program MARC (1997). The code solves the full equations for the velocity and stress-fields (Gudmundsson, 1999), based on the finite-element method. A four node isoparametric quadrilateral Hermann-element is used with a bilinear interpolation function. For each time step the two-dimensional stress and velocity-fields along the flowline are calculated. With the calculated surface flow velocities and the mass balance input, the new glacier surface is determined by the surface boundary Equation (3.10). This equation is approximated by finite differences using the Two-Step Lax-Wendroff Method (Press and others, 1996), which is based on a forward-time centered-space scheme and is second order in time and space. This approximation was used and tested for this application in detail by Leysinger (1998). Nodes at the calving front are moved according to the velocity vector and the time step. For each time step the terminus position is updated according to the modified flotation criterion and a new grid is defined for the updated glacier boundary. This procedure to determine the new terminus position after a time step is identical for a retreating and an advancing scenario.

In the following model calculations a time step of 0.1 year is used and the glacier length is updated at each time step by using the modified flotation criterion (Equation (3.4)). To test if the calculated length change and the resulting calving rate is



independent of the chosen time step, the model was run for the same scenarios with different time steps. For retreat scenarios the obtained cumulative length change since the start of the simulation differs by at most 0.3% during periods of fast retreat with time steps varying between 0.05 and 0.1 years. For the slowly retreating periods the maximum difference is less than 0.05%. We conclude that the model results are not significantly influenced by the chosen time step.

## 3.4 Model experiments

### 3.4.1 Model input

A retreating and an advancing scenario across a submarine basal depression are calculated with the numerical model. A synthetic bed topography is assumed, which should be representative for a tidewater glacier (Fig. 3.2). The model calculations

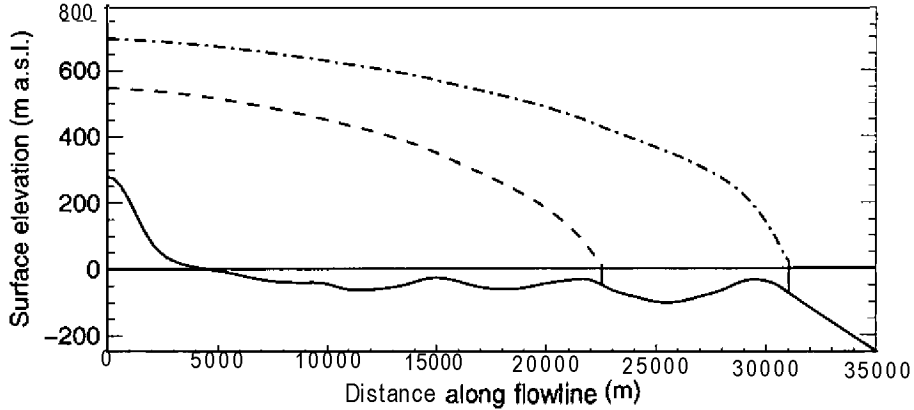


Figure 3.2: **Glacier bed (solid line)** and initial surface topographies **used** for model calculations for the retreating (dashed-dotted line) and the advancing scenario (dashed line). Both steady-state surface **profiles** are calculated by using the same mass **balance**.

start with steady state glacier surfaces obtained from model calculations for prescribed constant mass balances. A typical simplified mass balance function from a tidewater glacier in Svalbard (Hansbreen; Jania and Kaczmarek, 1997) is used, in which the mass balance linearly depends on altitude and is constant above a critical altitude  $h_a$  (Fig. 3.3):

$$b = \begin{cases} a_0 S(x) + a_1 + \delta b & S(x) \leq h_a \\ a_0 h_a + a_1 + \delta b & S(x) > h_a, \end{cases} \quad (3.12)$$

where  $S(x)$  is the surface elevation and  $\delta b$  is a Parameter to impose changes in mass balance and we specify the mass balance gradient as  $a_0 = 0.0061 \text{ a}^{-1}$ , the constant as  $a_1 = -2.3 \text{ m a}^{-1}$  and  $h_a = 450 \text{ m}$ . The scenarios are forced by shifting the mass

balance by  $\delta b$  (Fig. 3.3). For the model calculations a water pressure within the glacier corresponding to sea level is assumed. Seasonal variations of the inglacial water level are not included.

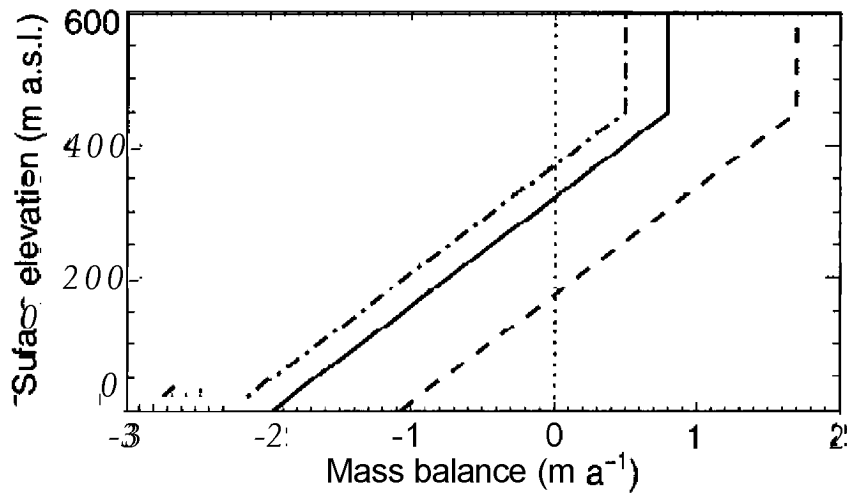


Figure 3.3: Parameterised mass balance used for the retreating (dashed-dotted line) and the advancing scenario (dashed line). The solid line indicates the mass balance used to calculate the initial steady state surface geometries.

### 3.4.2 Model results

#### Retreating scenario

The glacier retreat is forced by shifting the mass balance function (Equation (3.12)) of  $\delta b = -0.3 \text{ m a}^{-1}$  (Fig. 3.3) for the whole time period of model calculations. The modelled retreat is shown in Figures 3.4 and 3.5. Three different phases can be pointed out. In the first phase, the terminus is slowly retreating until the top of the submarine hill is reached (point A). From this point the rate of retreat increases as the glacier terminus gets into deeper water, resulting in a very rapid retreat and in high calving rates (second phase). Once the deepest part of the basal depression (point B) is passed, the glacier terminus moves into shallower water, the rate of retreat is reduced and the Situation resembles that of the first phase. With the retreat into deeper water, the calving rate and the velocity at the terminus increase (Fig. 3.5). However, the calving rate increases faster than the ice velocity resulting in a rapid terminus retreat. Although the ice thickness decreases, the surface flow velocity significantly increases along the flowline towards the calving front over the entire retreating period (Fig. 3.6). This is mainly due to increased basal sliding near the front, caused by the decreasing effective pressure. In the terminus region the ice flow velocities undergo large changes with time due to changes in basal sliding, whereas further upglacier the velocity changes are small (Fig. 3.6). During the phase of rapid retreat strong surface lowering takes places (Fig. 3.4), leading to the high calving rates (Fig 3.5 b).

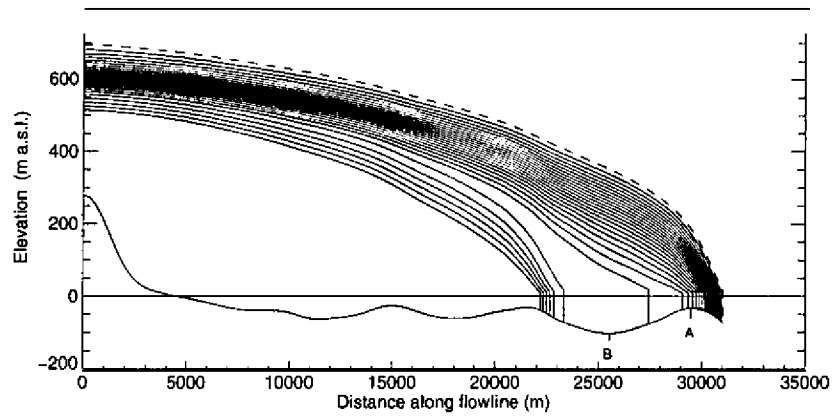


Figure 3.4: Evolution with time of the glacier surface for the retreating scenario. The time interval between two surface profiles is 50 years. The dashed line is the starting surface. The top of the bedrock hill and the deepest point in the basal depression are indicated by *A* and *B*, respectively.

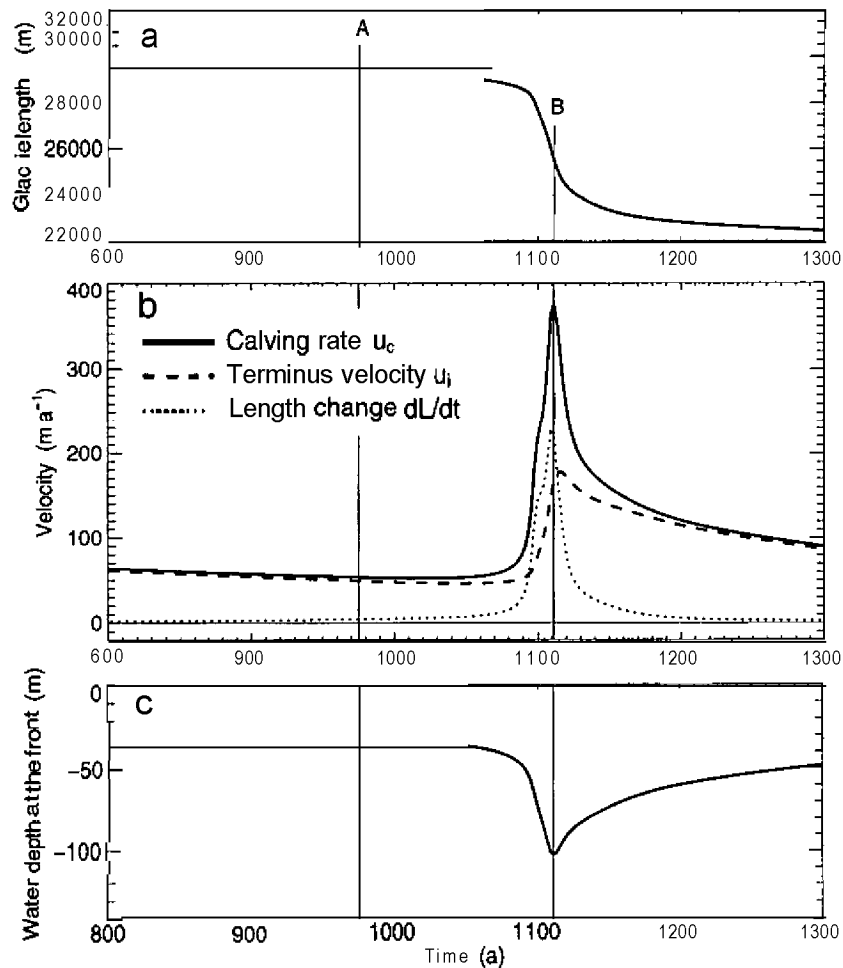


Figure 3.5: Retreating scenario: Evolution with time of (a) the glacier length  $L$ , (b) the calving rate  $u_c$ , the velocity at the terminus  $u_i$  and the length change  $dL/dt$  and (c) the water depth  $d$  at the terminus between 800 and 1300 years.

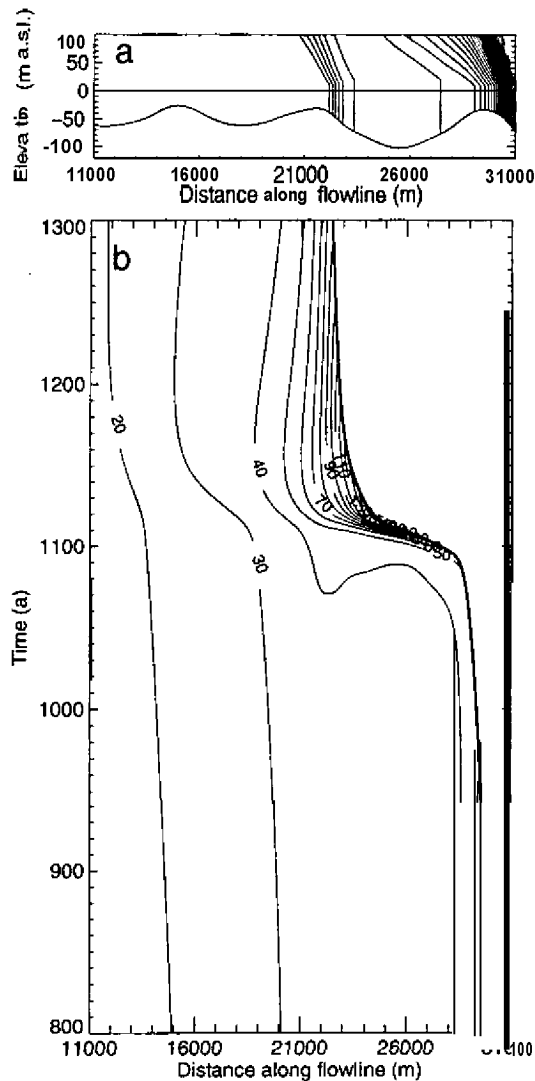


Figure 3.6: Retreating scenario: (a) Glacier bed elevation along the flowline and front position (same as Fig. 3.4). (b) Contour plot of temporal evolution of the surface flow velocity along the flowline. The contour line interval is  $10 \text{ m a}^{-1}$ .

The mass balance function was shifted at the beginning of the calculations but then kept constant for the whole model period, corresponding to constant climatic conditions. The sudden rapid retreat takes place at the location of the basal depression after a period of 1100 years of constant mass balance function or constant ELA (Fig. 3.7). Thus, the change of glacier length does not *immediately* reflect the climatic signal. Although the input mass balance function is constant with time, the average surface net balance (surface accumulation and ablation without calving) undergoes changes due to changes in surface elevation and geometry (Fig. 3.7b). During the phase of rapid retreat the ablation is dominated by calving and leads to a rapid shrinkage of the ablation zone which is the cause for the sudden increase of the AAR (Fig. 3.7c) and the average surface net balance. This illustrates that a time serie of average surface net balance of a glacier must be used with care if interpreted as indicator for changes in climate.

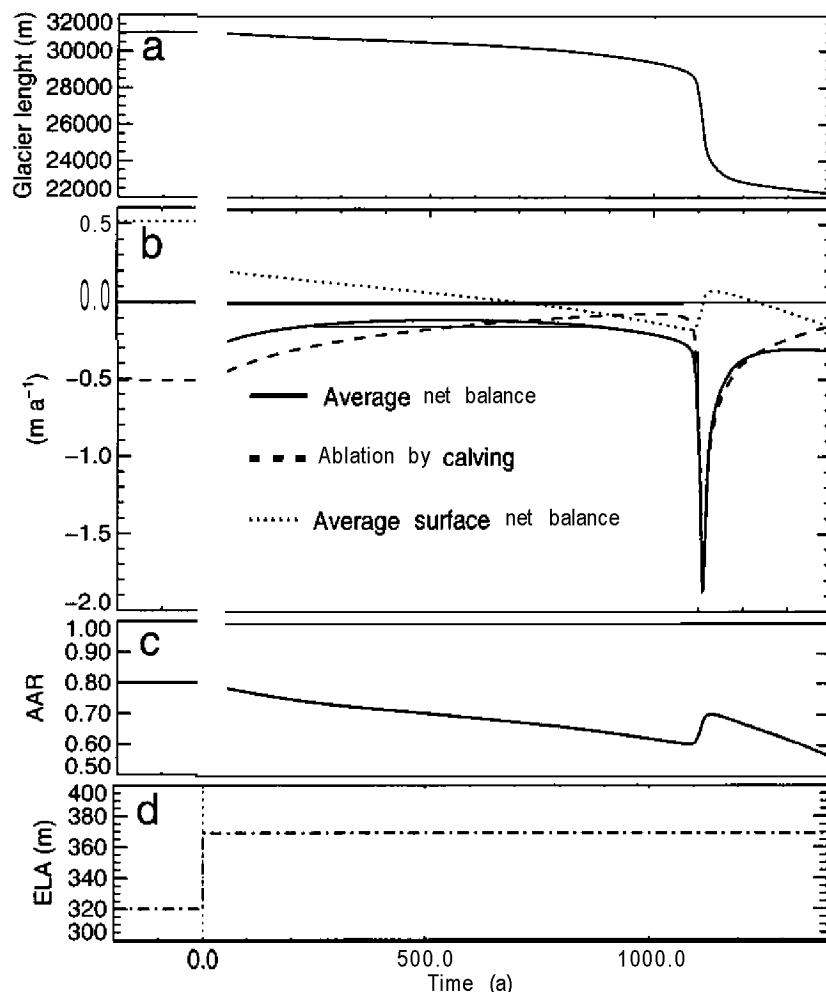


Figure 3.7: Mass balance changes with time for the retreating scenario. At time zero the shift in the mass balance function was performed and the model calculations were started. (a) Glacier length with time. (b) Net balance, surface net balance (surface accumulation and ablation without calving) and ablation by calving are shown with time as values averaged over the glacier area. (c) Accumulation ablation area (AAR) with time. (d) Equilibrium line altitude (ELA) as an index for the input mass balance function with time.

### Advancing scenario

A glacier advance is forced with a shift of the mass balance function (Equation (3.12)) of  $\delta b = +0.9 \text{ m a}^{-1}$  (Fig. 3.3). The glacier is thickening due to the positive mass balance and slowly starts to advance (Fig. 3.8 and 3.9). While the glacier is advancing, the calving front reaches deeper water leading to higher calv-

ing rates and ice velocities at the terminus. The rate of advance is very small and decreases with increasing water depth. Once the terminus passes the deepest point of the basal depression (B), the calving rate decreases rapidly accompanied by a smaller reduction of the terminus velocities. This leads to a rapid advance until the terminus overrides the basal hill (A). For a short time period the calving rate even vanishes because the terminus slides uphill and the critical height above buoyancy  $h_c$  is always exceeded during this step. During this phase, processes other than the flotation criterion may control the calving rate.

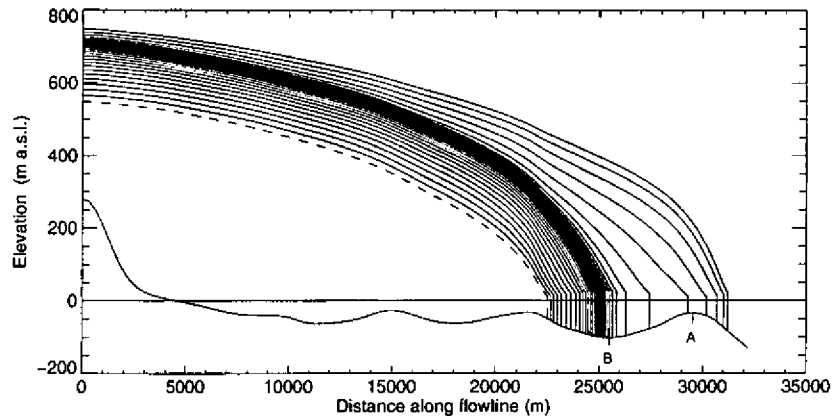


Figure 3.8: Evolution with time of the glacier surface for the advancing scenario. The time interval between two surface profiles is 20 years. The dashed line is the starting surface. The top of the bedrock hill and the deepest point in the basal depression are indicated by *A* and *B*, respectively.

For this reason an additional model run with the same scenario was performed which included melting at the waterline (Fig. 3.10). A constant melting rate  $u_c^{\text{melt}} = 80 \text{ m a}^{-1}$  at the calving front is assumed (Equation (3.5)): resulting in a constant calving rate  $u_c = u_c^{\text{melt}}$ . This prescribed melt induced calving rate is only considered if the calving rate inferred by the flotation criterion drops below  $80 \text{ m a}^{-1}$ . This is the case during the rapid advance. Due to the prescribed calving rate during this phase, the rate of advance is slightly reduced at the beginning of the accelerated advance (Fig. 3.10) but the height above buoyancy at the terminus starts to grow and exceeds the critical height  $h_c$ . This leads to higher frontal flow velocities (Fig. 3.10 b). Once the terminus passed the frontal moraine and reaches deeper water the buoyancy induced calving is again controlling the front position change. Despite the different length change during the fast period of advance compared to the case without a prescribed melt induced calving rate, the final positions of the glacier front are almost identical (Fig. 3.10).

For an additional model run with a slightly smaller shift of the mass balance function of  $\delta b = +0.7 \text{ m a}^{-1}$  instead of  $0.9 \text{ m a}^{-1}$  the glacier is not able to overcome the basal depression (Fig. 3.10). A steady state is reached already in the downslope region of the depression.

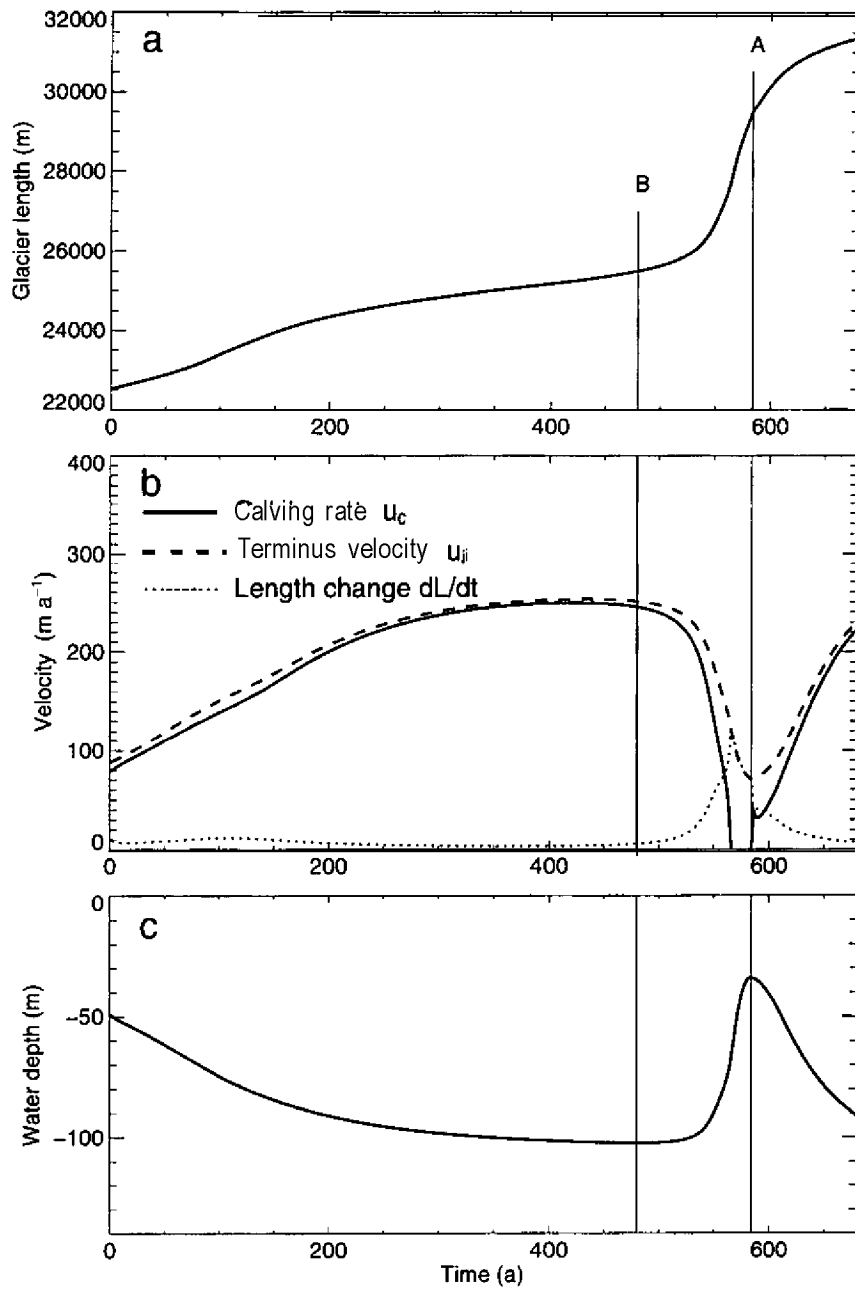


Figure 3.9: Advancing scenario: Evolution with time of (a) the glacier length  $L$ , (b) the calving rate  $u_c$ , the velocity at the terminus  $u_t$  and the length change  $dL/dt$  and (c) the water depth  $d$  at the terminus.

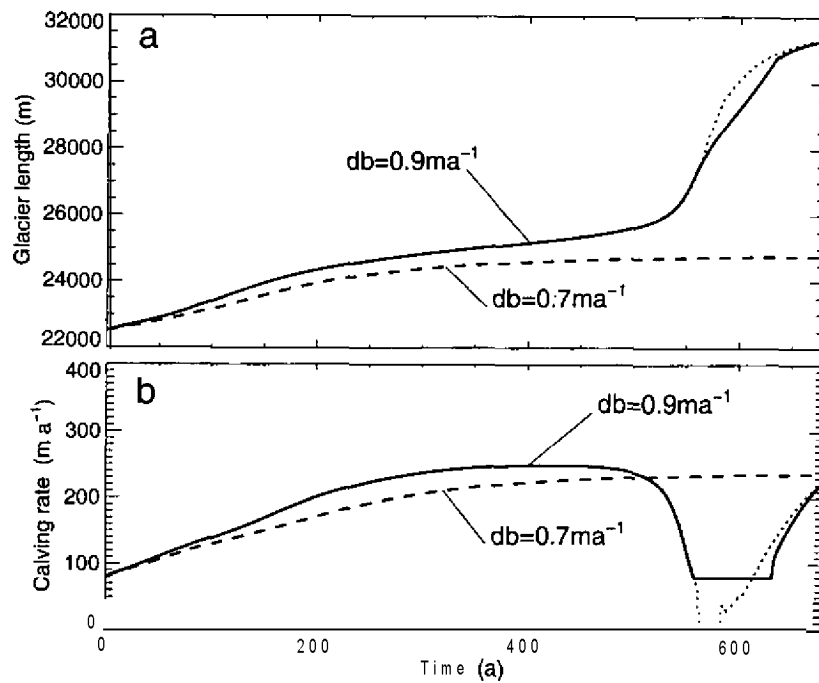


Figure 3.10: Different advancing scenarios: (a) Evolution of glacier length with time. The solid line represents the case of the advancing scenario with a prescribed melt induced calving rate of  $80 \text{ m a}^{-1}$ . The dotted line shows the advancing scenario without a prescribed calving rate (same as in Fig. 3.8) and the dashed line is the advance scenario with reduced mass balance shift of  $0.7 \text{ m a}^{-1}$  instead of  $0.9 \text{ m a}^{-1}$ . (b) Calving rates and terminus velocities corresponding to the advance scenarios that are shown in (a).

### *Sensitivity of the model results*

To examine the sensitivity of the modelled scenarios on the choice of the height above buoyancy, additional model runs with a slightly different  $q$  have been performed (Fig. 3.11). A larger  $q = 0.18$  instead of  $q = 0.15$  leads to higher calving rates and frontal flow velocities and therefore to a higher mass loss by calving, whereas a smaller  $q = 0.12$  leads to a reduced mass loss by calving. The retreat rates are not changed significantly, but the onset of rapid retreat is shifted in time, but still fixed to the location of the basal depression. Retreating scenarios are only affected to a small degree by changing  $q$ , whereas advance scenarios show a qualitatively different behaviour. For the advancing scenario a reduced  $q = 0.12$  results in a faster advance, because the mass loss by calving is reduced, with respect to  $q = 0.15$ . But the general advance behaviour with respect to basal topography is similar. With  $q = 0.18$  in the advancing scenario, the terminus does not overcome the basal depression because the mass loss by calving is too large and a steady state geometry is reached. In contrast to the retreating case, the total mass loss by calving is also high during the phase of slow position change. For this reason, a change in  $q$  has a significant effect on the change of terminus position for the advancing scenario.



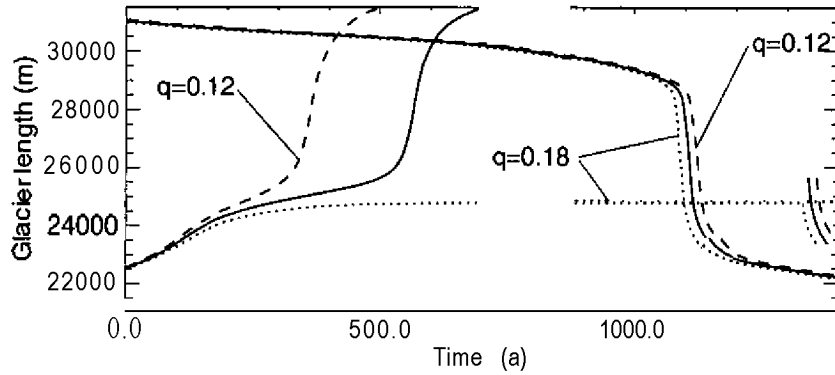


Figure 3.11: Retreating and advancing scenarios with variable height above buoyancy. The solid line represents the modelled evolution of the glacier length presented before ( $q = 0.15$ ) and the dashed and dotted lines show the evolution of glacier length for a slightly different height above buoyancy with  $q = 0.12$  and  $q = 0.18$  respectively.

Increased or reduced water depth in the region of the basal depression by 10% results in a qualitatively very similar dynamical behaviour (Fig. 3.12) as presented before with varied  $q$  (Fig. 3.11). The magnitude of the rate of retreat or advance is different in the region of the basal depression because the calving rate is sensitive to changes in basal slope and water depth. For the case of the shallower depression,  $dL/dt$  is reduced during the phase of rapid retreat due to a reduced mass loss by calving, whereas for the deeper depression the rapid retreat is accelerated due to enhanced calving. For the advancing scenario with increased water depth the glacier does not overcome the basal depression, because the mass loss by calving becomes too large.

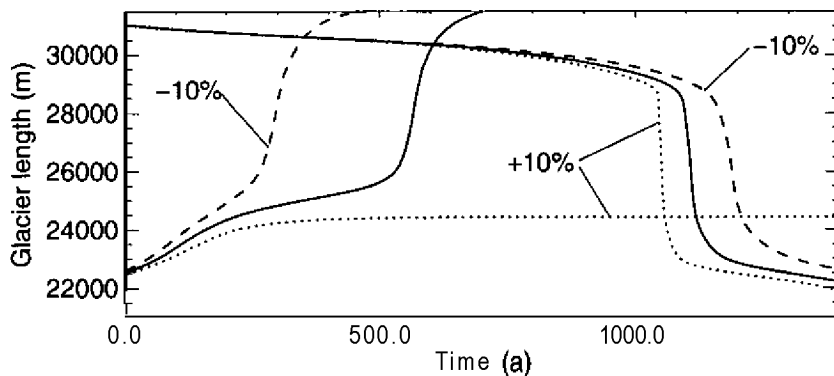


Figure 3.12: Retreating and advancing scenarios with variable water depth in the region of the basal depression. The solid line represents the modelled evolution of the glacier length presented before and the dashed and dotted lines show the evolution of glacier length for a change of water depth in the region of the basal depression of -10% and +10% respectively.

These sensitivity considerations on the critical height above buoyancy and the magnitude of the basal depression confirm the effect of basal topography on the dynamics of tidewater glaciers obtained with the advancing and retreating scenarios from before. Nevertheless, in the advancing case a Variation of  $q$  or the magnitude of the basal depression can have a significant effect on the qualitative behaviour of the glacier evolution.

### 3.5 Discussion

The modelled relation between calculated calving rate and water depth using the modified flotation criterion (Equation(3.4)) is qualitatively in good agreement with the linear relation suggested from observations (Brown and others, 1982), however, only for slow advances or retreats (Fig. 3.13 a and b). For situations of rapid changes the calving rate increases non linearly with water depth. Meier and Post (1987) pointed out that the linear calving law is probably limited to the case of slowly changing tidewater glaciers by arguing that in the case of rapid retreat, flotation may be the determining factor. This was also supported by the data from rapidly retreating Columbia Glacier (Van der Veen, 1996) and our model results clearly confirm this limited validity of the linear calving law.

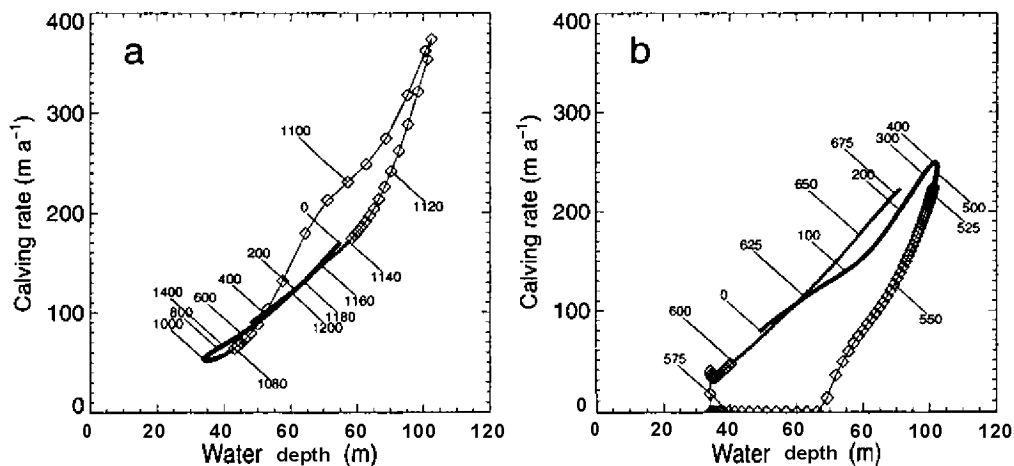


Figure 3.13: Calculated calving rates plotted against water depth for (a) the retreating scenario and (b) the advancing scenario. Each cross or diamond corresponds to the calculated values for a time step of one year. The numbers denote the time evolved in years. The diamonds mark periods of rapid front position changes which take place between 1080 and 1140 years for the retreat and between 520 and 600 years for the advance scenario.

Considering the flotation criterion for the calving process, the retreat or advance is primarily a consequence of thinning or thickening of the glacier in the terminus region, which is in general due to mass balance changes. The magnitude of the

thickness and the therefore length change depends, beside mass balance, on bed geometry and basal sliding. For example, during the rapid retreat through the basal depression, the typical flow acceleration towards the calving front is enhanced because basal sliding increases with water depth (Fig. 3.6). This leads to a much higher mass flux divergence in the frontal region and finally to an additional surface lowering.

In presence of a basal depression, a small change of mass balance can lead to a drastic change in the terminus position. It could be shown that thinning due to a slightly negative mass balance is the triggering process for a rapid retreat. This result supports the concept of Van der Veen (1996) to explain the observed rapid retreat of Columbia Glacier, which suggests that the rapid retreat is initiated and maintained by thinning of the glacier. The model calculations demonstrate that rapid changes of tidewater glaciers, as often observed, are mostly an effect of bed topography at and behind the terminus and only to a minor degree a *direct* reaction to a mass balance change. This was already described qualitatively on the base of observations by various authors (Meier and Post, 1987; Warren, 1993; Naruse and others, 1997).

The model calculations performed with the two scenarios confirm the concept of rapid retreat and slow advance of a tidewater glacier through a basal depression which was qualitatively described by Meier and Post (1987). The obtained simultaneous increase of the terminus velocity with increasing calving rate illustrates that an accelerated retreat through a basal depression is not obvious. The performed model experiments clearly show that whether a retreat or advance is slow or fast not only depends on water depth, but also on the sign of the basal slope at the terminus. Rapid changes of the terminus position occur where the bed slopes up in flow direction, whereas in regions where the bed slopes down the changes are slow.

In contrast to the slow advance with progression into deeper water, a fast advance into shallower water is predicted by the model, which has been observed qualitatively for Taku Glacier (Motyka and others, 1995) and Hubbard Glacier (Mayo, 1989). But for both cases sedimentation processes and the formation of a terminal push-moraine were involved in the rapid advance.

The model results enables us to identify regions of stable and unstable terminus positions. A downsloping bed in flow direction allows a stable or slowly changing position. On the other hand, when basal elevation increases in flow direction the terminus position is not stable and a rapid retreat or advance to a stable region is inevitable. As a consequence, in the presence of a basal depression in the terminus region of a tidewater glacier more than one steady state surface and terminus position exist for a given mass balance, depending on the initial geometry. In Figure (3.2) two different steady state geometries, calculated with the same mass balance, are shown. The lower steady state was calculated with an initial terminus behind the basal depression, whereas for the other steady state it was situated in front of the basal depression,

In the case of a progression of the terminus into deeper water the rate of advance slows down, because the mass loss due to calving increases. Thus, a long time is required to build up enough mass to advance. The model results of the advancing

scenario show that to overcome a basal depression, a long time period of large positive mass balances is required. If the mass balance is not large enough, the glacier will reach a steady state and the calving front will stay in the downslope region of the depression (Fig. 3.10). For deep basal depressions, such as beneath Columbia Glacier, a very large positive mass balance over very long time periods (>1000 a) may be anticipated as a necessary condition for a readvance across the depression. Looking at the long time periods needed for the advance through a bed depression, other processes may support the advance of the glacier terminus. Rock Sedimentation in the glacier forefield and the formation of morainal banks would reduce the water depth and the calving activity and facilitate an advance (Paterson, 1994; Motyka and Post, 1995; Fischer and Powell, 1998). These processes are not considered in the presented dynamic model, which is posing a limitation for modelling an advance of a tidewater glacier.

Other processes, such as lateral drag or cross section changes along the flowline may be important. For example a narrowing of a valley or an increase in lateral drag may lead to a slower retreat of a tidewater glacier. However, such 3-dimensional processes and the possible onset of floating of the ice tongue cannot be treated with the present model.

### 3.6 Conclusions

Advance and retreat of the terminus of rather small and slowly flowing grounded tidewater glaciers are simulated with a numerical glacier model. The model solves the full force balance equations to compute stress and velocity fields and calculates the time evolution of the glacier surface for a given mass balance scenario. Basal sliding is implemented through a sliding parameterisation based on basal water pressure corresponding to a water table at sea level. Calving is implemented with the flotation model, in which the calving front is shifted at each time step to the position where the frontal ice thickness exceeds flotation height by a prescribed value. Thus, the calving rate is an output of the model, which is in contrast to previous modelling approaches. For slowly flowing glaciers that are considered here, other processes such as melting along the waterline at the calving front may become the controlling process. Therefore a calving rate equivalent to the melt rate can additionally be prescribed in the model.

The performed model calculations confirm the cycles of slow advance and rapid retreat through a basal depression suggested by Meier and Post (1987). For a slowly advancing or retreating situation the known empirical relation between water depth and calving rate (Brown and others, 1982) is qualitatively reproduced by the model, but not for rapidly changing situations. Thus, this study demonstrates, that unstable rapid retreats of tidewater glaciers and the well known empirical relation between calving rate and water depth can be explained with a model in which a height above buoyancy criterion is prescribed.

The model calculations further show that calving not only depends on water depth but also on the sign of the basal slope in the terminus region. Rapid changes of

the terminus positions preferably occur in regions where the bed slopes up in flow direction and are therefore mostly an effect of bed topography rather than a direct reaction to changes in climate. In our model experiments thinning due to a change in climate and therefore in mass balance is only the triggering process for a rapid retreat through a basal depression.

If buoyancy, parameterised with the flotation criterion, is the dominant driving factor for calving, the obtained rate of advance or retreat is primarily controlled by changes in the surface elevation in the terminus region, and much less by the calving mechanism itself. This means that the magnitude of the calving rate is a result of the glacier dynamics and not vice versa. Surface elevation changes near the terminus are strongly affected by changes in basal sliding and bed topography. This sensitivity of glacier change to basal topography has important consequences regarding the future behaviour of tidewater glaciers with respect to climate change. A simple parameterisation in terms of easily available information such as surface topography, ice flow velocity and terminus height alone cannot be expected. Because basal depressions in the frontal region are typical for tidewater glaciers, rapid retreats are likely, even if the mass balance changes are small and slow. To predict the length change of tidewater glaciers, especially for short term changes, the basal topography in the frontal region must be known.

# Paper 4

## The retreat of a tidewater glacier: observations and model calculations on Hansbreen

### Abstract

Based on observations and model calculations the retreat over the last two decades of Hansbreen, a tidewater glacier in southern Spitsbergen, is investigated. The presented observations of the calving front position between 1982 and 1998 show an abrupt retreat in 1990, which is suggested to be related to a basal depression. The additionally observed seasonal variations of the front position are mainly due to variations of the calving rate. The observations of Hansbreen further indicate, that during periods of slow front position changes, melting at the waterline may play an important role for triggering the process of calving.

To give more insight on the causes of the observed abrupt retreat of Hansbreen between 1982 and 1998, its evolution is simulated with a numerical model for the dynamics of tidewater glaciers. A seasonal calving rate, estimated from the observations, is prescribed in the model and additionally a flotation model is implemented, in which for each time step the part of the glacier terminus, which is below a critical height above buoyancy, is removed. The model calculations show that the process of buoyancy induced calving is controlling the abrupt retreat of Hansbreen through the basal depression. The generally small retreat rate between 1982 and 1998 primarily is a consequence of the assumed mass balance and the prescribed seasonal calving rate, whereas the location of the jump in retreat is found to be independent on these parameters and is fixed to the position where the basal depression is located. Thus, the abrupt retreat of Hansbreen is mainly an effect of basal topography in the terminus region and not a direct response to a change in mass balance.

## 4.1 Introduction

The dynamical behaviour of tidewater glaciers, which are considered as *grounded* calving glaciers from which icebergs are discharged into the ocean, is important with respect to their reaction to changes in climate. Length changes of tidewater glaciers are not only a result of a change in surface mass balance, they are additionally affected by calving at the terminus. Rapid retreats related to increased calving rates have been observed for several grounded calving glaciers (Van der Veen, 1996; Warren and Aniya, 1999). These rapid changes in front positions were suggested to be less a direct response to changes in climate but are strongly affected by the local basal topography near the terminus (see Paper 3; Meier and Post, 1987; Warren, 1993; Naruse and Skvarca, 2000).

In this paper we focus on the dynamical behaviour of Hansbreen, a tidewater glacier, in southern Spitsbergen. With a length of 16km and frontal Aow velocities up to  $150 \text{ m a}^{-1}$ , Hansbreen is a relatively small, thin and slowly flowing tidewater glacier. Detailed front position records between 1982 and 1998 exist and the basal topography of the terminus region is known. Such a data set only exists for a few tidewater glaciers and gives us the opportunity to investigate the effect of basal topography on the change of terminus position based on observational data and by applying a numerical model of the dynamics of tidewater glaciers. A special focus is given on the observed rapid retreat of Hansbreen through a basal depression in 1990.

### *Calving*

Calving is a very efficient ablation mechanism and therefore it is an important process for the dynamics of tidewater glaciers. Based on observations, empirical relations for the calving rate  $u_c$ , which is defined as the difference between ice velocity at the terminus and the rate of change of the glacier length, have been determined. A linear relation between the calving rate  $u_c$  (in  $\text{m a}^{-1}$ ) and the water depth  $d$  (in m) at the terminus was suggested:

$$u_c = \beta \cdot d, \quad (4.1)$$

with coefficients  $\beta = 27.0 \text{ a}^{-1}$  for sea water (Brown and others, 1982) and  $\beta = 2.5 \text{ a}^{-1}$  for freshwater (Funk and Röthlisberger, 1989). For a given water depth the calving rate for freshwater is expected to be one order of magnitude below the value found for tidewater glaciers.

Basal depressions in the frontal region are observed to be typical for tidewater glaciers. According to the empirical relation (4.1) the calving rate increases with a retreat of the terminus into deeper water and a rapid unstable retreat through a basal depression is therefore expected. This has been observed for several tidewater and freshwater calving glaciers and suggests that these glaciers undergo cycles of slow advance and rapid retreat through basal depressions (Meier and Post, 1987). For the case of rapidly changing glaciers the validity of these linear empirical relations was questioned (Van der Veen, 1996; Meier and Post, 1987). Furthermore,

studies of the large Patagonian calving glaciers suggest a similar relation for glaciers calving into lakes and tidewater (Venteris, 1999).

During rapid retreat of Columbia Glacier in the 1980's, the terminus position appeared to retreat to the position where it did approach flotation thickness (Meier and Post, 1987). On the base of these observations Van der Veen (1996) suggested an alternative treatment of calving to the empirical relations for the calving rate discussed before. In this *flotation* model the part of the terminus that is too close to flotation calves off due to buoyancy forces and weakening of the ice by bottom crevasses (Van der Veen, 1998). The terminus of the glacier retreats to the position, where the ice thickness  $h$  exceeds the flotation height by an amount of  $h_o$  (Van der Veen, 1996). The height at the terminus  $h_c$  is then

$$h_c = \frac{\rho_w}{\rho_i}d + h_o, \quad (4.2)$$

where  $\rho_w$  is the density of sea- or freshwater and  $\rho_i$  the density of glacier ice. For Columbia Glacier  $h_o = 50$  m was found. This *flotation model* is found to be consistent with the observed rapid retreat of grounded calving glaciers in Patagonia, for which a similar critical height above buoyancy was derived (Venteris, 1999).

In a *modified flotation* model the fixed critical height above flotation  $h_o$  in Equation 4.2 is replaced by

$$h'_o = q \cdot \frac{\rho_w}{\rho_i}d, \quad (4.3)$$

which corresponds to a fraction  $q \sim 0.15$  of the flotation thickness (see Paper 3). The value of  $q$  may vary from glacier to glacier, but this does not significantly change the general dynamical behaviour of tidewater glaciers. Using the *modified flotation criterion* for calving in a numerical model for the dynamics of tidewater glaciers, the length change through a basal depression is discussed in Paper 3. These model calculations confirm that rapid changes of tidewater glaciers are mostly an effect of bed topography and to a minor degree a direct reaction on mass balance changes. Furthermore, it is shown that rapid retreats take place in regions where the bed slopes up in flow direction and that for periods of rapid changes calving rates do not follow the empirical relations.

#### Melting at the calving front

In most studies concerning the calving process, subaqueous melting at the terminus is neglected, because the total mass loss by melting at the calving front is found to be small compared to the mass loss by calving (Powell, 1988). For the submarine melt rate  $m_s$  (in  $\text{m a}^{-1}$ ), due to buoyant vertical convection, Neshyba and Josberger (1980) suggested a relation of the form

$$m_s = 2.14 \cdot T^{1.54}, \quad (4.4)$$



where  $T$  is the water temperature in °C above the freezing point. Based on this study, Jania (1988) estimated for Hansbreen a total mass loss by submarine melting below 5% to 10% of the mass loss by calving. The energy in the far-field water is often sufficient to melt ice at rates in the range of observed calving rates, but the problem is to bring this water to the calving front (Hanson and Hooke, 2000). From theoretical, laboratory and field studies on the deterioration of icebergs melting concentrated to the waterline is known to be one to two order of magnitudes higher than below the surface (El-Tahan and others, 1987), due to wave erosion. The melt rate  $m_w$  (in  $\text{m s}^{-1}$ ) at the waterline is specified as (White and others, 1980):

$$m_w = 1.46 \cdot 10^{-4} \left( \frac{R}{H} \right)^{0.2} \frac{H}{P} \cdot T, \quad (4.5)$$

where  $T$  is the water temperature in °C,  $H$  the the wave height in meters,  $P$  the mean wave period in seconds and  $R$  the roughness height of the ice surface in meters, for which a suggested value is  $R = 0.01$  m (El-Tahan and others, 1987). Melting concentrated to the waterline does change the shape of the front and leads to calving of overhanging ice slabs above the undercut notch. Although the total mass loss by melting is still small, melting at the waterline plays for icebergs an important role by triggering the process of calving. For icebergs 80% of the deterioration rate is found to be due to *melt induced* calving, which includes melting at the waterline and the resulting calving of the overhanging slabs, and only 2% is due to submarine melting by buoyant convection (El-Tahan and others, 1987). For icebergs in the open sea, melt rates in the range of  $2 \text{ m d}^{-1}$  are common (El-Tahan and others, 1987; Robe and others, 1977) and strong seasonal variations occur due to seasonal changes of sea temperature. During winter time sea-ice cover additionally prevents wave erosion at the waterline.

On several slowly flowing grounded calving glaciers a notch melted out at the waterline and the resulting breaking off of the thin ice lamellas above it is also observed (Warren, 1999; see Paper 3) and has been described in detail for Maud Glacier (NZ) by Kirkbride and Warren (1997). Laboratory studies support the validity of equation (4.5) for the Situation of tidewater glaciers (White and others, 1980; Josberger, 1977). Melt rates and therefore melt induced calving rates are expected to be smaller for tidewater glaciers than for icebergs in the open ocean, due to differences in the sea surface conditions and salinity, but the seasonal pattern may be very similar.

### *Basal sliding*

Basal sliding is an important process for controlling the dynamics of tidewater glaciers. Increasing basal sliding velocities are expected for a decreasing effective pressure  $p_e$  at the bed (Bindschadler, 1983; Boulton and Hindmarsh, 1987), which is defined as the ice-overburden minus the basal water pressure. Within a tidewater glacier the basal water pressure amounts at least to the water pressure that corresponds to sea level. Therefore the basal water pressure is expected to come closest to the ice-overburden pressure and leads to enhanced basal sliding near the terminus. This effect is indicated by the observed high sliding velocities for tidewater glaciers (Meier and Post, 1987) and the typical increasing flow velocities towards the calving front (Vieli and others, 2000).

## 4.2 Hansbreen: Geographical setting and observations

Hansbreen is a tidewater glacier situated at Hornsund in southern Spitsbergen (Fig. 4.1a). It is about 16 km long and covers an area of 57 km<sup>2</sup>. The glacier is grounded and ends with a 1.3 km wide calving front. Glaciological investigations were initiated during the 3rd International Geophysical Year by Kosiba (1960), continued by Baranowski (1977) and since 1982 extended by Jania (1988, 1994). Surface topography is known for the years 1936 and 1990 from aerial photogrammetry. Bed topography was investigated by radio-echo-soundings (Glazovsky and others, 1991) and depth soundings of the fjord in front of the glacier (Gizejewski, 1997). The AAR for Hansbreen is about 0.38 and the ratio of calving to the surface melt is about 0.22 (Jania and Kaczmarska, 1997). Glacier front positions and surface flow velocities have been measured by terrestrial photogrammetry in the frontal part of the glacier since 1982 (Jania and Kolondra, 1982) and in a longitudinal profile in 1998 by terrestrial survey (Vieli and others, 2000) and in 1999 by GPS (Fig. 4.1a; see Paper 2). First front position measurements date from 1918 and 1936. Since 1957 the calving front of Hansbreen has been monitored more frequently using the method of terrestrial photogrammetry. From 1936 until 1982 Hansbreen retreated by about 1.4 km, corresponding to a mean retreat rate of 22.5 m a<sup>-1</sup>. The retreat was interrupted by a few short periods of advance in 1957-1959 and 1973-1977 (Jania and Kaczmarska, 1997).

### 4.2.1 Frontal positions 1982-1998

Since 1982 the position of the calving front of Hansbreen has been monitored systematically by the method of terrestrial photogrammetry (Jania and Kolondra, 1982). From three different baselines, repeated stereoscopic photos were taken (Fig. 4.1b), at least once a year, usually during the summer season. For the years 1986 and 1991/92 nearly complete annual cycles were recorded with a temporal resolution of about two months. There are no observations in winter between November and February because of darkness during polar night. The observed front positions of Hansbreen between 1982 and 1998 are shown in Figure 4.1b. The glacier length averaged over a 200m wide stripe along the flowline for the same period is shown in Figure 4.2. A general slow retreat of Hansbreen since 1982 as well as seasonal variations of the terminus position are observed.

From 1982 until 1990 the terminus continuously retreated at a rate of about 28 m a<sup>-1</sup> (Fig. 4.2). Between the years 1990 to 1991 the front position record shows a jump in the retreat of about 280 m (Fig. 4.2). The front positions before and after this abrupt change are clearly separated from each other (Fig. 4.1b). This sudden retreat is more pronounced in the western part, where the water is deeper than in the eastern part. After 1991, the terminus was more or less stable with a slight advancing tendency.

The terminus positions of Hansbreen additionally show seasonal variations with an advance during winter and a retreat during summer (Fig. 4.2). During the well documented years 1986 and 1991/92 (Fig. 4.2b and Fig. 4.2c) the terminus advances

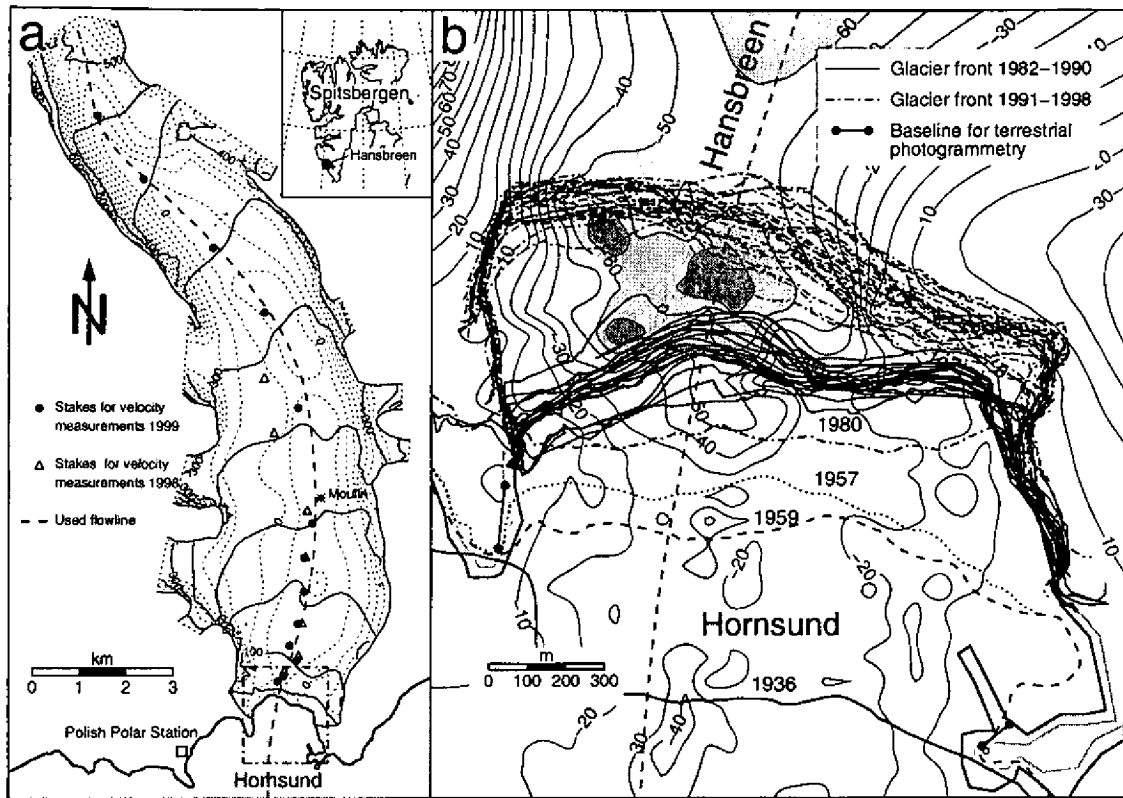


Figure 4.1: (a) Map of Hansbreen showing glacier surface (solid contour lines) and bed (dotted contour lines) topography. The contour intervals are 50m. The dashed line indicates the flowline used for the model calculations and the star symbol shows the location of the glacier moulin, in which water pressure was monitored. The locations of the stakes used for the velocity measurements are shown with triangles (1998) and black dots (1999). The dashed-dotted rectangular frame indicates the zoomed area shown in figure (b): Map of the frontal part of Hansbreen showing terminus positions before the abrupt retreat in 1991 (solid lines) and after it (dashed-dotted lines). Basal topography is shown as contour plot with a contour interval of 10 m. The dashed line indicates the flowline used for the model calculations.

from October until beginning of June with a rate of  $0.33\text{m d}^{-1}$  and  $0.55\text{m d}^{-1}$ , respectively. The retreating phase starts in June and continues until October with a retreat rate of  $1.04\text{m d}^{-1}$  for summer 1986. For other years with less temporal resolution of the front position measurements, estimations for the summer retreat generally give smaller values than the value of 1986 (Table 4.1). The inferred summer retreat and winter advance rates are consistent with results of Jania (1988).

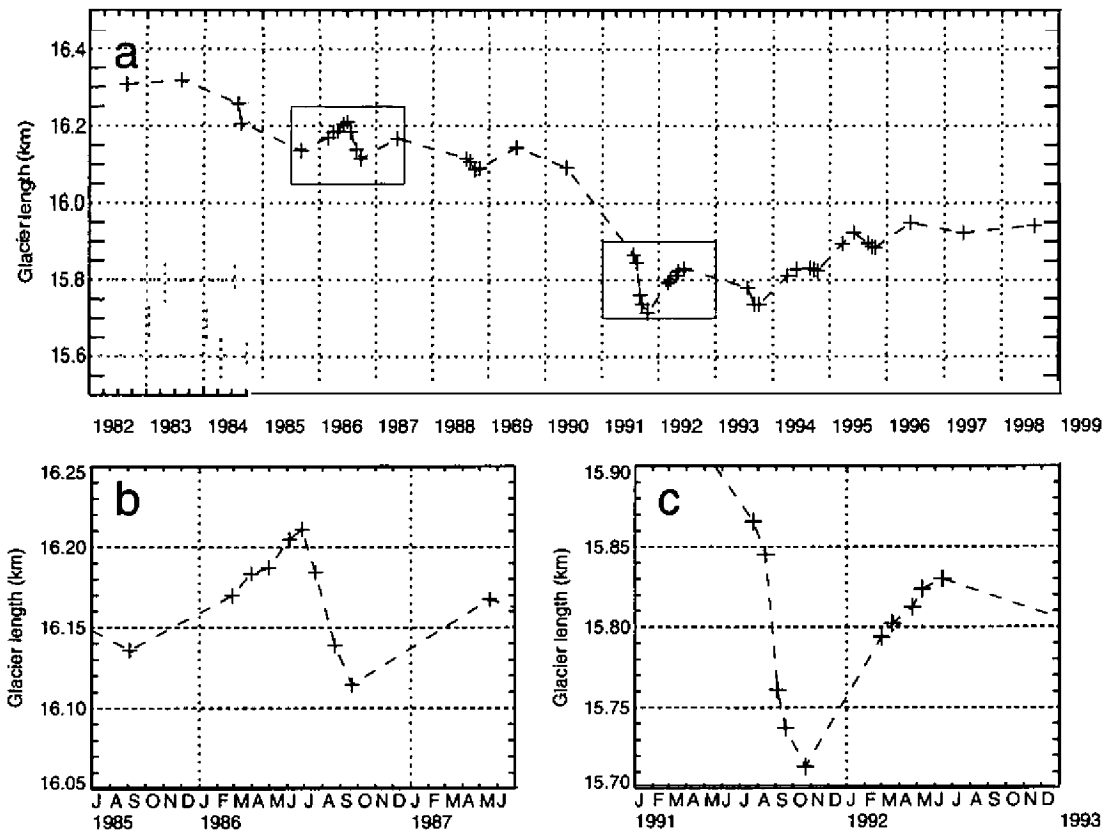


Figure 4.2: (a) Observed glacier front positions along the flowline for the period 1982-1998. A zoom of the seasonal cycles of the years 1986 and 1991/92 is shown in (b) and (c), respectively.

Table 4.1: Estimated maximum summer retreat rates and winter advance rates from observed front position changes. The \* indicates data from an earlier study by Jania (1988).

Year	Winter advance rate	Summer retreat rate
1983	0.29 m d <sup>-1</sup>	-0.99 m d <sup>-1</sup>
1984*	0.28 m d <sup>-1</sup>	-0.93 m d <sup>-1</sup>
1986	0.33 m d <sup>-1</sup>	-1.04 m d <sup>-1</sup>
1988	-	-0.54 m d <sup>-1</sup>
1991	0.55 m d <sup>-1</sup>	
1993	-	-0.95 m d <sup>-1</sup>
1995	0.42 m d <sup>-1</sup>	-0.32 m d <sup>-1</sup>

in late summer the velocities are usually slightly below. Sporadic speed-up events are additionally observed during the melting season with an increase in the surface flow velocities up to a factor of five but for a duration of only 1-2 days (Vieli and others, 2000, Paper 2). These speed-up events are related to periods of enhanced water input to the glacier due to rainfall or a föhn Situation associated with enhanced surface melt.

## 4.3 Interpretation and discussion of observations

### 4.3.1 Long term changes 1982-1998

The observed retreat from 1982 to 1998 follows the observed general retreat and surface lowering since 1936, except for the jump in the terminus retreat of about 280m from 1990 to 1991 (Fig 4.2). Before and after this abrupt retreat the frontal position undergoes only small changes in the range of seasonal variations. The rapid retreat of 1990/91 can be explained by a temporary strong increase in the calving rate.

Climatic or mass balance records do not indicate any abrupt change for this time period outside the range of the annual variability, however, the length change signal is strong and short. Therefore, the rapid retreat can not be a direct and immediate reaction to a sudden mass balance Change. A basal depression with a maximum depth of about 78m below sea level is located between the glacier front positions before and after the abrupt retreat of 1990/91 (Fig. 4.1b). This indicates that the retreat is affected by the basal topography. Earlier observations and numerical model experiments showed that such accelerated retreats are likely to occur through basal depressions (Meier and Post, 1987; see Paper 3). With continuing thinning and retreat of the glacier, due to a negative mass balance, the flotation level is approached in the region of the basal depression and increased calving due to buoyancy forces occurs. The decreasing effective pressure there leads to enhanced sliding, longitudinal stretching and bottom crevassing and may additionally weaken the ice (Van der Veen, 1996 and 1998). Thus the observations from Hansbreen suggest that the abrupt retreat is mostly an effect of the bed topography at and behind the terminus and the high calving rates are a result of the glacier dynamics in the region of a basal depression.

The slight readvance observed between 1993 and 1996 (Fig. 4.2) may be a consequence of reduced summer calving rates due to changes in climatic conditions. The observations clearly show that the summer retreat rates were significantly reduced in 1994 and 1995 (Fig. 4.2). The readvance may also be a dynamical reaction on the abrupt removal of the terminus part in 1990/91. The reason for the readvance can not be determined unambiguously because it is not observed whether the glacier was thinning or thickening near the terminus in the years between 1990 and 1999.

### 4.3.2 Seasonal variations

The seasonal Variation of the front position is determined by the seasonal change of the calving rate and the flow velocity at the glacier terminus. The observed speed-up events showed that on a time scale of days strong velocity variations occur on Hansbreen during the melt season (Paper 2). On time scales of months or seasons these events do not significantly change the ice flow. Thus seasonal variations of the frontal velocities are small in comparison to the fluctuations of terminus position and the seasonal changes of the front position are mainly due to a seasonal Variation of the calving rate. A calving rate close to zero during winter implies that the advancing rate matches the flow velocity at the terminus. The observed values for the winter advance rate in 1986 and 1991/92 are in the range of directly measured frontal flow velocities between  $0.30 \text{ m d}^{-1}$  and  $0.45 \text{ m d}^{-1}$  by terrestrial photogrammetry and survey (Jania, 1988; Vieli and others, 2000).

Assuming constant flow velocities over the year, a seasonal pattern of the calving rate can be estimated from the observed changes in front positions. The inferred annual cycle of calving yields no calving from October to beginning of June ( $\sim 8$  months) and high calving rates between June and October ( $\sim 4$  months). This step function is a first approximation for the annual cycle for calving. In nature the switch in the calving rate between the different seasons is expected to be more gradual.

The summer calving rate can be estimated from the observed summer retreat rate  $dL/dt$  and the frontal velocity  $u_i$ , which is assumed to be equal to the winter advance rate. For the best documented year 1986, a summer calving rate of  $u_c = dL/dt - u_i = -1.04 \text{ m d}^{-1} - 0.33 \text{ m d}^{-1} = -1.37 \text{ m d}^{-1}$  is obtained, which corresponds to a mean annual calving rate of  $164 \text{ m a}^{-1}$ . Rough estimations for the other years give values for the summer calving rate, which are similar or below the one of 1986 (Table 4.1). For the year 1991/92 it is difficult to see the annual signal of the frontal position because of the rapid retreat. The observed seasonal pattern of the calving rate correlates well with the seasonal Variation of climate. The period of main calving corresponds to the period of surface melting and highest sea water temperatures in the fiord (Fig. 4.4).

The observed notch at the calving front of Hansbreen suggests that melting at the waterline may play an important role for the process of calving by inducing the break off of the ice slabs above as observed for icebergs (El-Tahan and others, 1987). According to Equation (4.5) the melt rate at the waterline is zero when the temperature is below  $0^\circ \text{ C}$  or when wave activity is suppressed by sea ice covering in the vicinity of the calving face. In hydrological investigations in 1981/82 the seasonal Variation of the sea surface temperature and the sea ice covering in Hornsund was measured (Moskal, 1987; Swerpel, 1982). In summer sea surface temperatures of about  $2^\circ \text{ C}$  were measured, whereas from October to June the surface temperatures were below freezing and the fiord was mostly covered by sea ice (Fig. 4.4). From the weekly report of the National Ice Center, Washington D. C., USA (<http://www.natice.noaa.gov>) the Hornsund region was found to be covered by ice from end of November until beginning of June. Thus, the observed seasonal pattern of the sea surface temperatures and the duration of sea ice cover suggests that the melt rate at the waterline is close to zero from beginning of October until

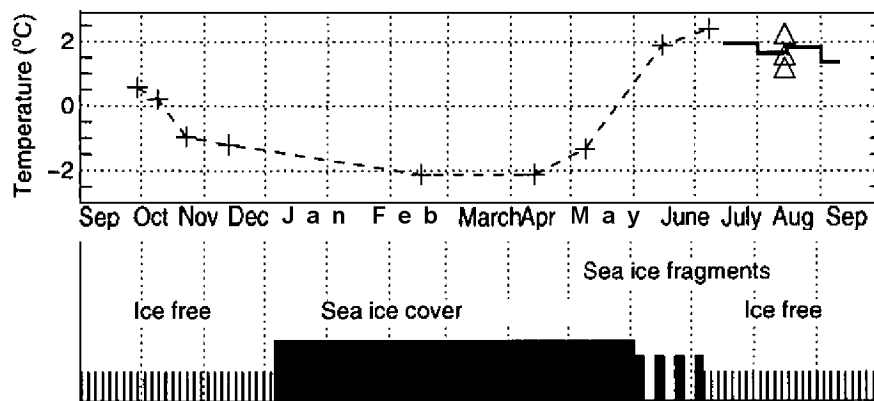


Figure 4.4: (a) Sea surface temperatures of Hornsund in the vicinity of Hansbreen shown for the year 1982/83 (crosses with dashed line; Moskal, 1987) and summer 1974 (triangles and thick solid line; Swerpel, 1982). (b) Observed seasonal pattern of sea ice covering on Hornsund in the vicinity of the calving front of Hansbreen for the year 1982/83 (Moskal, 1987).

June and is highest in late summer. This seasonal pattern is very similar to the one found for the calving rate and indicates a link between melting at the waterline and calving. If melting at the waterline is the inducing process for calving, as similarly suggested for Maud Glacier by Kirkbride and Warren (1997), their rates should be in the same range. Between 1982 and 1998 summer calving rates up to a value of  $1.37 \text{ m d}^{-1}$  occurred. Based on studies of Neshyba and Josberger (1980), Jania (1988) estimated a maximum cliff melt of  $0.16 \text{ m d}^{-1}$  for Hansbreen, which is one order of magnitude below the value of the calving rates. But this estimation is concentrated to submarine melting, due to buoyant convection and gives a vertically averaged melt rate. From studies on the deterioration of icebergs melt rates at the waterline are known to be one to two order of magnitudes higher than below (El-Tahan and others, 1987). Using Equation (4.5) a rough estimation for the melt rate at the waterline can be done for the situation of Hansbreen. For a surface water temperature of  $2^\circ \text{C}$ , a wave height of 0.1 m and a wave period of 1.5 s a melt rate at the waterline of  $1.06 \text{ m d}^{-1}$  would result. This value is in the range of the observed summer calving rates and therefore for Hansbreen melting at the waterline has to be taken into account as a possible triggering mechanism for calving and as a possible cause for the observed seasonal fluctuation of the front position during periods of slow retreats. The direct observations of calving and the permanently persisting notch melted out at the waterline during summer 1998 and 1999 suggests that this was the case at least during these periods. The estimation for the melt rate according to Equation (4.5) is based on assumptions for the temperature, wave height and period, which both undergo strong temporal changes. In addition Equation (4.5) is determined for open ocean, thus the value of  $1 \text{ m d}^{-1}$  is a maximum value and may overestimate the melt rate at the waterline during Summer. Although the melt rates at the waterline are smaller, the observations of Hansbreen indicate that melting at

the waterline affects the process of calving, by changing the shape of the calving face and therefore the stress field in the frontal ice body. Hanson and Hooke (2000) mentioned that an oversteepening due to increased submarine melting during summer may lead to enhanced summer calving.

The calving of ice lamellas above the waterline leads to a submarine ice foot. The large icebergs that occasionally rise to the sea surface in front of the calving front of Hansbreen indicate the development of an ice foot below the surface, which might be due to enhanced submarine melting near the surface (Hunter and Powell, 1998). Icebergs detach from the ice foot when buoyancy exceeds a critical stress for failure. Sediment layers on the observed icebergs indicate its origin from the glacier bed.

### 4.3.3 Calving rate water depth relation

The observations of Hansbreen during periods of slow calving do not support the calving rate to water depth relationship suggested by Brown and others (1982) for tidewater glaciers. For the year 1986 the annual calving rate is estimated to be  $164 \text{ m a}^{-1}$ . For the period 1982-1990 a mean calving rate between 150 and  $190 \text{ m a}^{-1}$  is found, assuming flow velocities according to observations between 0.3 and  $0.45 \text{ m d}^{-1}$ . The water depth at the terminus in the considered middle part of the glacier is about 50m. These observed calving rates are far below the value expected from the calving rate to water depth relationship suggested by Brown and others (1982), corresponding to a calving rate of  $1350 \text{ m a}^{-1}$  for 50 m water depth and  $810 \text{ m a}^{-1}$  for the water depth averaged over the glacier width of 30 m. The observed values of Hansbreen are in the range of the calving rate water depth relation suggested for freshwater calving glaciers (Funk and Roethlisberger, 1989). On a seasonal time scale the calving rates undergo strong changes from zero calving in winter up to  $1.37 \text{ m d}^{-1}$  in summer and show no relation to water depth, which is also known from Columbia Glacier (Sikonia, 1982).

## 4.4 Modelling the retreat of 1982-1998

A time dependent numerical model for the glacier flow of tidewater glaciers (see Paper 3) is applied on Hansbreen to investigate the suggested hypothesis derived from the observed changes in front position. In particular, the effect of the basal depression on the rapid retreat of 1990/91 will be tested with the model calculations. Furthermore, the observed seasonal variations of the glacier front is modelled by prescribing seasonal (melt induced) calving rates. We want to emphasize that the goal of the model calculations is to identify and check the governing processes during the retreat of Hansbreen rather than to reproduce the exact evolution in time.

### 4.4.1 Model description

The numerical model for the dynamics of tidewater glaciers used to study the retreat of Hansbreen was described and discussed in Paper 3. The model calculates the



surface evolution and the two-dimensional velocity and stress fields for a longitudinal section of the glacier. The 2D force balance and mass conservation equations are solved to compute stress and velocity fields using the finite-element method. Glens's flow law is used in the model with a flow law exponent  $n = 3$  and a rate factor  $A = 0.1 \text{ bar}^{-3} \text{ a}^{-1}$  (Gudmundsson, 1999; Hubbard and others, 1998; Albrecht and others, 2000).

### *Calving*

Calving is implemented in the model by two different schemes. The seasonal calving rates, for which melting at the waterline may be the controlling process, are included in the model by the seasonal calving scheme, in which the calving rate is prescribed according to the observed seasonal pattern (see Section 4.3).

In the *modified flotation criterion* (Equation (4.3); see Paper 3), for each time step the new terminus is moved to the position where the ice thickness  $h$  exceeds the flotation height by the fraction  $q=0.15$ . The ice mass that is removed corresponds to the mass loss due to calving. Following this method the calving rate is a result of the computation and is controlled by the ice velocity and the surface changes.

The calving process is implemented in the model as follows: At each time step first the front position is shifted according to the prescribed seasonal calving rate. Then the terminus position is updated according to the *modified flotation criterion*. Calving is governed by buoyancy as soon as a part of the glacier terminus is below the critical height  $h_c$ . With this approach, the model decides whether the prescribed seasonal or the *buoyancy* induced calving is the controlling process for calving.

### *Basal sliding*

A linear sliding law of the form

$$v_b = k \tau_b^m p_e^{-r}, \quad (4.6)$$

is included in the model, where  $v_b$  is the basal velocity,  $\tau_b$  the basal shear stress,  $k$  is an adjustable empirical positive Parameter and  $p_e$  the effective pressure. We set the Parameters  $m = 1$  and  $r = 1$  such that we get a linear sliding law.

This sliding relation (4.6) is implemented in the model by adding a thin soft layer at the glacier base. The viscosity of this basal layer has been chosen in order to fulfill the sliding relation (4.6) for a specific location (a detailed implementation is described in Vieh and others, 2000). The factor  $k p_e^{-1}$  in relation (4.6) is given as input for the model and the basal velocity and basal shear traction result by solving the system of field equations and boundary conditions. For each time step, the effective pressure changes and has to be updated with the actual ice thickness and basal water pressure.

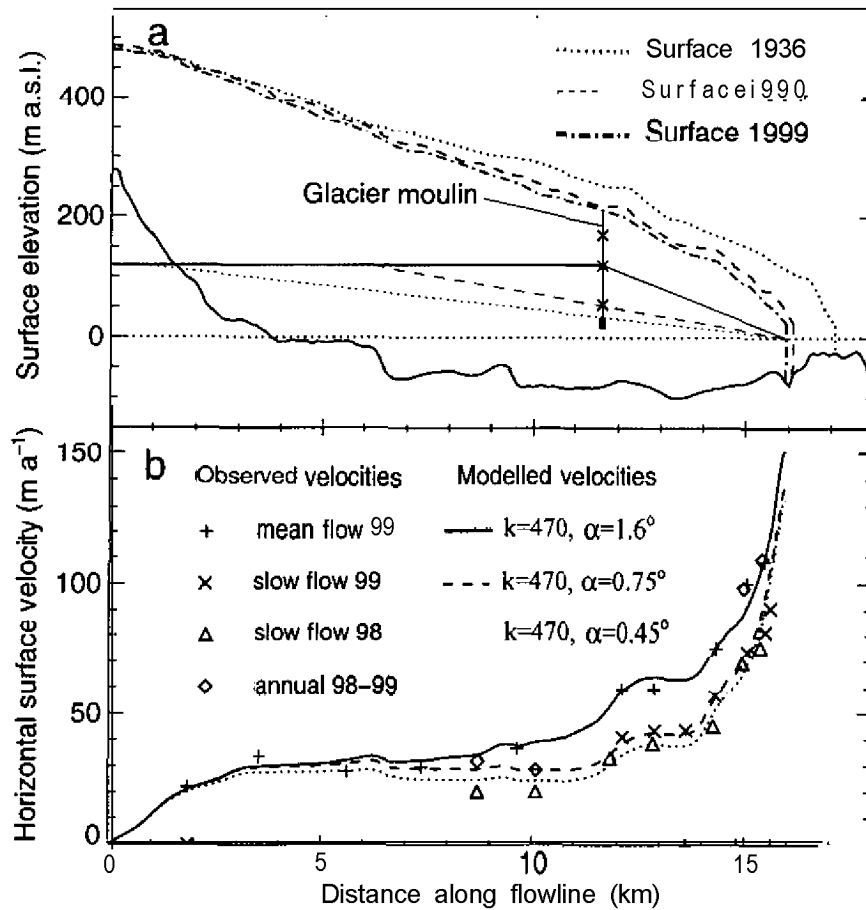


Figure 4.5: (a) Profile along the flowline of Hansbreen with glacier bed (solid line) and surface topography for the years 1936, 1990 and 1999. The lines within the glacier show the assumed water levels for the model calculations. The crosses show three observed water levels measured in a glacier moulin. (b) Measured (Symbols) and modelled (lines) surface flow velocities for the three different periods. For the mean flow 1999 (crosses) the solid line represents the best fit of the modelled velocities to the observed.

#### 4.4.2 Model input

Optimal sliding Parameter and water level

The sliding Parameter  $k$  and the water level for the numerical model are not known and have to be adjusted. The best values for sliding Parameter  $k$  and the water level were found by minimizing the root-mean-Square error between modelled and observed surface flow velocities on Hansbreen. Surface velocities along the flowline

were measured in summer 1998 (Vielí and others, 2000) and 1999 and are shown in Figure 4.5 (see Paper 2). Short-term variations of the surface velocities have been observed in the ablation zone. Speed-up events with velocities increased by a factor 2 to 5 and a typical duration of 1 to 2 days occurred. Because of the short duration of these events, they have only a minor effect on the mean annual and seasonal velocities. For the summer 1998 and 1999, the velocities during a short period immediately after a speed-up event (termed *slow-flow* 1998 and *slow-flow* 1999) were found to be slightly lower than the mean annual values, and may balance the enhanced velocities during the Speed-ups. Thus, the observations show that on a seasonal time scale the velocities are almost steady. In summer 1999 the velocities before such a speed-up event (termed *mean-flow* 1999) were nearly constant for two weeks with values very close to the mean annual velocities (Fig. 4.5b). The *mean-flow* 1999 velocities are assumed to be representative for the mean annual flow and are used for adjusting the model Parameters.

The measured velocity variations are related to variations of basal water pressure. The water pressure in a glacier moulin, located 4.5 km upstream of the terminus (Fig. 4.1a), was recorded in summer 1999, simultaneously with the velocity measurements (Fig. 4.5a). For the *slow-flow* period 1999 a water level of about 50 m a. s. l. was observed and for the *mean-flow* period it was 120 m a. s. l. The basal water pressure within Hansbreen is not known and assumptions must be made. Sea level is a lower limit for the water level, but especially during the melting season, it is higher. For the model calculations the water level is assumed to increase linearly with distance to the terminus, starting at sea level at the calving front. We additionally assumed that the water level does not exceed 120 m to take into account in a simple way a decreasing water level gradient glacier upstream. The water level gradient  $\alpha$  is therefore a tuning Parameter for the numerical model. For the *slow-flow* period,  $\alpha$  is expected to be smaller than for the *mean-flow* period. Because the velocities are almost steady with the seasons the tuning Parameters  $k$  and  $\alpha$  are assumed to be constant with time.

For the *mean-flow* period the best fit of the modelled to the observed velocities was found with  $k = 470$  and a water level corresponding to an inclination of the water table of  $\alpha = 1.6^\circ$  (Fig. 4.5). This value of the sliding Parameter  $k$  is equal to the value found for the *slow-flow* period for the summer 1998 (Vielí and others, 2000), but there a smaller water level inclination of only  $0.45^\circ$  was found, which represents a generally lower water pressure. Assuming the same sliding Parameter  $k = 470$  for the *slow-flow* period 1999, a slightly higher water level inclination of  $\alpha = 0.75^\circ$  results.

The water levels in the glacier moulin with the optimal water level inclinations of  $\alpha = 1.6^\circ$  (*mean-flow*) and  $\alpha = 0.75^\circ$  (*slow-flow*) are 120 m and 58 m respectively, which is in agreement with the observed values for the corresponding periods shown in Fig. 4.5a.

For the following model calculations we used  $k = 470$  and  $\alpha = 1.6^\circ$  corresponding to the *mean flow* 99 velocities.

### Input *geometry*

The model calculations were focused on the period 1982 until 1998 with a special interest on the period of 1990/91 in which the abrupt retreat occurred. For starting the model calculation the surface geometry along the flowline of 1936 is used (Fig. 4.5a). The observed surface lowering from 1990 to 1999 follows the general trend of glacier thinning from 1936 to 1990. There is an uncertainty in bed topography in a zone of 500 m length behind the front position of 1998, due to missing radio-echo-sounding data in this highly crevassed area.

### Input *mass* balance function

Mass balance measurements started in 1989, and thus there is no mass balance data available for the early part of the modelling period. Annual *mass* balance measurements are available since 1990 with a gap in 1996 and 1997 (Jania and Kaczmarek, 1997; IAHS, 1997). From the existing mass balance of the years 1991-1995, a *mass* balance function  $b$  was derived, depending on surface elevation  $S$

$$b = a_1 S + a_0, \quad (4.7)$$

with the coefficients  $a_1 = 0.00655$  and  $a_0 = -2.2043$ . This *mass* balance function includes surface accumulation and ablation without calving. The corresponding mean average net balance (without calving) over this period is  $-0.21$  m w. e. and the mean ELA is 338 m a. s. l.

The assumed *mass* balance  $b$  may not be representative for the entire period from 1936 until today. Even if the total *mass* balance did undergo large changes since 1936, the *mass* balance gradient is not expected to change very much. From the existing topographic maps of 1936 and 1990, the volume change of Hansbreen between 1936 and 1990, is estimated to be  $1.2 \text{ km}^3$  of ice (Jania and Kolondra, 1982). The surface area of the glacier decreased by about  $2 \text{ km}^2$  to  $57 \text{ km}^2$  in this period. Thus, the mean average net balance for the 54 year period 1936-1990 amounts to  $-0.35$  m w. e. a<sup>-1</sup>. This value includes the additional mass loss through calving of icebergs. The mean average net balance without calving for the period 1990-95 is slightly less negative with  $-0.21$  m w. e. a<sup>-1</sup>. This difference requires a mass loss through calving corresponding to an ablation rate of  $-0.14$  m w. e. a<sup>-1</sup>. The assumed *mass* balance parameterisation derived from the 1990-95 record is consistent with the estimated glacier volume change from the 1936-90. Therefore, the assumed *mass* balance function  $b$  (Equation 4.7) is an acceptable approximation for the mean *mass* balance since 1936 and is used as input for our model calculations. Because of the uncertainty in the *mass* balance input, additional model runs were performed with a shift of the *mass* balance function by  $\delta b = \pm 0.2$  m w. e. a<sup>-1</sup>.

### *Calving* rate

Beside the flotation criterion for calving, a seasonal cycle of calving rate  $u_c$  is prescribed from the observed front position changes and velocities, whatever the controlling process for calving is. For the 8 months period from the beginning of October

to the beginning of June, no calving is assumed and for the four summer months (June-October) the observed value of 1986,  $u_c^{\text{melt}} = 1.37 \text{ m d}^{-1}$  is used. The resulting mean annual calving rate amounts to  $0.45 \text{ m d}^{-1}$ . To show the sensitivity of the model results on the prescribed calving rates, additional model runs with slightly different summer calving rates of  $1.28 \text{ m d}^{-1}$  and  $1.46 \text{ m d}^{-1}$  were performed.

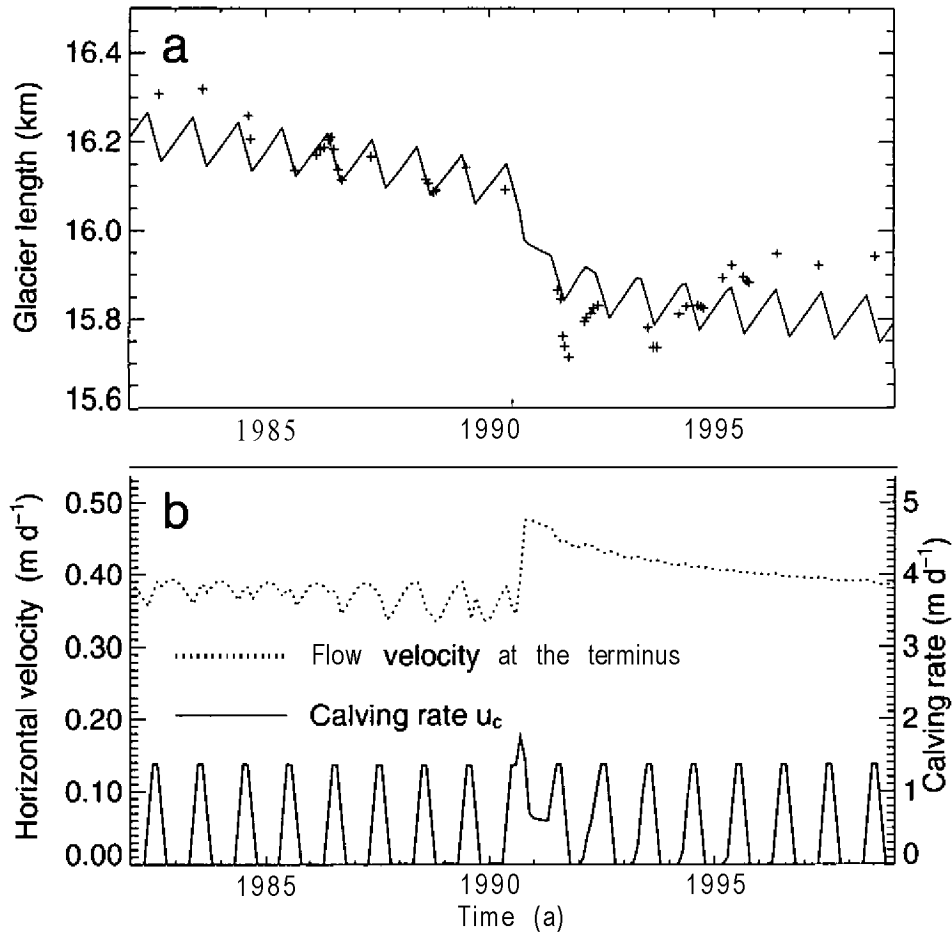


Figure 4.6: (a) Modelled (solid line) and observed (crosses) front positions of Hansbreen with time. The time axis corresponds to observed front positions. (b) Modelled horizontal surface velocities at the terminus (right scale) and prescribed calving rates (left scale) are shown with time.

## 4.5 Model results and discussion

The modelled front position shows a general slow retreat with a superimposed annual cycle (Fig. 4.6). A jump in the retreat of about 220m occurs in the modelled retreat in the year 47 after model start. The abrupt retreat takes place over the region where the basal depression is located (Fig. 4.7), which corresponds to the observations presented before. In Figure 4.7, the modelled evolution of the glacier surface is shown for every two years, starting with the 1936 surface. The glacier

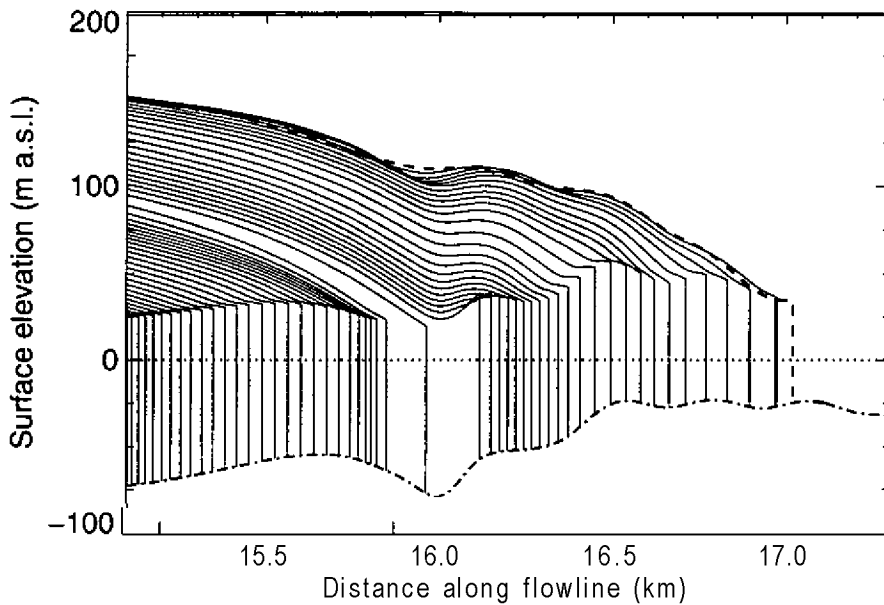


Figure 4.7: Modelled evolution of the glacier surface with time along the flowline. The time interval between two surface **profiles** is two years. The starting geometry of 1936 is indicated by the dashed line. The dashed-dotted line indicates the glacier bed topography along the flowline.

thins continuously from year to year due to the imposed negative mass balance. In the frontal region, where the basal topography at the terminus slopes up in flow direction, the thinning is found to be accelerated (Fig. 4.7). Due to the seasonal front position changes the frontal part of the glacier additionally undergoes small seasonal thickness changes.

The modelled retreat of the period 1982-1998 is not expected to be accurate in time, because the calculated mean retreat rate mainly depends on the assumptions made for the mass balance history and the annual prescribed calving rate (Fig. 4.8). The model calculations start in 1936 in order to have a long enough spin up period for realistic initial conditions for the jump in 1990 in which we are interested in. The position and shape of the jump in retreat is very robust with regard to different mass balance inputs and prescribed calving rates for the spin up, as discussed below. To obtain the modelled abrupt length change at the true time (1990/91), the model time is shifted accordingly (Fig. 4.6).

The modelled slow retreat before the jump is in agreement with the observed retreat (Fig 4.6a). Furthermore, the observed seasonal variations were well reproduced by the model calculations. The position where the modelled abrupt retreat takes place corresponds to the observations. Additional model runs with different values for the prescribed seasonal calving rate, a different input mass balance or a lower water level inclination  $\alpha$  also show the abrupt retreat at the same position (Fig. 4.8), although the model time of these jumps differs

For the model calculations the input mass balance function and prescribed seasonal

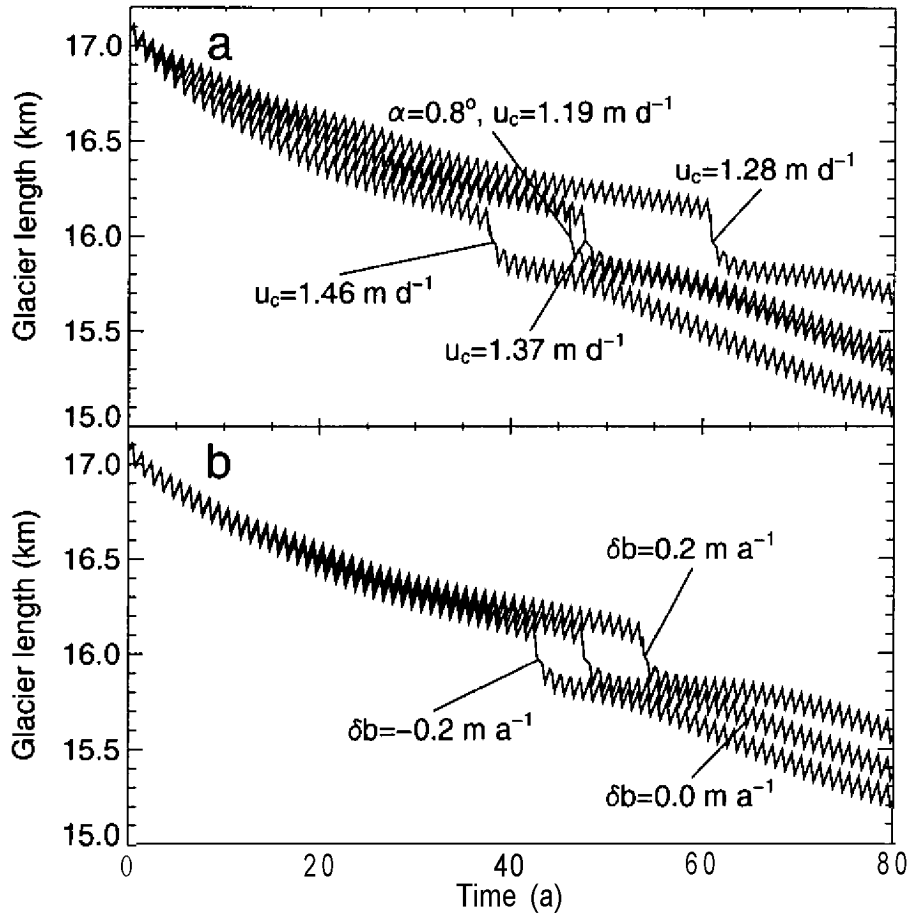


Figure 4.8: Glacier length with time shown for the additional model runs with (a) a slightly changed prescribed **summer** calving rate  $u_c$  and a changed water level gradient  $\alpha$  and (b) a shifted mass balance input by  $\delta b$ .

or melt induced calving rate are assumed to be constant with time. The modelled abrupt retreat of the terminus is therefore not an immediate reaction on this external forcing. The model calculations clearly show that the jump in retreat is fixed to the location of the basal depression.

The observations of the retreat between 1982 and 1998 are limited to some snapshots in time and are not continuous. The model calculations allow us to follow continuously the front position and additional variables, such as glacier surface, calving rates or flow velocities. The flow of a glacier through a basal depression results in a slight depression in the glacier surface above. Such a surface depression also occurs in the frontal region of Hansbreen (Fig. 4.7). Before the jump in retreat takes place, the surface elevation at the calving front is always above the critical height above flotation (Equation (4.3)) and the prescribed seasonal pattern of the calving rate is controlling the retreat. With thinning of the glacier, the surface depression gets more pronounced due to enhanced sliding. When the glacier surface thins below the critical height above buoyancy in the region of the basal depression, all the ice in front of the depression is removed, according to the flotation criterion (Equation (4.2))

and (4.3)). Instead of the prescribed seasonal calving, in this case buoyancy induced calving becomes the governing process. At this stage the retreat is mainly controlled by surface lowering in the terminus region, which is strongly affected by the bed geometry and changes in basal sliding. The enhanced sliding and steeper slope at the terminus in the region of the basal depression leads to an increase in the mass flux divergence and therefore to enhanced thinning (Fig. 4.7). The resulting high buoyancy induced calving rate leads to a very rapid terminus retreat through the basal depression and a region of a down slope bed in flow direction with shallow water is reached. There the buoyancy induced calving rate decreases rapidly and the prescribed seasonal calving again becomes the controlling process. Thus, the model calculations confirm the explanation for the jump in retreat suggested by the observations on Hansbreen.

The abrupt retreat is mainly an effect of basal topography and caused by the buoyancy induced calving in the region of basal depression. The negative net mass balance is driving the general surface lowering and is therefore triggering this rapid retreat. The additional model runs show that the mean retreat rate and the absolute time when the jump in retreat happens strongly depends on the assumptions made for the mass balance or prescribed calving rate (Fig 4.8). The location of the modelled abrupt retreat is independent of these two Parameters and thus further confirms the suggested effect of the basal topography on the retreat.

The modelled jump in retreat of 220m is smaller than the observed 280m. An explanation for this discrepancy may be found in the basal topography, which is not accurately known in the region behind the 1998 position (between 15.5 km and 16 km), because of missing depth sounding data.

With the used seasonal pattern of the calving rate the observed seasonal cycles of retreat and advance are well reproduced by the model (Fig. 4.6), especially for the years before the abrupt change. After the jump in retreat, the observations show a 4 year period of a slight advance whereas in the model calculations the terminus is slowly retreating. The observations indicate that the advance is mainly due to a reduction of summer calving rate and the duration of the summer retreat period. The surface elevation of the terminus region is not observed between 1990 and 1999 and it is not clear if the glacier was thickening during the readvancing period. For our model experiments the input mass balance and the prescribed seasonal cycle of the calving rate are assumed to be constant from year to year. In reality, they may vary seasonally and interannually. Lower air and sea temperatures and the longer duration of the winter season and the sea ice coverage possibly reduce the summer retreat. Thus, variations in the external forcing may be a possible cause for the observed slow glacier advance and may explain the discrepancy between observations and model calculations.

The modelled seasonal variations show that the flow velocities at the terminus can also undergo annual cycles (Fig. 4.9), although the sliding Parameters  $k$  and  $\alpha$  are kept constant with time. Figure 4.9 shows a period in which the prescribed seasonal calving rate controls changes in terminus Position. The velocity variations are a result of a seasonal changes of the cliff height caused by the externally forced annual cycles of the calving rate. With the retreat in summer the height of calving front increases, which causes higher driving forces at the terminus and leads to increased



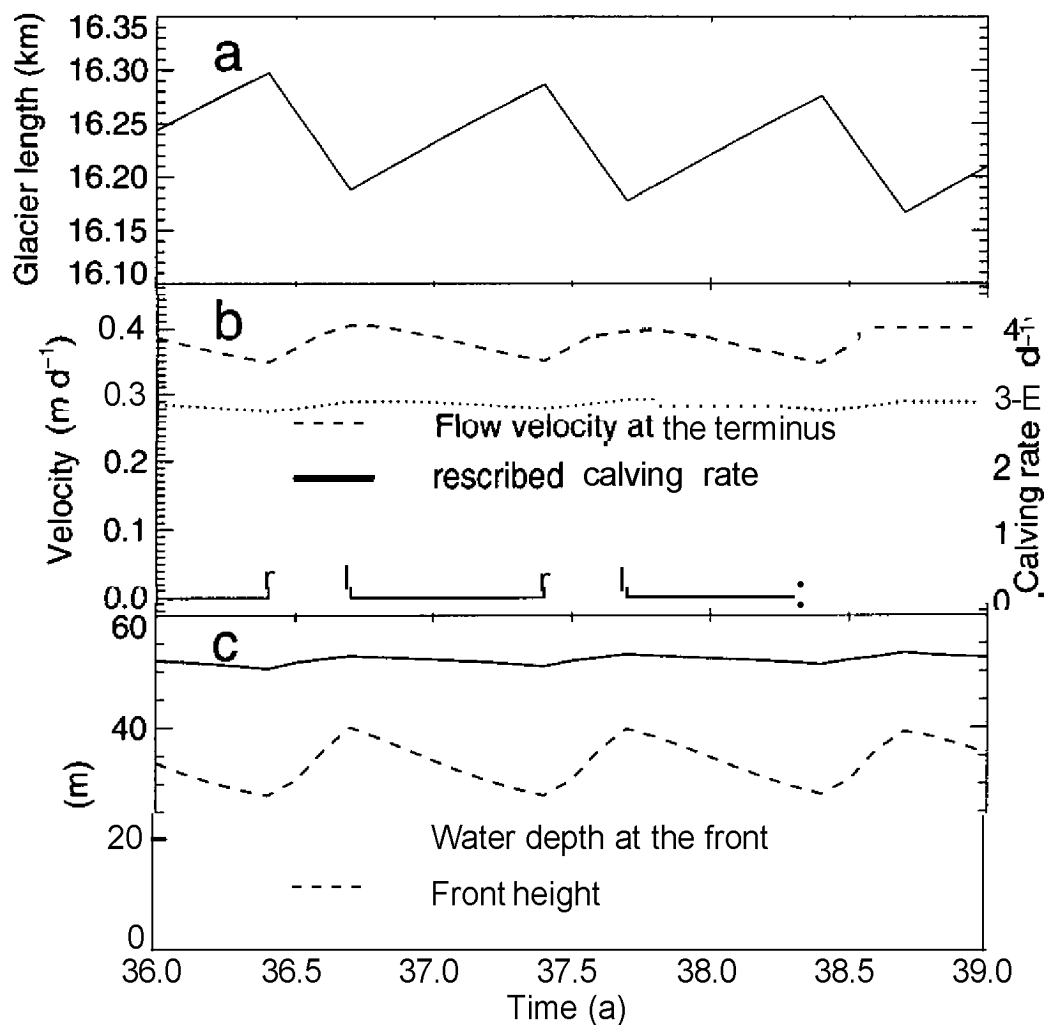


Figure 4.9: Modelled seasonal fluctuations of (a) the front Position, (b) the calving rate (solid line) and horizontal surface velocity at the calving front (dashed line) and 400 m behind it (dotted line). (c) Front height and water depth at the terminus.

velocities (Fig. 4.9). In winter, when the prescribed calving rate is assumed to be zero, the glacier slides forward and the cliff height decreases due to gravitational creep. This seasonal velocity increase is local and concentrated to the terminus region. Five frontal ice thicknesses behind the terminus (400m) the amplitude of the seasonal velocity variations is almost zero (Fig 4.9). This is confirmed by the observed velocities on Hansbreen, which are almost steady during the seasons further upglacier.

## 4.6 Conclusions and prospects

The observed rapid retreat of the front position of Hansbreen in 1990/91 is found to be related to a basal depression in the terminus region. The observed seasonal changes of the front position of Hansbreen are mainly due to variations of the calving rate. The period of main calving occurs during summer and corresponds to the period of surface melting and highest sea water temperatures in the fiord. In winter the calving rate is close to zero resulting in an advance corresponding to the ice flow at the calving front. The commonly observed notch at the waterline and the observed seasonal pattern of calving indicates that during periods of slow front position changes melting at the waterline may play an important role as a triggering mechanism for calving. Melting at the waterline mainly depends on sea water temperature and wave activity and is therefore highly sensitive on the duration of sea ice covering and climatic conditions in summer. For small tidewater glaciers with frontal flow velocities and calving rates similar or below that of Hansbreen the role of melting at the waterline on the calving process must be taken into account and be further investigated.

The performed model calculations confirm, that the cause of the abrupt retreat of Hansbreen in 1990/1991 is mainly an effect of basal topography, and governed by the process of buoyancy induced calving. This supports the concept of Van der Veen (1996) proposed for the rapid retreat of Columbia Glacier. The location of the jump is found to be independent on the external forcings, such as mass balance and the prescribed calving rates, and is fixed to the position of the basal depression. Thus, the general thinning of Hansbreen due to a negative net mass balance is only the triggering process for the rapid retreat. The enhanced calving rate is a result of the strong influence of bed topography to the surface change in the terminus region and therefore primarily a result of glacier dynamics and not vice versa. Rapid retreats through basal depressions were observed on several tidewater glaciers, but these studies were mostly focussed on large and fast flowing glaciers with calving rates and frontal velocities in the order of  $1 \text{ km a}^{-1}$ . The example of Hansbreen shows that the effect of basal topography on the dynamics of small slowly flowing tidewater glaciers is similar.

The proposed two relevant processes for calving do not distinguish between freshwater and tidewater, and therefore there is no fundamental restriction to apply our model to freshwater glaciers. The magnitude of the calving rate may be affected by the difference of buoyancy in fresh and tidewater or by the different melt rates at the waterline, due to differences in salinity and wave activity. The observed calving rates and corresponding terminus water depths for the slowly retreating period of Hansbreen result in a calving rate to water depth relationship, which is similar to the function inferred from observations of freshwater calving glaciers (Funk and Röthlisberger, 1989). Thus the **data** of Hansbreen supports a similar relationship for freshwater and tidewater glaciers.

From the observations and performed model calculations for Hansbreen, we conclude that rapid unstable retreats of grounded calving glaciers in fresh or tidewater are mainly related to basal depressions in the terminus region and are only to a minor degree a direct response to a change in climate. Because of the sensitivity of

length changes of grounded calving glaciers on basal topography, their future behaviour with respect to climate change is difficult to predict and requires an accurate knowledge of the glacier bed.

# Appendix A

## Interferometric radar observations of Hansbreen

### A.1 Introduction and method

In 1997 the surface flow of Hansbreen was only known at a few points in the terminus region. To determine a continuous velocity field with high resolution and emphasis to the ablation area the method of satellite radar interferometry was used (Rott, 1997). The interferometric analysis presented here were performed by the group of Prof. H. Rott, Institute for Meteorologie und Geophysics, University of Innsbruck, Austria. Hansbreen was imaged by the European Remote Sensing Satellite Synthetic Aperture Radar (ERS-SAR, specifications see Table A.1). The ERS-1/ERS-2 Tandem Mission operated between August 1995 and May 1996. The ERS-SAR operates on C-Band ( $\lambda = 5.7\text{ cm}$ ) with a spatial resolution of 6.5 m in azimuth (along-track) and 9.6 m in range (direction of the radar beam). The radar look angle from the vertical was 23 °. During the ERS-1/ERS-2 Tandem Mission the two satellites were coordinated in order to image the same areas on earth with a time difference of 24 hours.

Table A.1: ERS-SAR specifications.

ERS-SAR Sensor Characteristics	
Orbital altitude	785 km
Frequency	5.3 GHz (C-Band)
Wavelength	5.7cm
Swath width	100 km
Incidence angle	23°
Pulse band width	15.55 MHz
Range resolution	9.6 m
Azimuth resolution	6.5 m

Interferometric SAR measures the phase difference  $\Delta\Phi$  between two SAR images (Rott, 1997). If the repeat pass images are taken exactly from the same positions,  $\Delta\Phi$  only depends on the surface displacement in range, which can be split into a horizontal and a vertical component. If the antenna positions are separated by a distance (referred as baseline) the phase difference results from surface motion and topography. The topographic phase can be removed by using a terrain model or a second interferogram.

A precondition for an interferometric analysis is phase coherence between the signals of the two images. Surface melting, snow fall, ice deformation and changes of the surface roughness reduce coherence. For interferometric motion analysis of glaciers several factors have to be taken into account (Rott, 1997):

- The baseline length should be short, because the sensitivity to topography decreases with decreasing baseline.
- Only motion in the direction of the radar beam can be detected
- Decorrelation additionally results from rotation and deformation at pixel and subpixel scale, for example due to lateral shear at glacier margins.
- In case of fast flowing glaciers, the lateral motion gradient is very high and therefore the individual fringes can not be resolved.

## **A.2 SAR-data for Hansbreen region**

For Hansbreen, ascending and descending scenes are available. To obtain highest probability for phase coherence, SAR image pairs were selected from periods without surface melt (October to May). In addition, only image pairs with a short baseline were taken into account. The available SAR image-pairs that cover the region of Hansbreen and fulfill the criterions above are listed in Table A.Z. The direction of the radar beam for the descending scene is nearly perpendicular to the glacier flow in the frontal part of Hansbreen and therefore the descending scenes only provide information on the motion field in the upper part of the glacier. The look direction of the ascending scene would allow to determine also the motion field in the frontal part of Hansbreen, but from the existing image pair, one image was not available at the ERS data-Center. To get highest probability for phase coherence, image pairs were selected for which precipitation and wind velocities were small (Table A.2, Meteorological Station at Polish Polar Station of the Geophysical Institute of Polish Academy of Sciences ).

## **A.3 SAR interferogram April 9/10 1996**

Interferograms were calculated for the SAR image pair of December 13/14 1995 and April 9/10 1996, but only the interferogram of 9/10 April showed good coherence

Table A.2: Available SAR images pairs for the region of Hansbreen for the period between **October** and May and with short baselines.

Descending scenes					
Satellite	Orbit	Track	Frame	Date	Remarks
ERS 1	23028	495	2025	Dec. 10 1995	
ERS 2	3355	495	2025	Dec. 11 1995	strong wind, snowfall
ERS 1	23071	037	2025	Dec. 13 1995	no coherence
ERS 2	3398	037	2025	Dec. 14 1995	
ERS 1	24531	495	2025	March 24 1996	
ERS 2	4858	495	2025	March 25 1996	strong wind
ERS 1	24574	037	2025	March 27 1996	snowfall
ERS 2	4901	037	2025	March 28 1996	snowfall
ERS 1	24760	223	2025	April 9 1996	good coherence
ERS 2	5087	223	2025	April 10 1996	
Ascending scenes					
Satellite	Orbit	Track	Frame	Date	Remarks
ERS 1	30591	042	1575	May 21 1997	
ERS 2	10918	042	1575	May 22 1997	not available

(Fig. A.1). The phase differences shown in the interferogram in Figure A.2 results from surface motion and topography. Because of the short baseline of 39 m the sensitivity for topography is small. One color sequence (one fringe) in the interferogram represents a phase shift in range of  $2\pi$  between the two images, which corresponds to an altitude difference of 243m (in regions without motion) or to a horizontal or vertical displacement in the radar beam direction of 7.3 cm or 3.1 cm respectively. The sensitivity is higher to vertical than horizontal motion because of low incidence angle of the radar beam.

## Flow of Hansbreen

The flow in the frontal part of Hansbreen is nearly perpendicular to the radar beam direction for this descending scene and therefore a motion analysis of the interferogram in the frontal region is not possible. For the upper part of Hansbreen the angle between the flow and the radar beam direction is about  $45^\circ$ . There, only few fringes occur, which indicate rather slow surface velocities. For an exact determination of the surface flow the topographic phase must be removed. This was done for a transverse profile in the middle of the glacier (Fig. A.2) using the photogrammetric map of 1990. The velocity component perpendicular to the radar beam was derived from estimated flow directions. In this transverse profile surface flow velocities up to  $6.5 \text{ cm d}^{-1}$  result (Fig. A.3). These values are in good agreement with the velocities measured by terrestrial survey in 1998 (Vieli and others, 2000) and GPS in 1999 (in this thesis, Paper 2).



Figure A.1: Phase-coherence image of the SAR ERS-1/ERS-2 data from April 9/10 1996. Red color stands for high coherence and goes over orange, yellow, green and blue to low coherence.

### **Paierlbreen and Burgerbukta**

For Paierlbreen, which is situated north of Hansbreen with a similar size, surface slope and flow direction, the interferometric image looks very different (Fig. A.2). A high fringe frequency results which increases towards the terminus and the glacier margins where they can not be resolved. The glacier margins are also zones where phase coherence is lost (Fig. A.1). Because the slope is rather small ( $\sim 2^\circ$ ) the fringes on the glacier surface correspond in first approximation to the surface displacement in radar beam direction. A rough estimation by counting fringes from the top of the glacier (saddle Situation), where horizontal velocities are nearly zero, results in surface flow velocities in the range of  $500 \text{ m a}^{-1}$  for the lower part of Paierlbreen, which are one to two order of magnitudes above the observed values on Hansbreen, although the size and slope of the glacier are very similar. These unexpected high velocities suggest that Paierlbreen was in a surging phase on April 9/10 1996. In

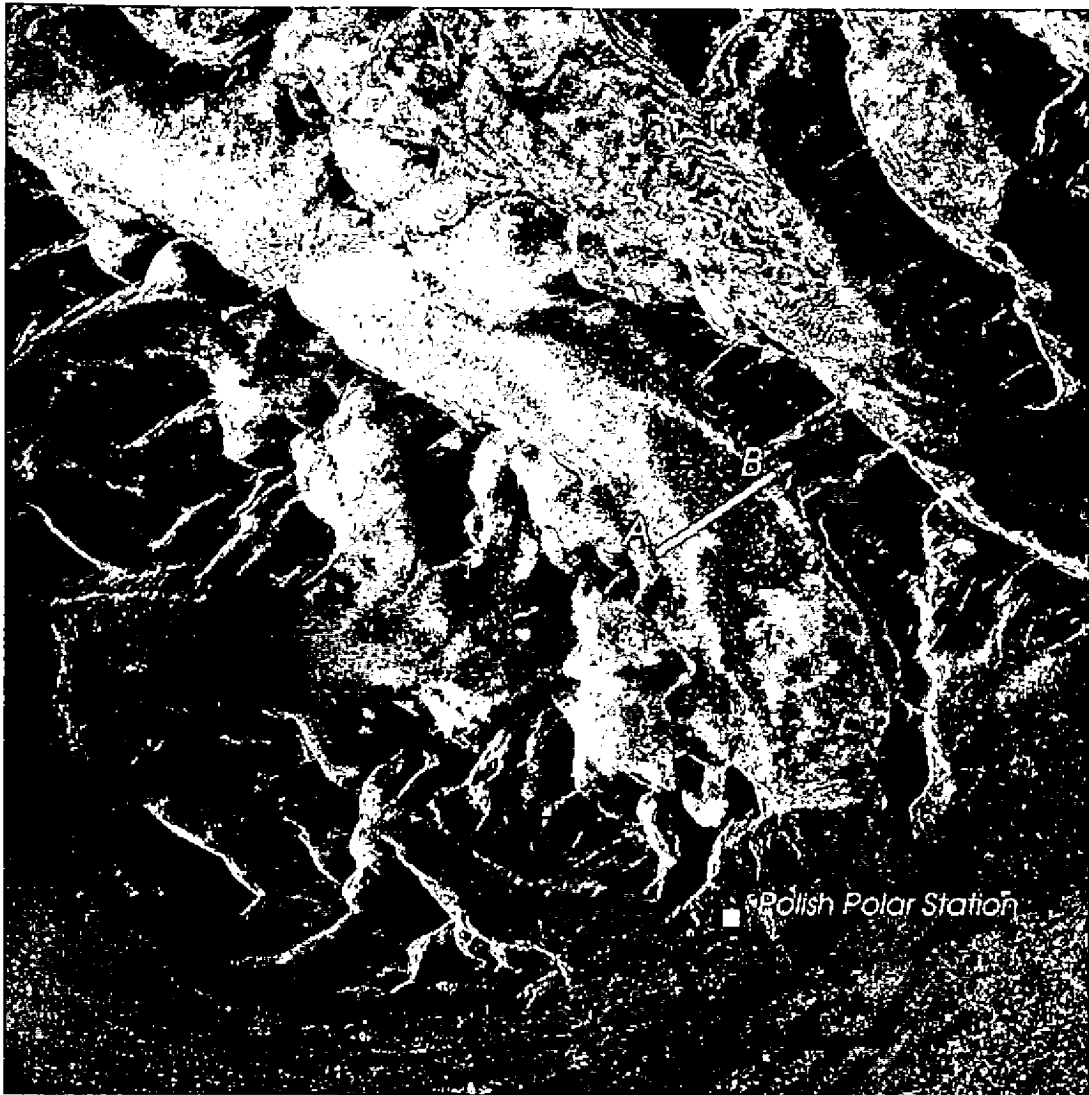


Figure A.2: Interferogram of Hansbreen region, based on SAR ERS-1/ERS-2 data from April 9/10 1996. The look direction of the radar beam is from right to left.

spring 1994 distinct changes of the surface topography (IAHS, 1998) and the opening of new large crevasses in the upper part of Paierlhreen were observed (personal communication from Prof. J. Jania, University of Silesia, Poland, Nov. 1998), which confirms a glacier surge of Paierlhreen. These new crevasses blocked the usual snow mobile route from Polish Polar Station to Longyearhyen. The loss of coherence mainly in the terminus and marginal parts also indicates very high internal ice deformation and rotation, which typically occurs during a glacier surge.

In the upper part of Paierlhreen a spot of zero coherence (dark blue) is visible (Fig. A.1). At this location a large meltwater lake was observed on the glacier surface in summer 1990. The loss of coherence at this spot may indicate that this lake also existed on April 9/10 1996, although surface melting is expected to be small or zero during this period. The daily temperatures on April 9 and 10 1996 recorded at the Polish Polar Station were  $-7.0^{\circ}$  and  $+0.2^{\circ}$  respectively.

The good coherence and the clear fringes on the ocean surface in the Burgerhukta in front of Paierlhreen is due to sea-ice covering (Fig. A.1). In contrast, in areas with



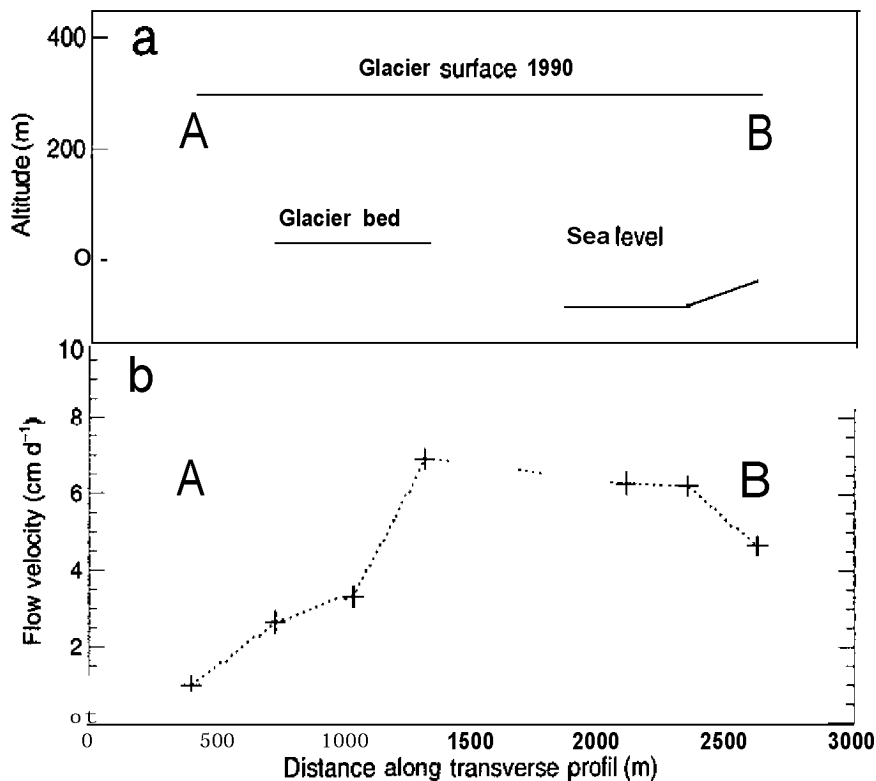


Figure A.3: Transverse profile of Hansbreen (indicated in Fig. A.2) showing (a) glacier surface and bed and (b) interferometrically derived surface flow velocities of April 9/10 1996.

open water the coherence is zero (blue). The phase shift (fringes) in areas covered by sea ice results from vertical displacement due tidal movement (Fig. A.2).

## A.4 Concluding remarks

From the performed interferometric analysis we were not able to derive a high resolution velocity field for the ablation area of Hansbreen, which was the main objective of this study. The reason is that the available ERS-SAR image pairs for which phase coherence is likely were limited to descending scenes with a radar beam direction perpendicular to the flow in the frontal part of Hansbreen. Thus an interferometric motion analysis for the region of main interest is not possible.

From the interferogram of April 9/10 1996 the velocities in a transverse profile in the upper part of Hansbreen are in good agreement with field measurements. There, in principle, a continuous motion field could be derived by removing the topographic phase using the map of 1990 or with a second interferogram. But the surface velocities are small (less than one fringe) and therefore the accuracy low. The probability of a second interferogram with phase coherence is small, because the other SAR image pairs are within periods of strong wind and high precipitation (Table A.2). In addition these image pairs are all from the descending scene and do not provide any information on the flow of the terminus part of Hansbreen, in which we are mostly interested. There is one additional image pair of an ascending scene (October 17/20

1991, ERS1), but the time interval is 3 days and the base line is 319 m, which is not optimal for an interferometric motion analysis. Therefore no further attempts to find an additional interferogram were done, instead velocity measurements in the field were carried out.

Although this interferometric analysis provides little information on the flow of Hansbreen, the calculated interferogram of April 9/10 1996 contains interesting additional information on the surroundings of Hansbreen, especially on the flow of neighbouring Paierlbreen. The SAR images could also be used to determine front positions of the surrounding glaciers. This study illustrates the high potential of satellite interferometry for glaciological studies, but also demonstrates the problems to derive specific information as for the case of Hansbreen.

---

Seite Leer /  
Blank leaf

# Bibliography

- Albrecht, O., Jansson, P., and Blatter, H. (2000). Modelling glacier response to measured mass balance forcing. *Annals of Glaciology*, pages 91-96.
- Alley, R. B., Blankenship, D. D., Rooney, S. T., and Bentley, C. R. (1987). Till beneath Ice Stream B 4. a coupled ice-till flow model. *Journal of Geophysical Research*, 92(B9):8931-8940.
- Baranowski, S. (1977). The subpolar glaciers of Spitsbergen seen against the climate of this region. Technical Report 410, Acta Universitatis Wratislaviensis, WrocBaw.
- Bindschadler, R. A. (1983). The importance of pressurized subglacial water in separation and sliding at the glacier bed. *Journal of Glaciology*, 29(101):3-19.
- Bindschadler, R. A. and Rasmussen, L. A. (1983). Finite-Difference Model Predictions of the Drastic Retreat of Columbia Glacier. Technical report, US Geological survey professional paper 1258-D.
- Blatter, H., Clarke, G. K. C., and Colinge, J. (1998). Stress and velocity fields in glaciers: Part ii. Sliding and basal stress distribution. *Journal of Glaciology*, 44(148):457-476.
- Boulton, G. S. and Hindmarsh, R. C. A. (1987). Sediment deformation beneath glaciers: Rheology and geological consequences. *Journal of Geophysical Research*, 92(B9):9059-9082.
- Broecker, W. S. (1994). Massive iceberg discharges as triggers for global climate change. *Nature*, 372(6505):421-424.
- Brown, C. S., Meier, M. F., and Post, A. (1982). Calving speed of Alaska tidewater glaciers, with application to Columbia glacier. Technical report, US Geological survey professional paper 1258-C.
- Budd, W. F., Keage, P. L., and Blundy, N. A. (1979). Empirical studies of ice sliding. *Journal of Glaciology*, 23(89):157-170.
- Clarke, G. K. C. (1987). Fast Glacier Flow: Ice Streams, Surging, and Tidewater Glaciers. *Journal of Geophysical Research*, 92(B9):8835-8842.
- Colinge, J. (1998). *Analyse numérique de la mécanique des galciers dans un état stationnaire*. PhD thesis, Université de Geneve.

- Dickson, D. (1978). Glacier retreat threatens Alaskan oil tanker route. *Nature*, 273:88–89.
- El-Tahan, M., Venkatesh, S., and El-Tahan, H. (1987). Validation and quantitative assesment of the deterioration mechanisms of arctic icebergs. *Journal od Offshore Mechanics and Arctic Engeneering*, 109:102–108.
- Fischer, M. P. and Powell, R. D. (1998). A simple model for the influence of push-morainal banks on the calving and stability of glacial tidewater termini. *Journal of Glaciology*, 44(146):31–41.
- Fischer, U. H. and Clarke, G. K. C. (1997). Stick-slip sliding behaviour at the base of a glacier. *Annals of Glaciology*, 24:390–396.
- Fowler, A. C. (1987). Sliding with cavity formation. *Journal of Glaciology*, 33(115):225–257.
- Funk, M. (1990). Gletscher-Kalbungsgeschwindigkeit im Süswasser. Bericht Nr. 20.8, unveröffentlicht, VAW. Im Auftrag der Kraftwerke Oberhasli AG, In- nertkirchen.
- Funk, M. and Röthlisberger, H. (1989). Forecasting the effects of a planned reservoir that will partially flood the tongue of Unteraargletscher in Switzerland. *Annals of Glaciology*, 13:76–80.
- Gizejewski, J. (1997). Bottom morphology of the Hans Glacier forefield (Hornsund, South-West Spitsbergen, Svalbard). Preliminary report. In Glowacki, P., editor, *Polish Polar Studies, 24th Polar Symposium, Warszawa*. Institut of Geophysics of the Academy of Sciences, Warszawa.
- Glazovsky, A. F., Kolondra, L., Moskalevsky, M. Y., and Jania, J. (1991). Studies on the tidewater glacier Hansbreen on Spitsbergen - summary. *Materialy Gljaciologicheskich Issledovaniy*.
- Gorski, M. (1997). Seismicity of the Hornsund region, Spitsbergen: icequakes and earthquakes. Technical Report B-20 (308), Institute of Geophysics Polish Academy of Science.
- Gudmundsson, G. H. (1999). A three-dimensional numerical model of the confluence area of Unteraargletscher, Bernese Alps, Switzerland. *Journal of Glaciology*, 45(150):219–230.
- Hanson, B. and Hooke, R. L. (1994). Short-term velocity variations and basal coupling near a bergschiund, Storglaciären, Sweden. *Journal of Glaciology*, 40(134):67–74.
- Hanson, B. and Hooke, R. L. (2000). Glacier calving: a numerical model of forces in the calving-speed/water-depth relation. *Journal of Glaciology*, 46(153):188–196.
- Hanson, B., Hooke, R. L., and Grace, E. M. (1998). Short-term velocity and water-pressure variations down-glacier from a riegel, Storglaciären, Sweden. *Journal of Glaciology*, 44(147):359–367.

- Heinrich, H. (1988). Origin and consequences of cyclic ice rafting in the northeast Atlantic Ocean during the past 130'000 years. *Quaternary Research*, 29(2):142–152.
- Holdsworth, G. (1978). Some mechanisms for the calving of icebergs. In Husseiny, A., editor, *Iceberg utilization*, pages 160–175. Pergamon Press.
- Hooke, R. L., Laumann, T., and Kennett, M. I. (1989). Austdalsbreen, Norway: expected reaction to a 40m increase of water level in the lake into which the glacier calves. *Cold Regions Science and Technology*, 17:113–126.
- Hubbard, A., Blatter, H., Nienow, P., Mair, D., and Hubbard, B. (1998). Comparison of three-dimensional model for glacier flow with field data from Haut Glacier d'Arolla, Switzerland. *Journal of Glaciology*, 44(147):368–378.
- Hughes, T. (1992). Theoretical calving rates from glaciers along ice walls grounded in water of variable depths. *Journal of Glaciology*, 38(129):282–294.
- Hunter, L. E. and Powell, R. D. (1998). Ice foot development at temperate tidewater margins in Alaska. *Journal of Geophysical Research*, 25(11):1923–1926.
- Hunter, L. E., Powell, R. D., and Lawson, D. E. (1996). Morainal-bank sediment and their influence on the stability of tidewater termini of valley glaciers entering Glacier Bay, Alaska, U.S.A. *Annals of Glaciology*, 22:211–216.
- Hutter, K. (1983). *Theoretical glaciology; material science of ice and the mechanics of glaciers and ice sheets*. D. Reidel Publishing Company/Tokyo, Terra Scientific Publishing Company.
- IAHS(ICSU)-UNEP-UNESCO (1997). Glacier Mass Balance Bulletin No. 5, 1994–1995. Technical report, WGMS.
- IAHS(ICSU)-UNEP-UNESCO (1998). Fluctuations of Glaciers 1990–1995. Technical report, WGMS.
- Iken, A. (1977). Variations of surface velocities of some Alpine glaciers measured at intervals of a few hours. Comparison with Arctic Glaciers. *Zeitschrift für Gletscherkunde und Glazialgeologie*, 13:23–35.
- Iken, A. (1981). The effect of the subglacial water pressure on the sliding velocity of a glacier in an idealized numerical model. *Journal of Glaciology*, 27(97):407–421.
- Iken, A. and Bindshadler, R. A. (1986). Combined measurements of subglacial water pressure and surface velocity of Findelengletscher, Switzerland: Conclusions about drainage system and sliding mechanism. *Journal of Glaciology*, 32(110):101–119.
- Iken, A., Röthlisberger, H., Flotron, A., and Haerberli, W. (1983). The uplift of the Unteraargletscher at the beginning of the melt season – a consequence of water storage at the bed? *Journal of Glaciology*, 29(101):28–47.

- Iken, A. and Truffer, M. (1997). The relationship between subglacial water pressure and velocity of Findelengletscher, Switzerland, during its advance and retreat. *Journal of Glaciology*, 43(144):328–33.
- Iverson, N. R., Hooyer, T. S., and Baker, R. W. (1998). Ring-shear studies of till deformation: Coulomb-plastic behavior and distributed strain in glacier beds. *Journal of Glaciology*, 44(148):634–642.
- Jania, J. (1988). Dynamiczne procesy glacialne na południowym Spitsbergenie w świetle badań fotointerpretacyjnych i fotogrametrycznych. (Dynamic glacial processes in South Spitsbergen in the light of Photointerpretation and photogrammetric research). Prace Naukowe Uniwersytetu Śląskiego 955, Katowice.
- Jania, J. (1994). Field investigation during glaciological expeditions to Spitsbergen in the period 1992-1994. Technical report, University of Silesia, Katowice.
- Jania, J. and Kaczmarek, M. (1997). Hans Glacier - a tidewater glacier in southern Spitsbergen: summary of some results. In Van Der Veen, C. J., editor, *Calving glaciers, Report of a Workshop*, BPRC Report No. 15, Byrd Polar Center.
- Jania, J. and Kolondra, L. (1982). Field investigations performed during the Glaciological Spitsbergen Expedition in 1982. Technical report, Uniwersytet Śląski, Katowice.
- Jania, J., Rudowski, L., and Gorski, M. (1985). Annual activity of Hans Glacier Spitsbergen as determined by photogrammetry and microtremors recording. In *Proc. Symp. Glacier Mapping and Survey, Reykyavik*.
- Jansson, P. (1995). Water pressure and basal sliding on Storglaciären, northern Sweden. *Journal of Glaciology*, 41(138):232–240.
- Jansson, P. and Hooke, R. L. (1989). Short-term variations in strain and surface tilt on Storglaciären, Kebnekaise, Northern Sweden. *Journal of Glaciology*, 35(120):201–208.
- Josberger, E. G. (1977). A laboratory and field study of iceberg deterioration. In *Proceedings of the First International Conference on Iceberg Utilization*, pages 245-264.
- Kamb, B. and Engelhardt, H. (1987). Waves of accelerated motion in a glacier approaching surge: the mini-surges of Variegated Glacier, Alaska, U.S.A. *Journal of Glaciology*, 33(113):27–46.
- Kamb, B., Engelhardt, H., Fahnestock, M. A., Humphrey, N., Meyer, M., and Stone, D. (1994). Mechanical and hydrologic basis for the rapid motion of a large tidewater glacier. 2. Interpretation. *Journal of Geophysical Research*, 99(B8):15231–15244.
- Kirkbride, M. P. and Warren, C. R. (1997). Calving processes at a grounded ice cliff. *Annals of Glaciology*, 6:116–121.

- Kosiba, A. (1960). Some results of glaciological investigations in SW-Spitsbergen carried out during the Polish I.G.Y. Spitsbergen Expeditions. Technical report, Zeszyty Naukowe Uniwersytetu WrocBawskiego. Serie B no. 4.
- Krimmel, R. M. (1992). Photogrammetric Determination of Surface Altitude, Velocity and Calving Rate of Columbia Glacier, Alaska, 1983-1991. Technical Report 92-104, U.S. Geol. Surv. Open File Report.
- Krimmel, R. M. and Vaughan, B. H. (1987). Columbia Glacier, Alaska: Changes in velocity 1977-1986. *Journal of Geophysical Research*, 92(B9):8961-8968.
- Leysinger, G. J.-M. C. (1998). Numerisches Blockgletschermodell in zwei Dimensionen. Diploma Thesis. Versuchsanstalt für Wasserbau, Hydrologie und Glaziologie (VAW) der ETH Zürich. pp. 64.
- Lliboutry, L. A. (1968). General theory of subglacial cavitation and sliding of temperate glaciers. *Journal of Glaciology*, 7(49):21-58.
- Lliboutry, L. A. (1979). Local frictions laws for glaciers: a critical review and new openings. *Journal of Glaciology*, 23(89):67-95.
- MacAyeal, D. R. (1989). Large-scale ice flow over a viscous basal Sediment: Theory and application to Ice Stream B, Antarctica. *Journal of Geophysical Research*, 94(B4):4071-4078.
- MARC (1997). *MARC/MENTAT User's Manual*. MARC Analysis Research Corporation, 260 Sheridan Avenue, Palo Alto, CA 94306, K7 edition.
- Mayo, L. R. (1989). Advance of Hubbard Glacier and 1986 outburst of Russell Fiord, U.S.A. *Annals of Glaciology*, 13:189-194.
- Meier, M., Lundstrom, S., Stone, D., Kamb, B., Engelhardt, H., Humphrey, N., Dunlap, W. W., Fahnestock, M., Krimmel, R., and Walter, R. (1994). Mechanical and hydrologic basis for the rapid motion of a large tidewater glacier. 1. Observations. *Journal of Geophysical Research*, 99(B8):15219-15229.
- Meier, M. F. (1994). Columbia Glacier during rapid retreat: interactions between glacier flow and iceberg calving dynamics. In Reeh, N., editor, *Workshop on the calving rate of West Greenland glaciers in response to climatic change, 13-15 Sept. 1993*, Copenhagen, pages 63-83. Danish Polar Center.
- Meier, M. F. (1997). The iceberg discharge process: observations and inferences drawn from the study of Columbia Glacier. In Van der Veen, C. J., editor, *Calving Glaciers: Report of a Workshop*, BPRC Report No. 15, pages 109-114, Byrd Polar Research Center, Ohio State University, Columbus, Ohio.
- Meier, M. F. and Post, A. (1987). Fast tidewater glaciers. *Journal of Geophysical Research*, 92(B9):9051-9058.
- Meier, M. F., Rasmussen, L. A., Krimmel, R. M., Olsen, R. W., and Frank, D. (1985). Photogrammetric determination of surface altitude, terminus position, and ice velocity of Columbia Glacier, Alaska. *U.S. Geological Survey Professional Paper*, 1258(F):F1-F41.



- Meinck, M. (1998). Untersuchungen zum Fließverhalten von Gletschern. Diplomarbeit, Hochschule für Technik und Wirtschaft Dresden.
- Moskal, W. (1987). Charakterystyka hydrologiczna zatoki białego niedziwida (Spitzbergen). Hydrological characteristic of the Isbjørnhamna (Spitsbergen). Technical report, Instytut Oceanografii, Uniwersytetu Gdańskiego.
- Motyka, R. (1997). Taku Glacier, Alaska: advance and growth of a tidewater glacier. In Van der Veen, C. J., editor, *Calving Glaciers: Report of a Workshop*, BPRC Report No. 15, pages 119-120, Byrd Polar Research Center, Ohio State University, Columbus, Ohio.
- Motyka, R. J. and Post, A. (1995). Taku Glacier: influence of Sedimentation, accumulation to total area ratio and channel geometry on the advance of a fjord-type glacier. In Ekstrom, D. R., editor, *Third Glacier Bay Symposium*, pages 38-45. National Park Service, Anchorage.
- Naruse, R. and Skvarca, P. (2000). Dynamic Features of Thinning and Retreating Glacier Upsala, a Lacustrine Calving Glacier in Southern Patagonia. *Artic, Antarctic, and Alpine Research*, 32(4):485-491.
- Naruse, R., Skvarca, P., and Takeuchi, Y. (1997). Thinning and retreat of Glacier Upsala, an estimate of annual ablation changes in southern Patagonia. *Annals of Glaciology*, 24.
- Neshyba, S. and Josberger, E. G. (1980). On the estimation of Antarctic iceberg melt rate. *Journal of Physical Oceanography*, 10:1681-1685.
- Ohmura, A. (2001). Physical Basis for the Temperature-Based Melt-Index Method. *Journal of Applied Meteorology*, 40:753-761.
- Paterson, W. S. B. (1994). *The Physics of Glaciers*. Pergamon, New York, third edition.
- Pelto, M. S. and Warren, C. R. (1991). Relationship between tidewater glacier calving velocity and water depth at the calving front. *Annals of Glaciology*, 15:115-118.
- Powell, R. D. (1988). Processes and facies of temperate and sub-polar glaciers with tidewater termini. In *GSA Centennial Annual Meeting, Denver, Colorado*. Geological Society of America.
- Powell, R. D. (1991). Grounding-line Systems as a second-order controls on fluctuations of tidewater termini of temperate glaciers. In *Glacial marine Sedimentation; paleoclimatic significance*, pages 75-93. Geological Society of America. GSA Special Paper 261.
- Press, W. H., Teukolsky, S. A., Vetterling, W. T., and Flannery, B. P. (1996). *Numerical Recipes in FORTRAN 77: The Art of Scientific Computing*. Cambridge University Press, Cambridge etc., second edition.

- PV-WAVE (1995). *PV WAVE Technical Reference Manual*. Visual Numerics, Inc., 6230 Lookout Road, Boulder, CO 80301, 6th edition.
- Rasmussen, L. A. and Meier, M. F. (1982). Continuity Equation Model of the Predicted Drastic Retreat of Columbia Glacier, Alaska. Technical report, US Geological survey professional paper 1258-C.
- Raymond, C. F. and Malone, S. D. (1986). Propagating strain anomalies on Variegated Glacier, Alaska, U.S.A. *Journal of Glaciology*, 32(111):178-191.
- Reeh, N. (1968). On the calving of ice from floating glaciers and ice shelves. *Journal of Glaciology*, 7(50):215-232.
- Robe, R. Q., Maier, D. C., and Kollmayer, R. C. (1977). Iceberg Deterioration. *Nature*, 267:505-506.
- Röthlisberger, H. (1972). Water pressure in intra- and subglacial channels. *Journal of Glaciology*, 11(62):177-203.
- Rott, H. (1997). Lecture Notes on Remote Sensing. EISMINT Summer School.
- Rott, H., Stuefer, M., and Siegel, A. (1998). Mass fluxes and dynamics of Moreno Glacier, Southern Patagonian Icefield. *Journal of Geophysical Research*, 25(B9):1407-1410.
- Sikonia, W. G. (1982). Finite element glacier dynamics model applied to Columbia Glacier, Alaska. Technical Report Professional Paper 1258-B, U. S. Geological Survey.
- Swerpel, S. (1982). Hydrological investigations of the coastal waters in the Hornsund fiord in the summer of 1975. Technical Report 525, Acta Universitatis Wratislaviensis.
- Tangborn, W. (1997). Using low-altitude meteorological observations to calculate the mass balance of Alaska's Columbia Glacier and relate it to calving and speed. In Veen, C. J. V. D., editor, *Calving glaciers, Report of a Workshop*, BPRC Report No. 15, pages 141-161, Byrd Polar Center.
- Truffer, M. (1999). *Till deformation beneath Black Rapids Glacier, Alaska, and its implication on glacier motion*. PhD thesis, University of Alaska, Fairbanks.
- Van der Veen, C. J. (1996). Tidewater calving. *Journal of Glaciology*, 42(141):375-385.
- Van der Veen, C. J., editor (1997). *Calving Glaciers: Report of a Workshop*, BPRC Report No. 15, Byrd Polar Research Center, Ohio State University, Columbus, Ohio.
- Van der Veen, C. J. (1997a). Controls on the position of iceberg-calving fronts. In Veen, C. J. V. D., editor, *Calving glaciers, Report of a Workshop*, BPRC Report No. 15, pages 163-172, Byrd Polar Center.

- Van der Veen, C. J. (1998). Fracture mechanics approach to Penetration of bottom crevasses on glaciers. *Cold Regions Science and Technology*, 27:213–223.
- Vaughan, D. G. (1993). Relating the occurrence of crevasses to surface strain rates. *Journal of Glaciology*, 39(132):255–266.
- Venteris, E. R. (1999). Rapid tidewater glacier retreat: a comparison between Columbia Glacier, Alaska and Patagonian Calving Glaciers. *Global and Planetary Change*, 22:131–138.
- Vieli, A., Funk, M., and Blatter, H. (2000). Tidewater glaciers: frontal flow acceleration and basal sliding. *Annals of Glaciology*, 31:217–221.
- Vieser, P. (2000). GPS-Kampagne Spitzbergen 1999. Diplomarbeit, Fachhochschule beider Basel.
- Voigt, U. (1979). Zur Blockbewegung der Gletscher. Technical Report 44, Geodätische und Geophysikalische Veröffentlichungen. Reihe III.
- Warren, C. and Aniya, M. (1999). The calving glaciers of southern South America. *Global and Planetary Change*, 22:59–77.
- Warren, C. R. (1993). Rapid recent fluctuations of the calving San Rafael Glacier, Chilean Patagonia: climatic or non-climatic? *Geografiska Annaler*, 75:111–125.
- Warren, C. R. (1999). Calving Speed in Freshwater at Glaciar Ameghino, Patagonia. *Zeitschrift für Gletscherkunde und Glazialgeologie*, 35:21–34.
- Warren, C. R., Glasser, N. F., Harrison, S., Winchester, V., Kerr, A. R., and Rivera, A. (1995b). Characteristics of tide-water calving Glaciar San Rafael. *Journal of Glaciology*, 41(138):273–288.
- Warren, C. R., Greene, D. R., and Glasser, N. F. (1995a). Glaciar Upsala, Patagonia: rapid calving retreat in fresh water. *Annals of Glaciology*, 21.
- White, F. M., Spaulding, M. L., and Gominho, L. (1980). Theoretical Estimates of the Various Mechanisms Involved in Iceberg Deterioration in the Open Ocean Environment. Technical report, U. S. Coast Guard Report. No. CG-D-62-80.
- Willis, I. C. (1995). Intra-annual variations in glacier motion: a review. *Progress in Physical Geography*, 19(1):61–106.

# Acknowledgements

First of all, I thank Prof. Heinz Blatter and Dr. Martin Funk for their continuous support and the helpful discussions and suggestions concerning this study. They initiated this thesis and gave me the possibility to perform field work in Spitsbergen.

The support given by Dr. G. Hilmar Gudmundsson for the development of the numerical model and for his open mind for all kind of scientific questions is gratefully acknowledged.

I thank Prof. Keith Echelmeyer (University of Alaska) for the review of the final manuscript and the valuable comments to improve this work. Prof. Atsumu Ohmura is gratefully acknowledged for providing support in various aspects and for acting as co-examiner.

The observational part of this thesis is partly based on data provided by the group of Prof. Jacek Jania of University of Silesia, Poland. Thanks to Lezek Kolondra, who did the photogrammetrical analyses of Hansbreen.

During the thesis I had the opportunity to perform field investigations on Hansbreen in Spitsbergen. Many thanks to Jacek Jania, who made the two field expeditions possible and helped greatly in the field. He also provided valuable support for all kind of data and questions concerning Hansbreen and helped to improve the manuscript. Many thanks also to his wife Elzbieta for her warm help and support during my stay in Spitsbergen, especially in times of trouble. I highly appreciated the company and help of their son Jacek Junior in the field. A special thank goes to Pascal Vieser, who was responsible for the GPS-Survey. He was an excellent partner during the expedition to Spitsbergen and did a very good job in the field.

The Geophysical Institut of Polish Academy of Science provided the infrastructure on the Polish Polar Station in Hornsund, Spitsbergen, during the field investigation. I thank the various members of the Polish Polar Station for their support in logistics and in the field and for their warm hospitality.

I thank all colleagues at the Section of Glaciology of Versuchs Anstalt für Wasserbau (VAW) ETH and at the Institut of Climate Research ETH for their contribution to a pleasant and stimulating academic environment. During most part of the thesis I was a guest in the office of Andreas Bauder. I thank him for the hospitality and his continuous support concerning Software and Computer Problems. I am very grateful to Martin Lüthi, Gudfinna Adalgeirsdottir, Urs Fischer and Martin Truffer (University of Alaska) for spending time on parts of the manuscript and for giving critical and valuable comments. I also thank Sepp Luthiger and Karl Schroff for their technical

support for the field equipment and Hermann Böschi for his help in questions dealing with terrestrial or GPS survey.

The Glaciological Section of VAW (ETH), provided the finite-element Software MARC/MENTAT for the modelling part and the equipment for the field investigations.

The satellite interferometry investigations of Hansbreen were performed by the group of Prof. H. Rott from University of Innsbruck, Austria, thank you.

I thank my parents for making this interesting study possible. My deepest thanks go to my wife Gwendolyn and my daughter Anna-Lydia for sustaining me and keeping me smiling also in times of trouble.

This thesis was financed by the Swiss Federal Institute of Technology (ETH) Zürich, Switzerland, grant No. 0-20-400-97.

# Curriculum Vitae

Name: Andreas Vieli  
Address: Rotachstr. 50, 8003 Zürich, Switzerland  
Date of birth: 21. June 1970  
Citizenship: Vals (GR), Switzerland

1977-1983 Primary school in Dietlikon (Switzerland)  
1983-1986 Secondary school in Dietlikon  
1986-1990 Gymnasium Typus C in Winterthur (Switzerland)  
1991-1996 Studies in Physics at ETH Zürich  
with Diploma thesis in Glaciology at VAW, ETH Zürich  
1996-1997 Employment at VAW, ETH Zürich,  
1997-2001 Doctoral study in Glaciology at Institute of Climate Research',  
ETH Zürich

---

<sup>1</sup>former Geographisches Institut der ETH, Zürich